WT-103 (SAN)

OPERATION GREENHOUSE

SCIENTIFIC DIRECTOR'S REPORT

VOLUME III

GREENHOUSE HANDBOOK OF NUCLEAR EXPLOSIONS

NUCLEAR EXPLOSIONS

1951, Sanitized Version

[redacted]

[redacted] document contains restricted [redacted]s
defin[redacted]tomic En[redacted]1946.
Its transmitta[redacted] of its
contents [redacted]ner to an[redacted]d
per[redacted]ohibited.

[redacted]

REVIEWED BY DTRA (OSI).
DECLASSIFIED WITH DELETIONS.
COORDINATED WITH DOE, ARMY, NAVY, and AIRFORCE.
DATE 2 May 2001

DISTRIBUTION STATEMENT A
APPLIES PER NTPR REVIEW.
DATE 2 May 2001

[redacted]

WT-103 (SAN)

This document consists of 89 pages
(counting pre[illegible] pages)
No. 4 of 125 copies, Series A

Scientific Director's Report of Atomic Weapon Tests at Eniwetok, 1951

Volume III

Greenhouse Handbook of Nuclear Explosions,

Sanitized Version

[redacted]

This document contains restricted data as defined in the Atomic Energy Act of 1946. Its transmittal or disclosure of its contents in any manner to an unauthorized person is prohibited.

[redacted]

Distribution

	Copy
DEPARTMENT OF DEFENSE	
Armed Forces Special Weapons Project (Sandia)	1–3
Armed Forces Special Weapons Project (Washington)	4–15
ARMY	
Army Field Forces	16
Assistant Chief of Staff, G-3	17
Assistant Chief of Staff, G-4	18–19
Chief Chemical Officer	20–23
Chief Signal Officer	24–25
Chief of Engineers	26–27
Chief of Ordnance	28–31
Operations Research Office (Johns Hopkins University)	32–33
Quartermaster General	34–38
Surgeon General	39–40
NAVY	
Bureau of Aeronautics	41
Bureau of Ordnance	42–44
Bureau of Ships	45–46
Bureau of Yards and Docks	47
Chief of Naval Operations	48–49
Chief of Naval Research	50
Commandant, Marine Corps	51
AIR FORCE	
Air Force Cambridge Research Center	52
Air Research and Development Command	53–56
Air Targets Division, Directorate of Intelligence (Phys. Vul. Branch)	57–58
Assistant for Atomic Energy	59
Assistant for Development Planning	60
Assistant for Materiel Program Control	61

	Copy
AIR FORCE	
Deputy Chief of Staff for Development (AFDRD)	62
Director of Operations (Operations Analysis Division)	63
Director of Plans (AFOPD-P1)	64
Director of Requirements	65–66
Director of Research and Development	67–68
Eglin Air Force Base, Air Proving Ground	69
Ent Air Force Base, Air Defense Command	70–71
Kirtland Air Force Base, Special Weapons Center	72–74
Langley Air Force Base, Tactical Air Command	75–76
Maxwell Air Force Base, Air University	77–78
Offutt Air Force Base, Strategic Air Command	79–81
1009th Special Weapons Squadron	82
Rand Corporation	83–84
Scott Air Force Base, Air Training Command	85–86
Wright Air Development Center	87–89
Wright Air Materiel Command	90–91
ATOMIC ENERGY COMMISSION	
Atomic Energy Commission, Washington	92–94
Los Alamos Scientific Laboratory, Report Library	95–99
Sandia Corporation	100–101
University of California Radiation Laboratory, Livermore	102
Technical Information Service, Oak Ridge (surplus)	103–124
Weapon Test Reports Group, TIS	125

[redacted]

THE SCIENTIFIC DIRECTOR'S REPORT

Volume III

Greenhouse Handbook of Nuclear Explosions

Edited by

B. R. SUYDAM

Contributing Authors

P. G. Galentine F. B. Porzel
W. H. Langham B. R. Suydam
E. J. Zadina

Approved by
ALVIN C. GRAVES
Scientific Director

Los Alamos Scientific Laboratory
Los Alamos, New Mexico

March 1951

[redacted]

[redacted]

Editor's Note

This report was written prior to Operation Greenhouse and contains only the theory and preoperational outline of the experimental programs. A detailed account of the results of the individual operations may be found in the specific reports dealing with each project and will be summarized and evaluated in Parts I, II, and III of Volume II of the Scientific Director's Report for Operation Greenhouse.

[redacted]

Preface

Since the Sandstone tests in 1948, considerable advancement has been made in the design of fission weapons. The Los Alamos Scientific Laboratory program of developing physically small fission weapons has led to the design of smaller high-explosive systems [redacted] Design work is advancing on even smaller systems.

[redacted] It was hoped that this handbook might contain the results of the Ranger Program, but this has, for the most part, proved unfeasible.

Concurrently with the development of smaller fission weapons, the Los Alamos Scientific Laboratory has been advancing in its work on a "Super" bomb. In this field, theoretical studies have advanced to the point that the experimental study of a simple thermonuclear reaction becomes necessary. [redacted]

A full list of acknowledgments for this handbook would read like a list of the members of the Los Alamos Scientific Laboratory. For the most part, material has been quoted from many sources without specific mention. Of particular value in the preparation of this volume have been the Los Alamos Technical Series and the many volumes of the Scientific Director's Report of Operation Sandstone. In addition to those whose names appear as authors of particular chapters of this handbook, the following have given unusual assistance in its preparation in the way of advice and criticism: David B. Hall, William E. Ogle, Harris Mayer, Frederick Reines, Leslie B. Seely, and Bob E. Watt. Without their assistance, this volume could not have been written.

B. R. Suydam

CONTENTS

[redacted]

CONTENTS (Continued)

CONTENTS (Continued)

ILLUSTRATIONS

CHAPTER 2 GAMMA RADIATION

CHAPTER 3 NEUTRONS

CHAPTER 4 BLAST AND THERMAL RADIATION

ILLUSTRATIONS (Continued)

TABLES

[redacted]

Chapter 1

Purpose of the Tests

By B. R. Suydam

The three broad objectives of the 1951 Greenhouse Test Program are (1) to test fission weapons [redacted] (2) [redacted] (3) to increase the knowledge of the effects of nuclear weapons. The purpose of this handbook is to outline the manner in which these three objectives will be met.

1.1 TESTS OF FISSION WEAPONS

The Los Alamos Scientific Laboratory (LASL) has undertaken the development of fission weapons [redacted] is the first of such designs to be completed and will be tested in the Greenhouse Program.

Theoretical calculations [redacted] lead to surprisingly high values. These results depend, of course, on the assumption of perfect symmetry, on perfect initiation, and on knowledge of the equation of state of the bomb materials. [redacted] predicted by the International Business Machine (IBM) implosion calculations and could be incorrect for either of two reasons: (1) The equation of state for uranium and plutonium used in the implosion calculations could be incorrect or (2) asymmetries in the implosion could spoil the actual compressions. [redacted]

Concern [redacted] led to a series of special shots in Nevada, the Ranger Program. At the time of writing, the results of the Ranger shots have not been completely analyzed. [redacted]

1.2 THERMONUCLEAR TESTS

A second program of LASL is the advancement of work on a thermonuclear "Super" bomb. Thermonuclear reactions have received a great deal of theoretical study at Los Alamos. [redacted]

[redacted]

[redacted]

TABLE 1.1 THE EXPERIMENTAL PROGRAMS

Program No.	Agency	Experiment
1	Los Alamos	Diagnostic measurements. Gamma rays, neutrons, thermal radiation, and blast
2	Military and AEC	Biomedical program. Thermal-burn studies, gamma-ray and neutron damage to living tissues
3	Military	Blast damage to structures
4	Military	Cloud physics. Cloud tracking, updraft, tropical meteorology
5	Military	Test of radiological monitoring instruments
6	Military	Physical measurements. Cloud-particle size, thermal radiation on materials, exposure of combat vehicles, fall-out distributions, aircraft contamination, etc.
7	Military	Long-range detection
8	Military	Blast damage to aircraft and radar-scope photography

TABLE 1.2 SHOT SCHEDULE

Date (Tentative)	Island	Bomb Model	Approximate Yield (kt)
7 April	Runit	[redacted]	[redacted]
18 April	Engebi		
9 May	Eberiru		
3 June	Engebi		

* The yield of this weapon will depend on the efficiency to which the tritium is burned.

[redacted] SECURITY INFORMATION

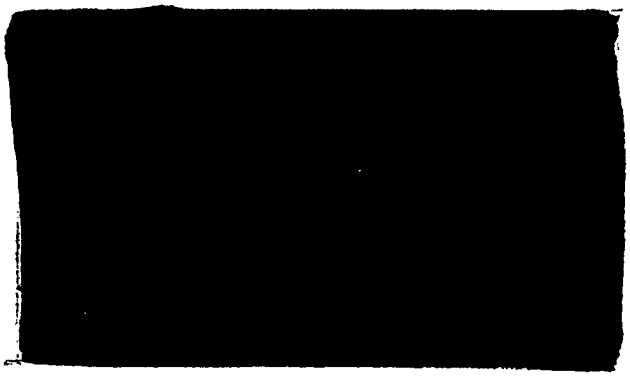

1.3 EFFECTS OF FISSION WEAPONS

By far the greater part of the Greenhouse Program is devoted to the determination of the effects of nuclear weapons. This portion of the program divides naturally into two broad parts:

1. Measurements of what might be called the "field variables" of the bomb. These measurements are concerned with the determination of air blast, neutrons, gamma rays, and thermal radiation in, as nearly as possible, their pure and undisturbed states.

2. Determination of the effects produced by these field variables on animate and inanimate objects.

The field-variable measurements consist in complete gamma-radiation measurements (Chap. 2), neutron measurements (Chap. 3), and blast and thermal-radiation studies (Chap. 4). The radiation studies, gamma, neutron, and thermal, are quite elaborate and, if successful, will essentially complete the knowledge of these phenomena. The blast studies to be effected are as complete as possible under the conditions of a tower burst. They should settle the questions of the curves of free-air pressure vs distance and the validity of scaling from HE to nuclear explosions.

The effects measurements include such experiments as the biomedical program, the structures program, cloud studies, meteorology, and long-range detection. These programs are briefly outlined in Chaps. 5 and 6.

1.4 THE EXPERIMENTAL PROGRAMS

In Table 1.1 are listed the experimental programs by number with a brief description of the program objectives. The descriptions of the various experimental programs are not intended to be complete but rather to indicate their general natures.

1.5 SHOT SCHEDULE

The schedule as planned for the firing of the various shots of the Greenhouse Program is given in Table 1.2.

The wind directions at the Atoll would make the shot order Engebi, Eberiru, Runit somewhat more advantageous because then no cloud would pass over a future shot island. However, the schedule in Table 1.2 is felt to be better in general, since it allows more time on the islands where the most work is to be done. Thus, conducting the Runit shot first will permit a checking of instruments and techniques before the heavily instrumented shot on Engebi is fired; it will also permit a longer time for setting up and checking the very complicated thermonuclear diagnostic experimental apparatus on Eberiru.

[redacted]

Chapter 2

Gamma Radiation

By B. R. Suydam

2.1 SOURCES OF GAMMA RADIATION

There are two distinct sources of gamma radiation in a nuclear explosion. The so-called "prompt" gamma rays are those created while the nuclear reaction is going on. Some of these gamma rays are the direct result of fission, and some are the result of n,γ reactions in the assembly (radiative capture or inelastic scattering of neutrons). The time during which prompt gamma rays are liberated is the reaction time of the bomb. This time depends on the model but will generally be some fraction of a microsecond.

Later, when the bomb components have disassembled and the reaction has ceased, there is still gamma radiation being produced by the radioactive decay of the fission fragments. This later radiation is called the "delayed" gamma radiation. The delayed radiation continues for some time after the burst, and its exact time dependence is determined by the fate of the fission fragments, i.e., the time at which they are swept up into the upper atmosphere or to the points where they are deposited. In any air burst, even on a very low tower, the vast majority of the fission fragments will be carried high into the air by the buoyant rise of the ball of fire. Because of this, the majority of the delayed radiation comes during the first minute or so after the explosion, although weak gamma radiation from a few fission fragments trapped in the surrounding soil may continue for a long time afterward. In addition to the gamma radiation from these two sources, there is gamma radiation from n,γ reactions in the soil and in the air surrounding the bomb. Gamma rays arising from this source are usually lumped together with the delayed gamma rays.

The amounts of energy liberated in the prompt and in the delayed gamma rays are roughly equal. However, the source of the prompt radiation is the dense assembled bomb which acts as an excellent shield to prevent the escape of the radiation, whereas the source of the delayed radiation is in the form of a tenuous gas which shows essentially no gamma-ray absorption. The net result is that, of the total gamma-ray dosage delivered, only about 1 or 2 per cent is from the prompt gamma rays.

2.2 RESULTS FROM PAST MEASUREMENTS

Knowledge of gamma radiation from a nuclear explosion has resulted almost entirely from the Sandstone experiments. These experiments are described in detail in Sandstone Report, Vol. 7, "The Scientific Director's Report." Briefly, the following measurements were made:

1. Prompt gamma rays were measured in the alpha experiment, using Rossi-type chambers.
2. Good-geometry measurements were made, using collimating tubes containing various amounts of absorbing material. There were two types of such measurements: (a) integral measurements using film badges and thimble chambers as detectors and (b) time-dependent measurements with naphthalene and photocells as detectors.
3. Two types of measurements were made in bad geometry: (a) integral measurements using film badges and (b) time-dependent measurements using thimble chambers and recording electrometers.

[redacted]

For many reasons, as pointed out in "The Scientific Director's Report," these measurements left much to be desired. Nevertheless, certain conclusions can be drawn; they will be discussed in the following sections.

2.2.1 Prompt Gamma Rays

A careful calculation of the prompt gamma rays which escape from the bomb assembly would require a detailed quantitative knowledge of all the processes involved in a nuclear explosion, such as the fission gamma spectrum, the precise neutron and material distributions at all times, the inelastic scattering and radiative-capture cross sections that all the materials used in the bomb present to neutrons, and the gamma spectrum of all possible n,γ reactions. Little is known about many of the details of these processes, and in any case the amount of labor involved would prohibit making such a detailed calculation. However, the gamma-ray absorption coefficients of the active material and tamper are so large that it is difficult to imagine that a significant number of gammas would penetrate very much of these materials. It is accordingly believed that most of the prompt gamma radiation observed is that which has its origin in n,γ reactions (inelastic scattering and radiative capture) involving neutrons in the outer layers of the tamper. Accordingly, the number of gammas per fission which reach the surrounding air will depend critically on the bomb model, in particular on the value of alpha, the tamper thickness, and on the amount of material surrounding the tamper.

For several experiments, especially the Dinex experiment, it is important to know the number of prompt gammas escaping the assembly per fission inside. As pointed out, this quantity is hopelessly difficult to calculate accurately; however, experimental estimates of this quantity are available. The alpha measurements [redacted]

Moreover, it turned out that the total gamma-ray measurements in good geometry essentially measured only the prompt gamma rays,[2] and this allows a somewhat better estimate of the quantity Γ_0, the number of gammas reaching the air per fission [redacted]

and from this, Γ_0 for the various Greenhouse shots may be estimated according to the following:

1. It is assumed that essentially all the escaping gamma rays are formed in the outer layers of the tamper. Accordingly, Γ_0 is proportional to the neutron density in the outer centimeter of the tamper and to the n,γ cross sections of the tamper material.
2. The gamma rays formed in this manner [redacted]

In this manner the estimates of Γ_0 given in Table 2.1 have been made. It is to be emphasized that the values of Table 2.1 are not to be taken as precisely known values [redacted]

About the best that can be said is that these values are probably of the correct order of magnitude.

TABLE 2.1 GAMMAS AT A DISTANCE PER FISSION

[redacted]

2.2.2 Delayed Gamma Radiation

Since the source for the delayed gamma radiation is a tenuous gaseous cloud of fission fragments, the total amount of such radiation would be expected to depend not at all on the bomb model but only on the total number of fragments formed and hence only on the yield of the bomb. However, the total amount of delayed gamma radiation should actually depend slightly on the model since the fragment yields and the energy released per fission are slightly different for U^{235} and Pu^{239}, but these effects are quite small.

[redacted]

For all three shots of the Sandstone experiments the total gamma-ray dosage as a function of distance was measured by means of film badges. These films were calibrated and used with a lead covering of such a thickness that equilibrium was attained at all calibration energies but not at the energies measured in the explosions. The result of this is that the number of electrons striking the film per incident erg of gamma radiation should have been higher on the calibration runs than during the measurements. The absolute gamma-ray levels encountered during the experiments are therefore very doubtful, although the relative values should be correct within experimental scatter. A rough estimate of the effect of using a nonequilibrium thickness of lead in front of the film indicates that the levels reported[3] should be corrected upward by a factor of about 1.7. When this correction is applied to the results of the three Sandstone shots, when the spherical geometry factor is removed by plotting dosage times distance squared vs distance, and when all measurements are normalized to a 24-kt yield according to the best available Sandstone yields, the results may be plotted as shown in Fig. 2.1. It is seen that all the data fit the single curve. In plotting the curve of Fig. 2.1, no attempt was made to fit the data, except for a choice of scale factor. Instead the dosage-vs-distance curve for a point source was calculated. This point source decayed in time according to the known gross fission-product decay curve, rose into the air as the ball of fire was observed to rise, and emitted radiation obeying the exponential absorption law observed in the good-geometry measurements. A calculation showed that the actual finite size of the source had no significant effect on the calculated curve. It is seen that a curve calculated in this simple manner agrees with the results as well as any other curve that might be drawn. It should be noted that the gamma-ray absorption curve of Fig. 2.1 has been corrected to standard conditions for the air (0°C and 760 mm Hg).

In making these calculations, the gross decay of the fission fragments and the height of the ball of fire vs time were required. These are shown in Figs. 2.2 and 2.3, respectively. (The data for Fig. 2.3 were actually taken from the Trinity measurements since no measurements of the cloud height were made at Sandstone at short times.) From these two curves and as a by-product of the calculation, the curves of Fig. 2.4, which show the gamma dosage vs time, were also obtained. In this figure the results of the time-dependent total dosage measurements made on shot Zebra are also plotted. Here the agreement between measurement and calculation is not striking, but it is probably within experimental error. It must be pointed out that the actual experimental data are not as consistent as the points appear. In particular, the two chambers, both at the same location, differed by a factor of nearly 3 regarding the total dose.

The following conclusions may be drawn from the experimental results of total gamma-ray dosage measurements in poor geometry:

1. Over a range of 500 to 2500 meters distance from the explosion (about 7 mfp) the apparent mean free path is independent of distance and corresponds with a gamma energy of 4.6 Mev. The apparent increase of mean free path at large distances can be accounted for, within experimental error, by the buoyant rise of the ball of fire.

2. The yield of the bomb can be estimated from total gamma-ray dosage measurements. For distances not too large the gamma-ray dosage in roentgens is given by

$$\text{Dosage} = 2.9 \times 10^9 \frac{W}{D^2} e^{-D/\lambda} \qquad (2.1)$$

where W is the bomb yield in kilotons, D is the distance from the explosion in meters, and λ is the mean free path in meters. The quantity λ will be given by

$$\lambda = 283 \left(1 + \frac{T}{273}\right) \qquad (2.2)$$

when the air temperature T is expressed in degrees centigrade. At large distances the formula for the dosage (Eq. 2.1) must, of course, be corrected for the rise of the source. The value of λ is quite good. On the other hand, because of the uncertainty regarding the film calibration, the numerical factor in Eq. 2.1 is quite uncertain. Nevertheless, if films similar to those used at Sandstone are used in a similar manner, the numerical factor can be applied, and the yield measured in this manner should be accurate to about 30 per cent.

There has been no direct measurement of the gamma-ray spectrum. The observed fact that the mean free path is independent of distance,

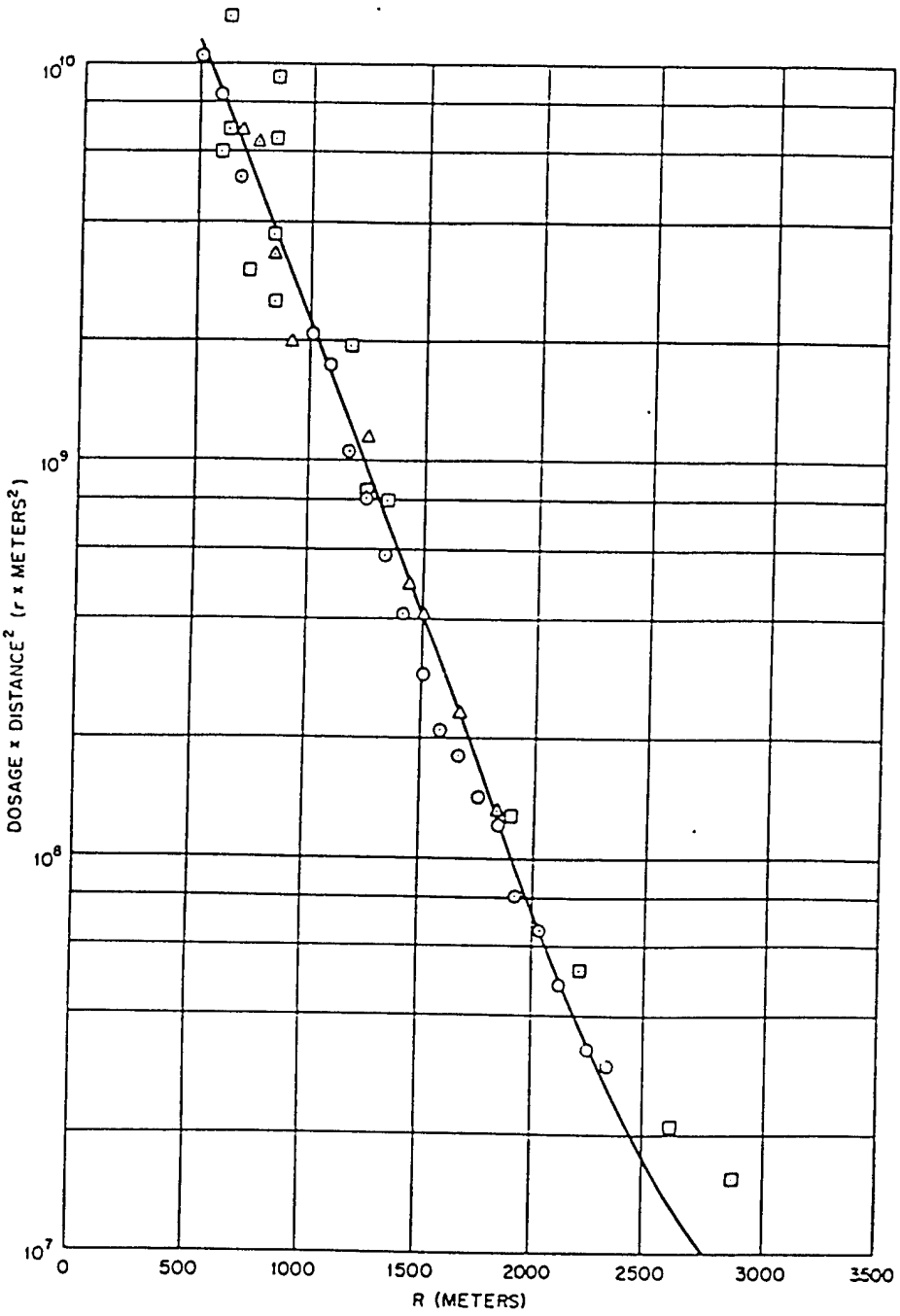

Fig. 2.1 Total Gamma Dosage vs Distance. Normalized to Trinity yield and to air at 0°C and 760 mm Hg, corrected for lead cross. □, X-ray shot. △, Yoke shot. ○, Zebra shot.

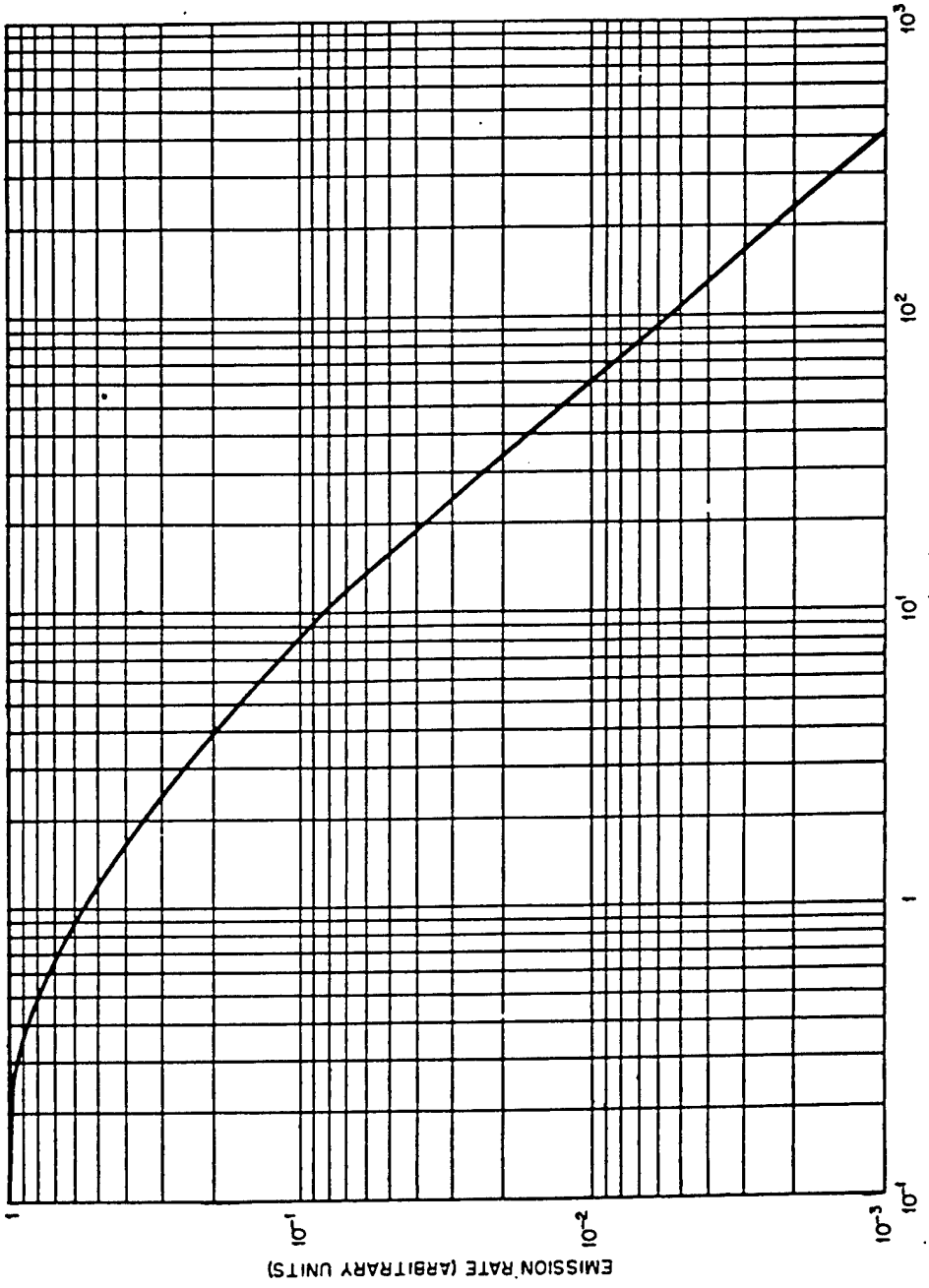

Fig. 2.2 Rate of Gamma-ray Emission from Fission Fragments

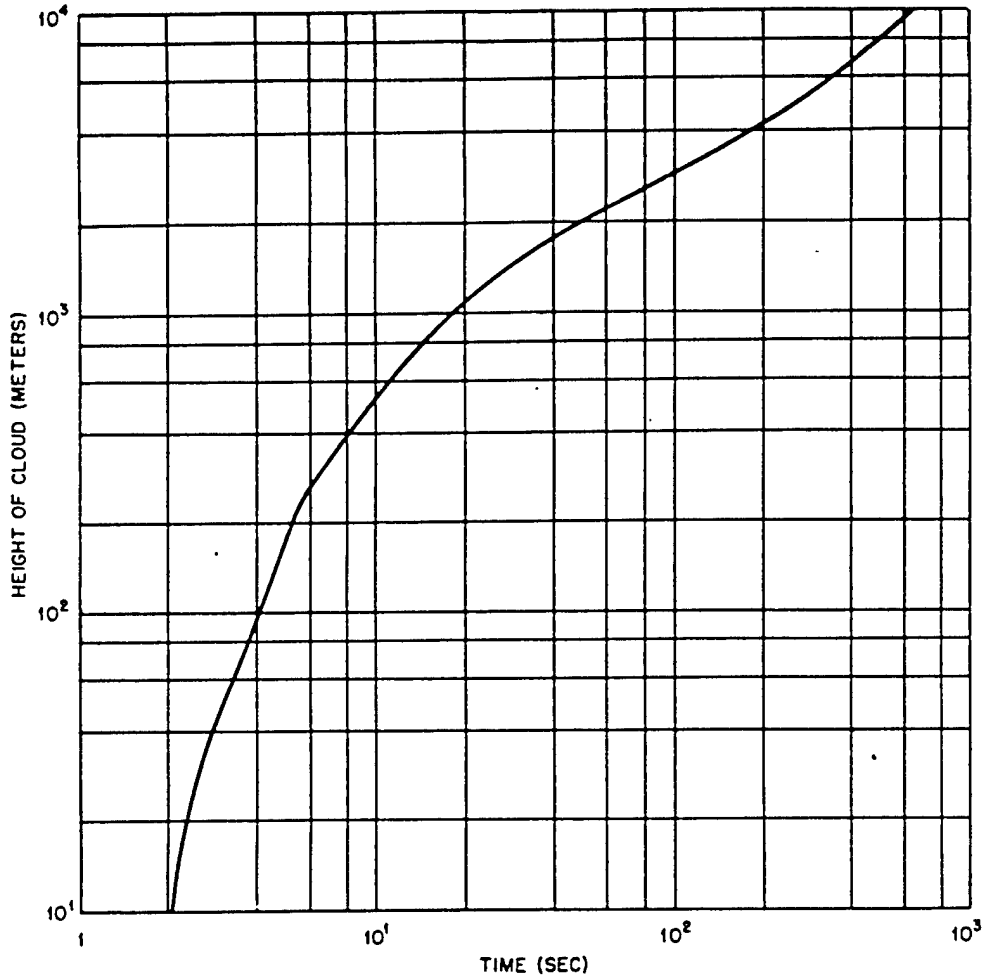

Fig. 2.3 Cloud Height vs Time, Trinity Shot

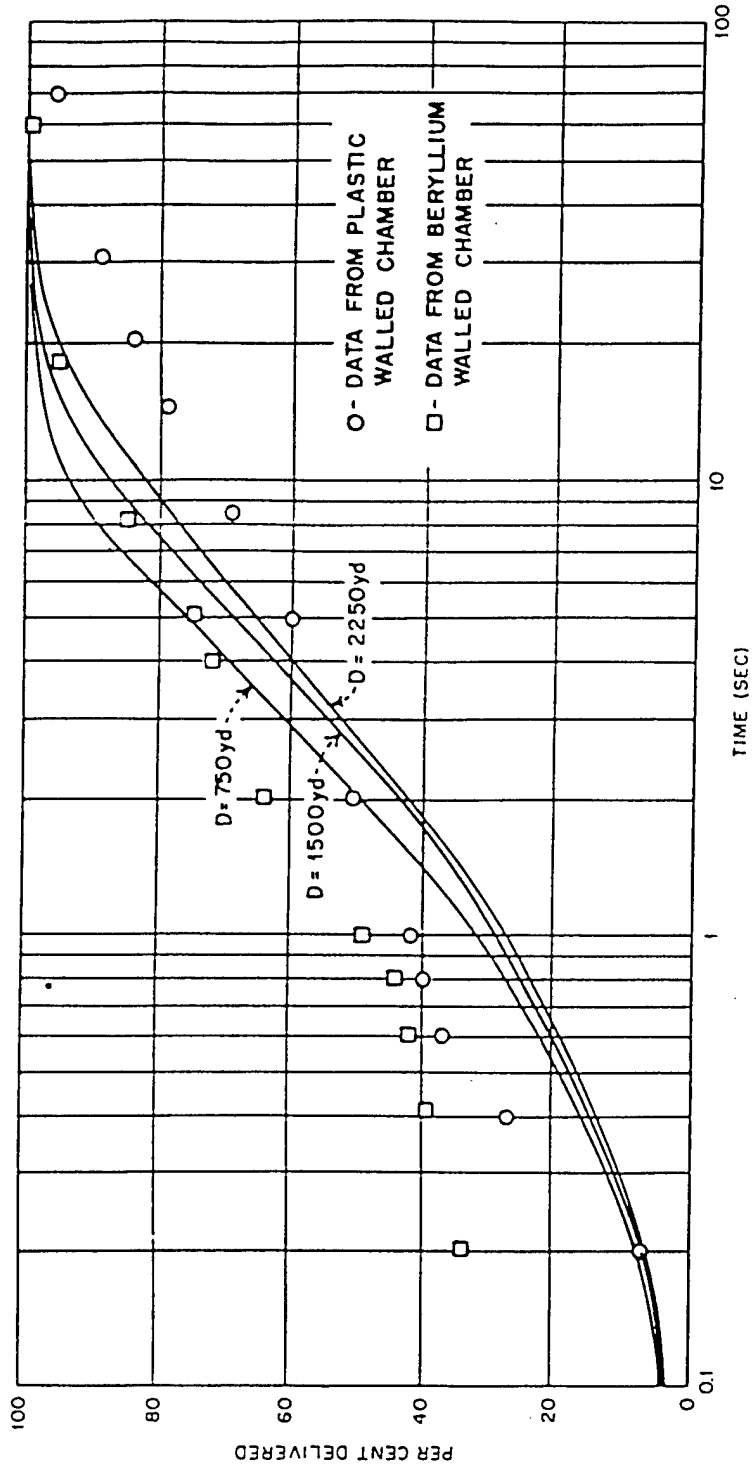

Fig. 2.4 Percentage of Total Dosage Delivered from a Blaling Source up to Time t for Various Horizontal Distances D.

however, gives indirect evidence from which qualitative conclusions may be drawn. Since the gamma-ray absorption curve appears to yield an absorption coefficient which corresponds to an energy of 4.6 Mev and is independent of distance, the spectrum probably does not differ markedly from that which would be obtained at a great distance from a 4.6-Mev source. This latter spectrum can be calculated by the following scheme: Let $n(\vec{k},x)$ represent the number of quanta per unit volume at the point x which have the momentum $\vec{k}$ (and the energy $k = |\vec{k}|$; momenta will be in energy units). In one dimension the diffusion equation will be

$$\cos\theta \frac{\partial n(\vec{k},x)}{\partial x} = -\sigma(k)\ n(\vec{k},x) + \int \phi(\vec{k}';\vec{k})\ n(\vec{k}';x)\ d\vec{k}' \quad (2.3)$$

where $\sigma(k)$ is the total cross section as a function of the energy k, $\phi(\vec{k}';\vec{k})$ is the differential cross section for scattering from momentum $\vec{k}'$ to $\vec{k}$, and θ is the angle between $\vec{k}$ and the x axis. At very large distances

$$\frac{\partial n}{\partial x} = -\sigma(k_0)n \equiv -\sigma_0 n$$

where σ_0 is the total cross section for the assumed initial energy, in this case 4.6 Mev. The diffusion equation becomes

$$(\sigma_0 \cos\theta - \sigma)\ n(\vec{k}) = -\int \phi(\vec{k}';\vec{k})\ n(\vec{k}')\ d\vec{k}' \quad (2.4)$$

This integral equation can be solved approximately for the gamma spectrum, as follows:

1. Divide the energy range $(0,k_0)$ into a finite number of cells, and replace the integral by a finite sum.

2. In each energy cell, replace the continuous angular distribution by a single "average" or "most probable" value of the angle θ.

There results from this a system of algebraic equations by which the number of photons in each energy cell may be determined. The result of such a calculation using a few rather wide energy cells is shown in Fig. 2.5. Since the result is not, in any case, to be believed to high precision, it was not felt necessary to use many small cells in the calculation. The shape of the curve in the neighborhood of 4.6 Mev is definitely not correct, but the total energy in the highest cell is probably fairly accurate.

The result of this calculation indicates a maximum energy of 4.6 Mev. This value is known to be untrue, since a few gamma rays above 9.6 Mev were detected at Sandstone. However, it is probably true that there is very little energy above 4.6 Mev. The result further indicates an average energy of 3 Mev, i.e., half the gamma energy is carried by photons exceeding 3 Mev and half by photons of less than 3 Mev. This result is felt to be approximately correct.

2.3 PLANS FOR 1951 TESTS

In the preceding sections of this chapter an attempt has been made to give a complete picture of the present knowledge of the gamma radiation accompanying a nuclear explosion, as well as estimates of what is expected in the forthcoming tests. It is quite apparent that the data are at many points quite sketchy if not altogether nonexistent. In order to remedy this situation, a rather large measurement program is planned for the 1951 Greenhouse operation.

Knowledge of the prompt radiation in general and of the number of gammas escaping per fission in particular will certainly be increased by the improved alpha measurements to be made. The use of differential- rather than integral-type detectors should give much more reliable results in the variable alpha region. This, together with recently completed "Hippo" efficiency calculations, is expected to increase the knowledge of the quantity Γ_0 (gammas per fission) by confirming or modifying the present ideas and by establishing some sort of confidence limits.

In addition to the alpha experiments, which measure the prompt gamma rays the following set of measurements of delayed gamma rays will be conducted by the National Bureau of Standards:

1. Short-time measurement of the absolute gamma level. These will be time-dependent measurements over a period of time extending to about 100 msec with a time resolution of 1 msec. Two detector geometries will be used: one sees gamma rays over a solid angle of 2π and the other employs a 4π solid angle of detection. This experiment will be conducted on all tower shots.

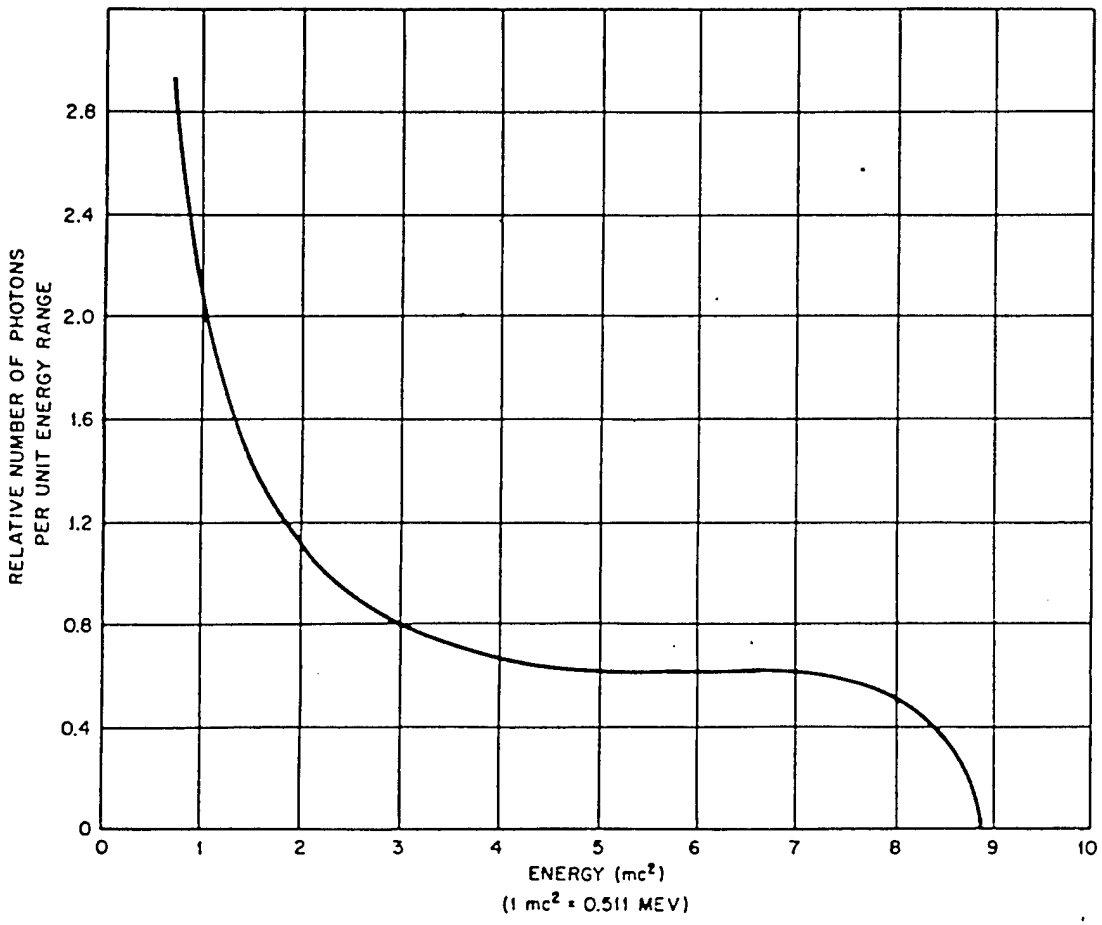

Fig. 2.5 Equilibrium Spectrum

2. Measurement of gamma-ray spectrum over the range 0.5 to 10 Mev. This will be accomplished by analyzing the secondary electrons ejected from a radiator in a beta-ray spectrometer. The spectrum will be measured only on the Engebi and Runit shots.

3. The spatial distribution of the fission fragments as a function of time will be measured on the Engebi and Runit shots.

4. The total gamma dosage as a function of time and distance using bad-geometry (2π and 4π) detectors will be measured on all tower shots.

In this handbook the experiments are merely outlined sufficiently to describe the objectives.

The principal objective of experiment 1 is to make an absolute determination of yield in a manner independent of radiochemistry. Knowledge of the short-time decay characteristics of the fission fragments, together with a knowledge of the gamma spectrum, allows in principle the deduction of the number of fission fragments, and hence the yield, from the absolute gamma measurements. This experiment will further confirm the knowledge of gamma-ray intensities at all times by being intercalibrated with other time-dependent measurements, i.e., the alpha experiment.

Experiment 3, the measurement of the distribution of the fission fragments in space and time, is aimed primarily at increasing the knowledge of the hydrodynamics of the early phases of the explosion. The experiment consists, briefly, in placing a cluster of collimating tubes at various points lying on a radius through the bomb and observing the time dependence of the gamma radiation which comes down the collimators. Determination in this manner of the spatial disposition of the bomb materials within the ball of fire is expected to yield information on material densities and velocities inside the ball of fire and also some information regarding the extent of mixing during the early stages of the explosions.

Experiments 2 and 4 are self-explanatory. From experiment 2, direct information should be obtained on the gamma-ray spectrum which will be valuable in the design of shielding, the interpretation of the biomedical experiments, and the mocking-up of sources for future laboratory experiments. Experiment 4 should largely eliminate the uncertainty regarding total dosage levels and will further aid in the interpretation of the biomedical experiments.

An additional function of experiment 4 is the obtaining of relative yields of the various bombs [redacted] It hardly seems possible that the gamma-ray measurements could fail to the extent that knowledge of the gamma rays from a nuclear explosion is not significantly increased. If all measurements succeed as planned, knowledge on this subject should be essentially complete.

REFERENCES

1. Sandstone Report, Vol. 8, Chap. 8.
2. Sandstone Report, Vol. 8, Chap. 4.
3. Sandstone Report, Annex 8, Part IV, Vol. 29.

Chapter 3

Neutrons

By B. R. Suydam

3.1 SOURCE OF NEUTRONS

The major source of neutrons in a nuclear explosion is the fission reaction itself. Each fission consumes one neutron, which is required to produce the fission, and releases about two neutrons (actually 2.5 for U^{235} and 2.95 for Pu^{239}). Therefore the net result is that, at the end of the chain reaction, somewhat more than one neutron net has been produced per fission. Some of the neutrons thus produced suffer radiative capture in the bomb materials, giving rise to gamma rays, but many of them eventually escape the assembly. In escaping the assembly, most of the neutrons are slowed down by inelastic scatterings in the heavy core materials, by elastic scatterings in the light HE materials, or by both; a few neutrons will escape with relatively little energy loss.

A few neutrons are emitted by the fission fragments, but the number of such delayed neutrons is relatively small, only about 1 per cent of the total number produced. On the whole, the fission fragments prefer to decay to their ground states by beta and gamma emission.

The majority of the neutrons resulting from a nuclear explosion are thus seen to be prompt neutrons, i.e., those liberated by the fission process. However, as has been shown, many of the prompt neutrons escape the assembly only after being slowed down in the HE. In escaping the assembly the majority of the prompt neutrons are actually thermalized in the HE and are temporarily trapped there. Later the nuclear shock traverses the HE, blowing all this material outward and carrying with it the neutrons trapped therein. The neutrons which have been trapped in the HE are thus swept outward with epithermal velocities of about 300 to 500 ev. These neutrons then diffuse out into the surrounding air, are slowed down to about 0.2 ev, and are then captured by nitrogen.

A picture of the neutrons accompanying a nuclear explosion is now seen to be roughly as follows: There is an essentially instantaneous burst of relatively fast neutrons, i.e., those which escape with little or no slowing down, and these neutrons propagate into the surrounding air, obeying approximately an exponential transmission law. Accompanying this burst of fast neutrons is a flood of epithermal neutrons which diffuse into the surrounding air, being slowed down in the process until they are captured by nitrogen or by the soil. Therefore at any point there will be neutrons of many energies, such as fast neutrons which have succeeded in penetrating bomb materials and air with little or no slowing down, thermal neutrons which have diffused outward, other thermal neutrons which started out fast but were slowed down by the air, and, in addition, neutrons of intermediate energies. There will also be delayed neutrons, but these account for only a small fraction of the total.

3.2 PAST EXPERIMENTS

The most extensive neutron measurements to date are those made at the Sandstone test in 1948. Detectors of three general types were used: (1) arsenic for slow neutrons, (2) sulfur threshold detectors which make use of the n,p reaction, and (3) a number of threshold detectors which undergo n,2n reactions. The

arsenic detectors are sensitive to neutrons of approximately thermal energies, the reaction being

$$As^{75}(n,\gamma)As^{76}$$

$$As^{76} \xrightarrow{26.8h} \begin{Bmatrix} Se^{76} \\ Ge^{76} \end{Bmatrix} + \text{mixture of } \beta^-,\ \beta^+, \text{ and } \gamma$$

The sulfur detectors have a threshold of 3 Mev and undergo the following reaction:

$$S^{32}(n,p)P^{32}$$

$$P^{32} \xrightarrow{14.3d} S^{32} + \beta^-(1.8 \text{ Mev})$$

The cross section for this reaction can be reasonably well represented by a step function which is zero for all neutron energies below 3 Mev. Thus the specific activity of a sulfur sample measures the total number of neutrons of energy not less than 3 Mev which pass through the sample.

Of all the n,2n threshold detectors tested, only iodine, which undergoes the reaction

$$I^{127}(n,2n)I^{126}$$

$$I^{126} \xrightarrow{13d} Xe^{126} + \beta^-(1.1 \text{ Mev}) + \gamma(0.5 \text{ Mev})$$

gave positive results. The threshold for the iodine n,2n reaction is 9.45 Mev. It is readily seen that an n,2n detector is not ideal because the γ,n reaction will always lead to the same result. Thus the measured activity of the iodine samples was always the combined result of n,2n and of γ,n reactions. For this reason, n,2n detectors must be used with and without lead shielding in order to separate neutron- and gamma-induced activities.

In all cases the sulfur results are best because of the cleanness of the reaction and the advantageous shape of the curve of cross section vs energy. Iodine results are probably the poorest because of the difficulty of separating neutron- from gamma-induced activity. The arsenic detectors suffer from the fact that the cross section cannot be accurately known unless the slow-neutron spectrum is known. A further difficulty encountered with the arsenic detectors, and probably the most serious, is that the arsenic activity was found to be impure. The arsenic samples contained antimony impurities; moreover arsenic itself has a second possible reaction, the n,2n reaction with high-energy neutrons. Thus three periods had to be separated in order to obtain arsenic results: (1) the arsenic slow-neutron capture, (2) the antimony slow-neutron capture, and (3) the arsenic n,2n plus arsenic γ,n period.

3.2.1 Fast Neutrons

B. E. Watt has shown[1] that the thermal-neutron-induced fission spectrum of U^{235} can be well represented by the equation

$$n(E)\,dE = (\text{const}) \times \sinh\sqrt{2E}\; e^{-E} \qquad (3.1)$$

where n(E) dE represents the number of neutrons with energies in the range (E, E + dE) and E is the neutron energy in millions of electron volts. From this equation it can be calculated by a simple integration that N(E), the relative number of neutrons whose energies exceed E, is given by the expression

$$N(E) = \frac{1}{2}\sqrt{\frac{1}{2}}\left[\Phi_1\left(\sqrt{E}-\sqrt{\frac{1}{2}}\right) - \Phi_1\left(\sqrt{E}+\sqrt{\frac{1}{2}}\right) + \sqrt{2}\left[2 - \Phi_0\left(\sqrt{E}-\sqrt{\frac{1}{2}}\right) - \Phi_0\left(\sqrt{E}+\sqrt{\frac{1}{2}}\right)\right]\right] \qquad (3.2)$$

where $\Phi_1(x)$ and $\Phi_0(x)$ represent, respectively, the error function and the error integral as tabulated in Jahnke and Emde.[2] Thus

$$\Phi_1(x) = \sqrt{\frac{2}{\pi}}\; e^{-x^2}$$

and

$$\Phi_0(x) = \sqrt{\frac{2}{\pi}} \int_0^x e^{-y^2}\, dy$$

Equation 3.2 is plotted in Fig. 3.1. In particular, it is shown that 0.21 of all fission neutrons have energies in excess of 3 Mev. It is to be emphasized that Fig. 3.1 represents the neutron spectrum from fission induced by thermal neutrons and hence is probably not an exact representation of the neutron spectrum within a reacting bomb.

The results of the neutron measurements with sulfur samples gave, for all three Sandstone shots and also for the Bikini-Able shot, neutron-flux-vs-distance curves which fit the formula

$$n = \frac{Q}{4\pi R^2}\, e^{-R/\lambda} \qquad (3.3)$$

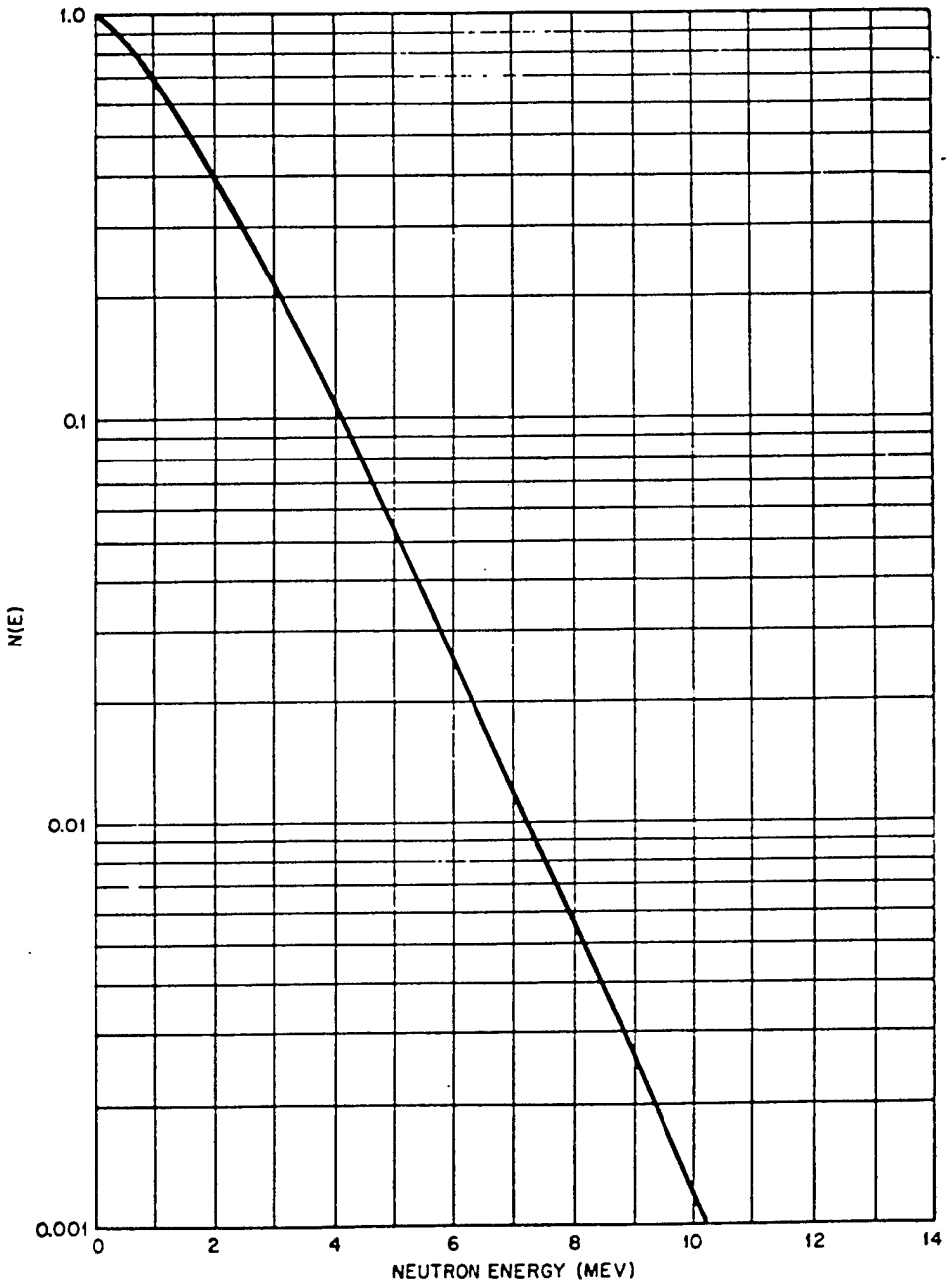

Fig. 3.1 Neutron Spectrum from Fission Induced by Thermal Neutrons. Given in the form of the fraction of fission neutrons exceeding some energy as a function of that energy.

[redacted]

TABLE 3.1 EXPERIMENTAL NUMBER OF SULFUR NEUTRONS PER FISSION NEUTRON

Shot	Q per Fission Neutron	Transmission	Number of Mfp
X	0.0048	0.023	3.77
Y	0.012	0.057	2.87
Z	0.0077	0.036	3.33
Bikini A	0.0059	0.028	3.58

TABLE 3.2 ESTIMATED NUMBERS OF SULFUR NEUTRONS EXPECTED FOR GREENHOUSE MODELS

Bomb Model	HE Thickness (mfp)	Tamper Thickness (mfp)	Total Trans-mission	Ratio, Sulfur Neutrons / Fission Neutrons	Q, Sulfur Neutrons (neutrons/kt)
[redacted]					

* These are only fission neutrons and do not count D-T neutrons.
† See text for the meaning of the three different values give[redacted]
‡ On axis.
§ Through HE.
¶ Asymptotic.

where λ equals 182 meters in air at 0°C and 760 mm Hg. The source strengths Q for the various shots can be expressed in terms of neutrons detected per fission neutron liberated (see Table 3.1).[3] The third column of Table 3.1 is the transmission calculated by dividing the numbers in the second column by 0.21, the fraction of the fission spectrum which lies above 3 Mev. The fourth column is this same quantity, the transmission of the bomb assembly, expressed in terms of mean free paths.

[redacted]

If, for these two models, it is assumed that the thicknesses of the HE, measured in mean free paths, are identical and that the mean free paths corresponding to the transmission of the inner components are proportional to $\int \rho \, d\gamma$ evaluated over the tamper[redacted]

This is admittedly a crude method of estimating the transmission of the bomb materials, but it is about the best that can be done without an extremely involved neutron-diffusion calculation, i.e., an alpha calculation which includes all bomb materials, including the HE.

On this basis the numbers of sulfur neutrons to be expected for the various models to be tested can be estimated (see Table 3.2). The

values in column 5 can readily be converted to sulfur neutrons per kiloton. The result is that Q in Eq. 3.3 takes values in the last column of Table 3.2 for the various bomb models.

[redacted] materials is such that it is extremely difficult to make an estimate of the fast-neutron transmission. Nevertheless, such an estimate is attempted here, and it will, of course, be subject to considerable uncertainty [redacted]

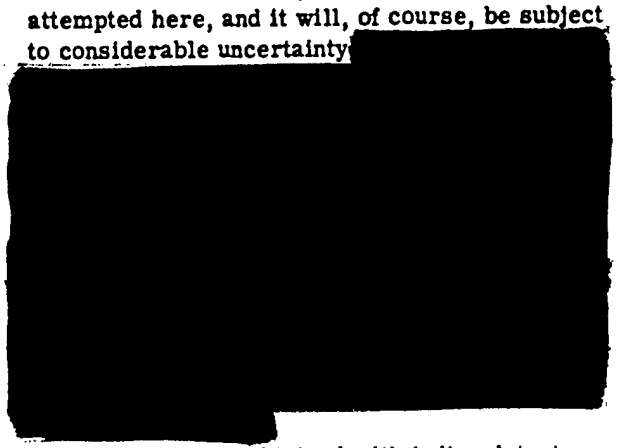

Some data were obtained with iodine detectors with and without lead shielding in order that the neutron activation could be separated from that due to the γ,n reaction. Unfortunately the lead shielding extended only halfway around the samples, i.e., the samples were unshielded toward the rear.

Because of the lead differences observed, it is clear that gamma rays in excess of 9.45 Mev were detected. One of the important sources of such hard gamma rays is now believed to be neutron capture by nitrogen in the air. Because such a gamma source is distributed throughout the air, it is not clear whether the shielded detectors were activated by neutrons or by gamma rays created in the air on the unshielded side of the detectors. It is probable that a mixture of these two sources is responsible for the iodine activities, and it may be possible to effect a separation, but the necessary calculations have not been completed at this time.

At present there is no firm knowledge of experimental nature concerning neutrons above the iodine threshold. It should be possible, however, to predict the ratio of iodine neutron to sulfur neutrons, with moderate confidence, on the basis of the fission spectrum as presented in Fig. 3.1. The predicted value is 5.7×10^{-3} iodine neutron per sulfur neutron. This estimate is only approximate but should not be incorrect by a factor exceeding 2 or 3.

3.2.2 Slow Neutrons

For reasons previously mentioned, the slow-neutron data are somewhat less reliable than are the sulfur data. The slow neutrons were measured by the activation produced in arsenic samples with and without cadmium shielding, and the cadmium difference was interpreted as slow neutrons. Thus, in the following discussion, slow neutrons are to be considered as those below cadmium cutoff and consequently are of energies lying between 0.2 and about 1 ev (nitrogen capture eliminates neutrons much below 0.2 ev).

When normalized to the same yield, the slow-neutron results for all three Sandstone shots lie on a single curve within a fairly large experimental error. These results, normalized to a yield of 1 kt, are plotted in Fig. 3.2.

In an attempt to discover the sources of the slow neutrons, several curves have been plotted in Fig. 3.2 in order to examine how well they fit the data. If the slow neutrons were mainly the result of neutrons which left the assembly with high energies and were subsequently slowed down in the surrounding air, they should be distributed with an approximately exponential absorption law, i.e., they should follow the fast-neutron law of Eq. 3.3. Accordingly, a curve is plotted, labeled A in Fig. 3.2, of the form $(1/R^2)\, e^{-R/\lambda}$, selecting $\lambda = 200$ meters as given by the sulfur neutron data. A second curve labeled B was calculated according to the diffusion theory and is of the form $(1/R^2)\, e^{-(3/2)(R/a)^2}$, with $a = 285$ meters. This would be the expected curve if all the slow neutrons left the bomb as epithermals of 300 to 500 ev energies. Curve C is the sum of curves A and B.

None of the theoretical curves fits the data very well, but, on the other hand, the data are not very precise. Both curves A and C of Fig. 3.2 are reasonable fits to the data if a point or two are ignored; the data are inadequate to decide between the two curves. For theoretical reasons it appears that curve C, which is based on slow neutrons diffusing from the bomb plus fast neutrons being slowed down, is the most likely to be approximately correct.

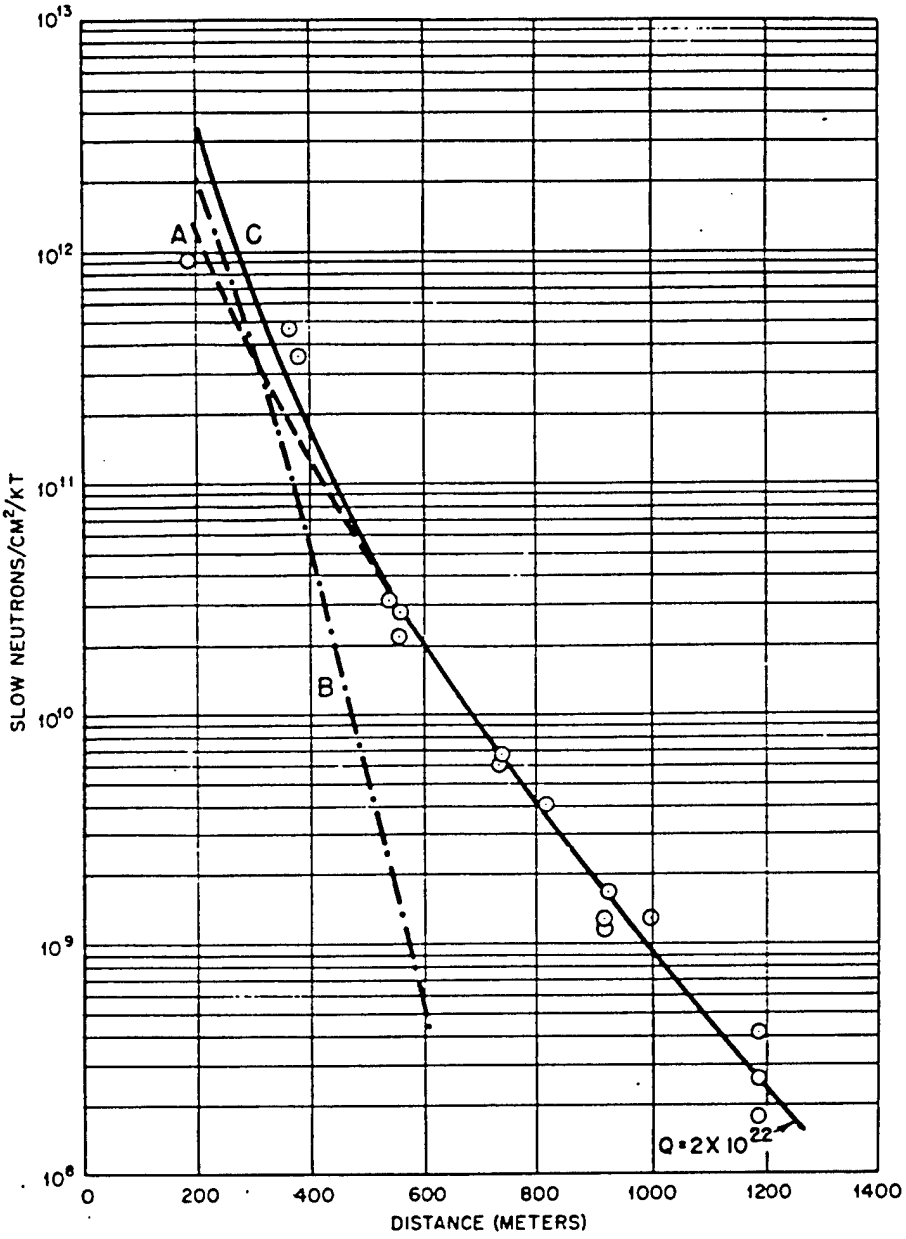

Fig. 3.2 Slow-neutron Results from Sandstone Measurements. O, Sandstone measurements. Curve A, $(1.41 \times 10^{7})/R^{2}\, e^{-R/200}$. Curve B, slow-neutron curve, according to the diffusion theory. Curve C, sum of curves A and B.

Slow neutrons were measured by means of gold samples for the five shots of the Ranger Program. Excellent results were achieved, principally because gold is such a good material; it has no spurious periods and it has a convenient half life. There has been insufficient time to include the Ranger results in this chapter, but two important conclusions from the experiments can be given:

1. It was noted on all five shots that the neutron-flux-vs-distance curves fit very well a curve of type C, Fig. 3.2, indicating a superposition of neutrons diffusing outward and fast neutrons becoming thermalized.

2. It was noted that the slow-neutron flux at a given distance does not scale with the yield but depends on the bomb model as would be expected if these neutrons were prompt.

Among the results of the Ranger experiments was a radiochemical determination of the ratio of neutron captures in the tamper to the total number of fissions; let this quantity be called ϵ. The gold neutron measurements indicate a neutron source whose strength is quite accurately proportional to the bomb yield multiplied by $\nu - 1 - \epsilon$, just as would be expected. Thus each fission produces ν neutrons, of which one is required to maintain the chain reaction and ϵ neutrons are captured, thus allowing $\nu - 1 - \epsilon$ neutrons per fission to escape.

3.3 NEUTRON EXPERIMENTS FOR GREENHOUSE SHOTS

It will be appreciated that the knowledge of the neutrons resulting from a nuclear explosion has some very large gaps. Knowledge of the energy distribution is quite poor, especially in the energy range between 3 Mev and cadmium cutoff. In fact, even the total number of neutrons as a function of distance is not known. The experiments planned for the Greenhouse shots are designed to fill in this gap to a considerable extent but will not give a complete picture of the neutrons.

[redacted] Because neutron detectors either are very sensitive to neutron energies or will respond strongly to gamma radiation, all the experiments which are designed to increase the knowledge of the neutrons released from a fission bomb are attempts to measure various portions of the neutron spectrum.

The following neutron experiments planned for the Greenhouse shots will be performed on all shots by Group J-3, LASL, under the direction of W. E. Ogle and L. Rosen:

1. Neutron spectrum will be measured by means of cameras utilizing nuclear-particle photographic plates. This experiment measures all neutrons above ½ Mev in energy. By placing cameras at several distances from the explosion, spectrum-vs-distance information will be obtained. The cameras used for the measurement of the neutron spectrum consist of a collimator to define a neutron beam, a hydrogenous foil which serves as a proton radiator, and a cavity in which are placed nuclear-particle plates which record proton tracks. From the known angle at which a proton leaves the radiator and from the length of its track, the energy of the neutron which ejected the proton can be deduced.

2. Neutron flux will be measured as a function of distance by threshold detectors. Sulfur, a very clean detector which has given excellent results in the past, will be used again. Other detectors have been intensively investigated since the Sandstone shots, and use of those listed in Table 3.3 has been decided upon. Both of the n,2n detectors will be placed in pairs, one with and the other without lead shielding, in order that the n,2n reactions may be separated from the γ,n reactions.

3. Slow neutrons, i.e., neutrons below cadmium cutoff in energy, will again be measured as a function of distance. Gold foil detectors will be used for this experiment.

4. An improved version of the cellophane catcher camera used at Trinity will be employed to obtain time-dependent neutron measurements. The principle of operation of this device is to expose a thin foil of fissionable material to the neutron flux. A strip of cellophane, which is drawn past this foil at a known rate, catches fission fragments from the foil. The activity thus deposited on the cellophane strip is then measured as a function of distance

TABLE 3.3 THRESHOLD NEUTRON DETECTORS

Detector	Reaction	Threshold (Mev)	Period	Other Periods
Au	n,γ	Thermal	2.69 days	None
S^{32}	n,p	3*	14.3 days	None
I^{27}	n,2n γ,n	9.45	13 days	25 min (n,γ)
Zr^{90}	n,2n γ,n	12.0	78 hr	62 hr (n,p) 17 hr (n,γ)

* Effective.

TABLE 3.4 FOILS FOR CELLOPHANE CATCHER CAMERA

Foil	Threshold	Reaction
U^{235}	Thermal	Fission
U^{238}	1 Mev	Fission

along the strip. The characteristics of the foils to be employed are given in Table 3.4. The U^{235} foils will be used with and without cadmium shielding.

It is seen that even the rather elaborate set of experiments planned for the Greenhouse shots will leave some gaps in the knowledge of the neutrons resulting from a fission bomb explosion, notably the gap between ½ Mev and 1 ev. However, the prospects are good for combining the results of these measurements with neutron-diffusion theory to obtain a reasonably credible picture of the complete neutron spectrum.

REFERENCES

1. Energy Spectrum of Neutrons from Fission Induced by Thermal Neutrons, Los Alamos Scientific Laboratory Report LA-718.
2. E. Jahnke and F. Emde, "Funktionentafeln," Dover Publications, Inc., New York, 1943.
3. Sandstone Report, Vol. 8, p. 52.

Chapter 4

Blast and Thermal Radiation

By E. J. Zadina

4.1 BLAST

4.1.1 Scaling Laws

(a) Scaling from One Explosion to Another in the Same Medium. Consider two separate and noninteracting explosions, not necessarily produced by the same type of explosive but occurring in the same medium under the same ambient conditions.

Let W_1 = energy released by first explosion
W_2 = energy released by second explosion
R_1 = distance from W_1 to point where the pressure P_1 is produced
t_1 = time after explosion W_1 at which the pressure P_1 exists at R_1
R_2 = distance from W_2 to point where the pressure P_2 is produced
t_2 = time after explosion W_2 at which the pressure P_2 exists at R_2

The two explosions are said to be similar if, at some particular pair of instants t_1 and t_2,

$$P_2(R_2,t_2) = P_1(R_1,t_1) \tag{4.1}$$

for all values of R_2 and R_1 that are connected by the relation

$$R_2 = \lambda R_1 \tag{4.2}$$

where λ is a constant. If similarity exists in this sense, then the hydrodynamic equations guarantee that

$$P_2'(R_2',t_2') = P_1'(R_1',t_1') \tag{4.3}$$

for all values of R' and t' that satisfy the relations

$$\begin{aligned} R_2 - R_2' &= \lambda(R_1 - R_1') \\ t_2 - t_2' &= \lambda(t_1 - t_1') \end{aligned} \tag{4.4}$$

Thus two similar explosions have pressure contours which are identical except for a constant scale factor in distance and time. The Hugoniot conditions, together with the equation of state, guarantee that the same scaling law applies to all other hydrodynamic variables. It turns out that the scale factor λ is given by

$$\lambda = \left(\frac{W_2}{W_1}\right)^{1/3} \tag{4.5}$$

Substituting the value of λ from Eq. 4.5 into Eqs. 4.4 and taking $R_1' = R_2' = 0$ and $t_1' = t_2' = 0$, the very important blast scaling laws for scaling from one similar explosion to another are obtained:

$$\begin{aligned} \frac{R_2}{R_1} &= \left(\frac{W_2}{W_1}\right)^{1/3}_{P = P_1} \\ \frac{t_2}{t_1} &= \left(\frac{W_2}{W_1}\right)^{1/3}_{P = P_1} \end{aligned} \tag{4.6}$$

(The subscripts in the equations, $P = P_1$, emphasize the fact that the same pressure, P_1, is being considered for both explosions.) These equations state that, if a specified peak overpressure P_1 occurs for one explosion at a certain distance and time, then that same peak overpressure P_1 will exist for a second similar explosion at a distance and time which are directly proportional to the cube root of the ratio of the energy releases. For example, if an overpressure of 40 psi exists at a time of 1 msec and at a distance of 20 ft from a given explosion,

then, if the energy release is increased 27-fold, a 40-psi overpressure will be found at 3 msec and 60 ft. Durations also scale according to Eqs. 4.6. For example, if the positive phase at a given peak overpressure has a duration of 0.5 sec for one explosion, it will have a duration of 1.5 sec at the same peak overpressure if the energy release is increased 27-fold.

These scaling laws give no information on how blast-wave characteristics change at a given distance as the energy release is varied. They can be applied only when a particular overpressure has been specified for one explosion and when it is desired to know the corresponding locations, times, and durations for that same overpressure for a second similar explosion of different energy release.

To facilitate the application of scaling laws, $(W_2/W_1)^{1/3}$ vs (W_2/W_1) is plotted in Fig. 4.1.

(b) Scaling of an Explosion to an Identical Medium with Different Ambient Conditions. The details of theory can be found elsewhere;[1] only the final formulas are given here.

The object of this section is to determine the free-air-pressure–distance curve, $P_h(R)$, for a given energy release in air at an arbitrary altitude h when the pressure-distance curve is known for a similar explosion at sea level. The similar explosion at sea level is defined by Eq. 4.7. It is intuitively obvious that a larger bomb will be required to produce a given pressure at a specified distance in air of low density than will be necessary to produce the same pressure at the specified distance at sea level.

Let W_h = energy release of bomb to be detonated at altitude h
P_0 = ambient pressure (atm) at altitude h
W_S = energy release at sea level which is similar to W_h at altitude h
$P_S(R)$ = pressure-vs-distance curve of W_S
$P_h(R)$ = pressure-vs-distance curve of W_h at altitude h

Then it can be proved that

$$W_S = \frac{W_h}{P_0} \tag{4.7}$$

and

$$P_h(R) = P_0\, P_S(R) \tag{4.8}$$

In general, the low overpressures will be most affected by this transformation.

Suppose it is desired to find the pressure-distance curve for a 50-kt bomb when detonated at an altitude of 6 km, where the ambient pressure is approximately one-half that at sea level. Then W_h is 50 kt, P_0 is 0.5 atm, and W_S is 50/0.5 or 100 kt. The pressure-distance curve $P_S(R)$ for 100 kt at sea level is found, and the pressure at each distance is multiplied by a P_0 of 0.5 to obtain the pressure-distance curve for 50 kt detonated at 6 km.

It should be pointed out that the derivation of Eqs. 4.7 and 4.8 assumes that the atmosphere is infinite and homogeneous, a condition which will obviously not obtain for large bombs. The magnitude of the error introduced by violation of this assumption has not been estimated.

4.1.2 Determination of Yield from Ball-of-fire Photography

The only aspect of blast which has thus far proved useful for the quantitative calculation of nuclear explosion yields is the observation by fast photography of the ball of fire up to about the time of breakaway. Such photography yields shock radius vs time. Two methods of treating these data exist and are discussed in the following sections.

(a) Yield from Simple Scaling Laws. It has been shown in Sec. 4.1.1a that, for two similar explosions, assuming a given P,

$$\frac{R_2}{R_1} = \left(\frac{W_2}{W_1}\right)^{1/3}$$

$$\frac{t_2}{t_1} = \left(\frac{W_2}{W_1}\right)^{1/3}$$

Equating and assuming a given P,

$$\frac{t_2}{t_1} = \frac{R_2}{R_1} \tag{4.9}$$

or

$$\frac{t_2}{R_2} = \frac{t_1}{R_1} \tag{4.10}$$

is obtained. Equation 4.10 shows that the pressures from two similar explosions are equal when t_2/R_2 is equal to t_1/R_1. Yields may thus be calculated from Eq. 4.6 by selecting fireball radii for which $t_2/R_2 = t_1/R_1$. Then

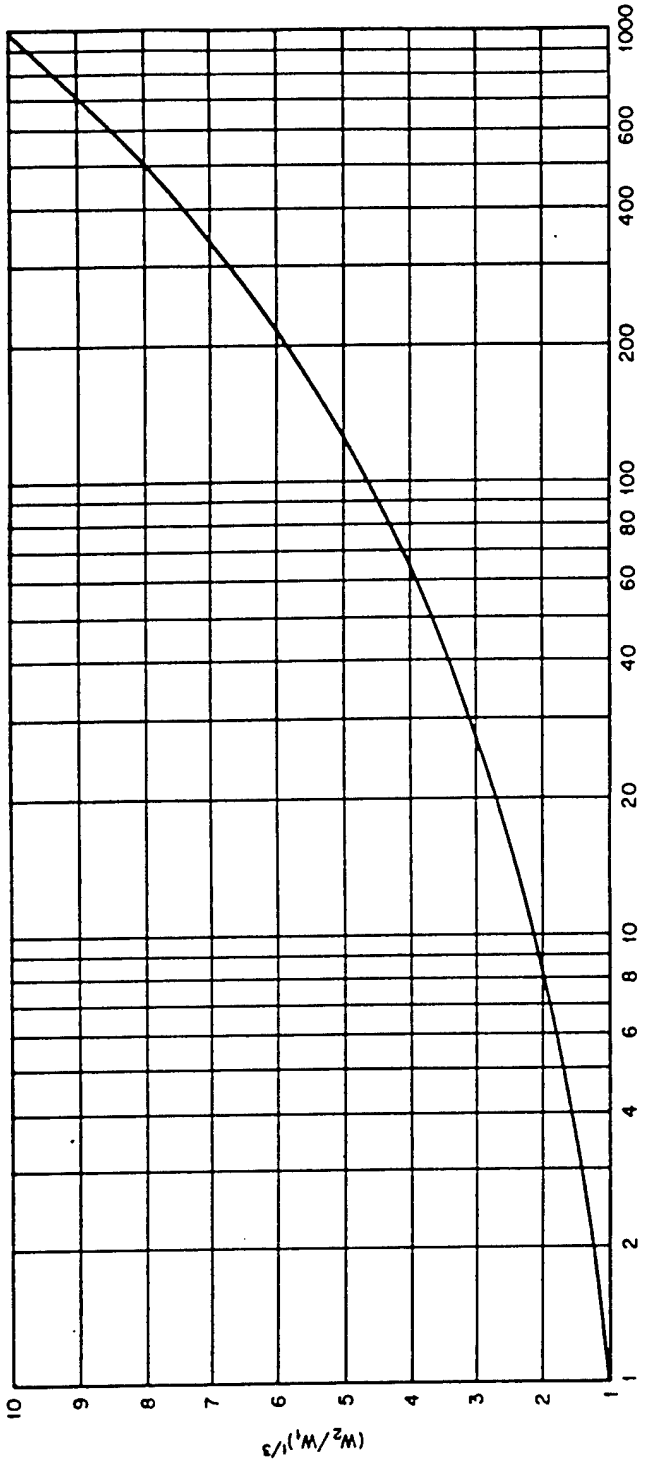

Fig. 4.1 Graph of $(W_2/W_1)^{1/3}$ vs (W_2/W_1)

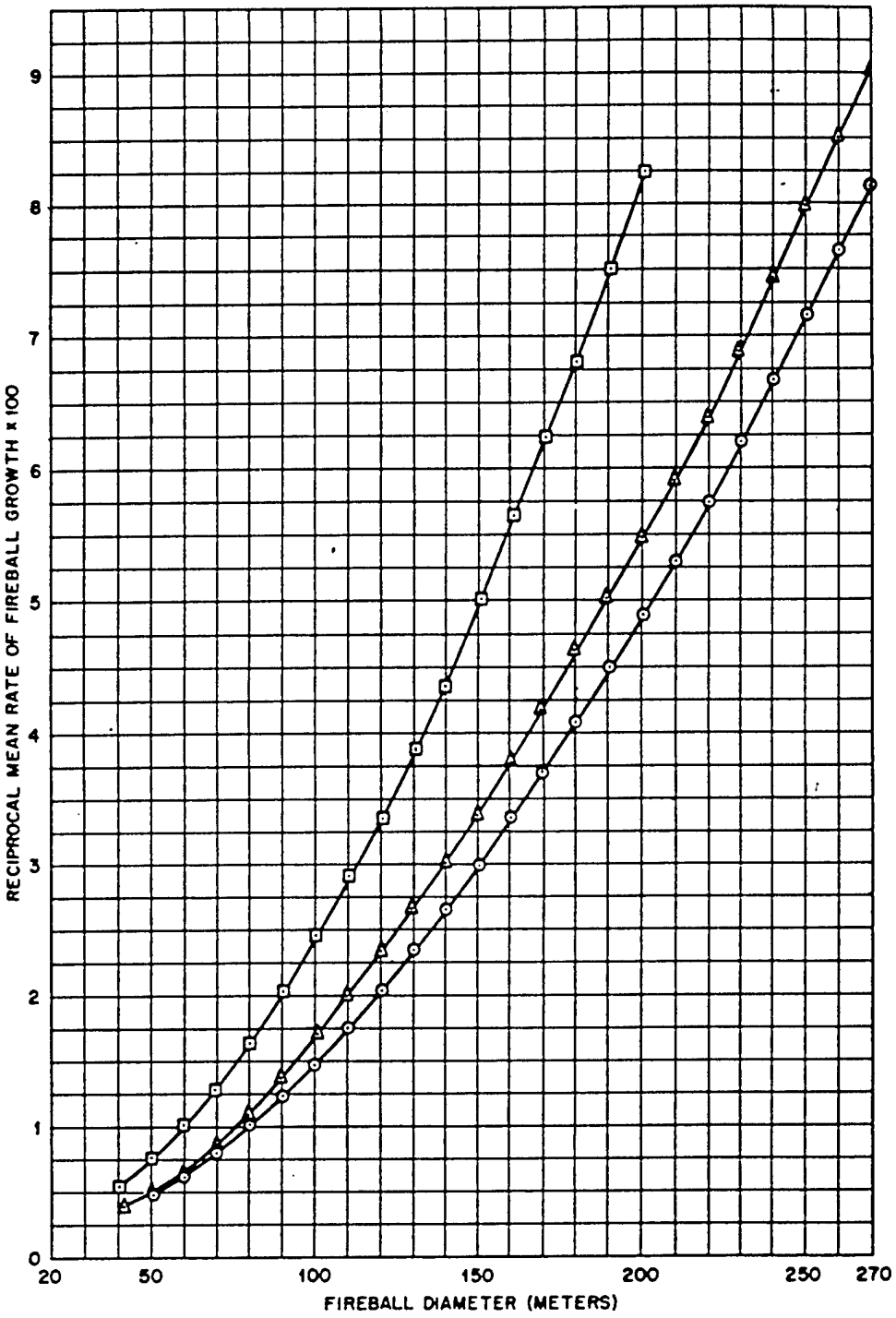

Fig. 4.2 Reciprocal Mean Rate of Fireball Growth vs Diameter, Sandstone Shots. □, Zebra shot. △, X-ray shot. ○, Yoke shot.

$$\frac{W_2}{W_1} = \left(\frac{R_2}{R_1}\right)^3_{t_2/R_2 = t_1/R_1} \qquad (4.11)$$

Figure 4.2 is a graph of t/D vs D (diameter) for the Sandstone shots. Of course D can be used as a variable rather than R and is, in fact, customarily used since the diameter rather than the radius is actually measured.

In order for this simple scaling procedure to be valid, the bombs must be exploded in identical atmospheres.

(b) Porzel's Method. A more general approach to fireball analysis has been given by F. B. Porzel. This approach can be shown to contain, after simplifying assumptions have been made, both the method described in the preceding section and the approximate $R \propto t^{2/5}$ law previously used for photographic determinations of yield. The following discussion is from Porzel.

A theory of rate of growth of the fireball has been formulated[2] by integration of the equations of motion, using the model of an early radiative phase and a theory of strong shocks. The resultant curve cannot be stated in analytic form. When plotted as log R vs log t, it displays a variable slope, the average value of which is 0.377 over the usual range of measurement, in good agreement with the observed slope of 0.374 ± 0.005 from Sandstone.

The theory shows that no method of scaling is valid unless comparisons are made at points where the hydrodynamic variables are equal and an appropriate method of scaling follows. The shock velocity U is readily available from the R-t graph. This value of U is determined mechanically from a log R–log t graph by observing that, in any small region, the curve can be approximated with arbitrary accuracy by $R = ct^n$. Differentiating,

$$U = \frac{dR}{dt} = \frac{nR}{t}$$

is obtained, where n is the local value of the slope. The real invariant between different bombs is U/C_0 rather than U itself, C_0 being the ambient sound velocity. The equation

$$\frac{U}{C_0} = \frac{n}{C_0}\frac{R}{t} \qquad (4.12)$$

is plotted in Fig. 4.3 as a function of R, on a log-log basis. A similar procedure is followed for a bomb of known yield; the displacement between the curves is log $(W_2/W_1)^{1/3}$.

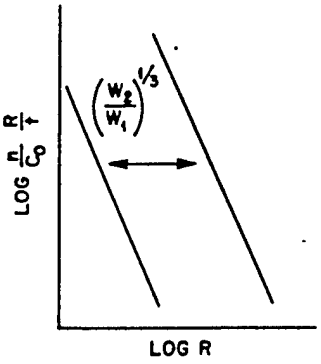

Fig. 4.3 A Method of Scaling from Fireball Measurements

This procedure has the advantage that constant errors in radius or time are eliminated because, if such errors are present, they do not affect dR/dt; the log R–log t slope will be distorted exactly to compensate for a constant error in R or t. Proportional errors will be included in the scaling factor. If the log R–log t graph has been approximated by a straight line in both cases, these small errors in slope are somewhat compensated. A failure to achieve a constant value of $(W_2/W_1)^{1/3}$ will indicate a failure of scaling, quite likely due to bomb mass effects during early stages of fireball growth, even prior to the time of actual measurement.

If the values of n and C_0 are observed to be the same for two explosions, this procedure may be simplified to plot D/t as a function of D. At equal values of D/t, the yields will be proportional to the cubes of the radii as shown in Sec. 4.1.2a.

The graph has the additional advantage that, from U/C_0, the pressure ratio P/P_0 is readily deduced by using strong shock theory with variable γ. By this simple transformation of the ordinates, the peak-pressure-vs-distance curve is obtained in a region where the shock velocity calculation is most accurate and physical measurement is difficult.

[redacted]

4.1.3 Blast Characteristics of a Nuclear Explosion

The development of the blast wave has been treated adequately elsewhere,[3-5] and hence this section will be confined to the present state of knowledge regarding blast waves produced by nuclear explosions.

The most significant blast-wave characteristic for atomic bombs is the peak-pressure-vs-distance curve. This curve will have different characteristics according to whether the pressure is measured on a reflecting surface or in the absence of such a surface.

(a) Free-air-pressure–Distance Curve. The importance of a free-air-pressure–distance curve lies in two facts:

1. It provides the data to be used in height-of-burst tables for the calculation of pressure distributions over the ground resulting from air bursts.

2. Its theoretical calculation is feasible, and a comparison between such a calculation and an experimental determination of the free-air curve would indicate the correctness or lack of correctness of current ideas as to the influence of initial conditions, radiation transport, etc., on the propagation of the blast wave.

Unfortunately, no satisfactory free-air-pressure–distance curve, either theoretical or experimental, exists for atomic bombs. IBM Problem M was an attempt at theoretical calculation but is not entirely satisfactory because of errors in numerical calculation and the neglect of possibly important physical processes. No attempt has been made in previous tests of nuclear weapons to obtain an experimental free-air-pressure–distance curve.

In view of this situation, it is necessary to rely on Bikini-Able, which is the best approximation to a free-air burst for which blast measurements are available. This bomb was detonated at a height of 520 ft, and pressure measurements were carried out on the water surface. To obtain a free-air-pressure curve from Bikini-Able blast data, the measured pressures must be corrected for increase due to reflection. Because of the absence of small-charge reflection data at reflected pressures greater than about 20 psi, it was impossible to correct the Bikini-Able curve at reflected pressures higher than this value. It appears, as a result of such corrections as were possible, that the free-air-pressure–distance curve for atomic bombs in the 2- to 20-psi region is about the same as that for three-fourths the same tonnage of pentolite. If it is desired to estimate the curve at higher pressures, the most that can be done is to extrapolate on the basis of the pentolite curves, obtained by Bleakney and Stoner,[6] which extend to about the 50-psi region. A further extrapolation to higher pressures has been made by attaching to the pentolite data a theoretical curve, obtained by Kirkwood,[7] which predicts the correct shape of the pressure-distance curve characteristic for HE. The resulting tentative free-air-pressure–distance curve for atomic bombs (based on the work of Bleakney, Stoner, and Kirkwood and on the assumption that the pressure-distance curve is equivalent to that for three-fourths the same tonnage of pentolite) is given for several yields in Fig. 4.4.

It cannot be emphasized too strongly that the curves of Fig. 4.4 must be used with extreme caution for the following reasons: The accuracy of the experimentally determined Bikini-Able pressure-distance curve and the accuracy of reflection data used for correcting to free air the Bikini-Able measurements in the 2- to 20-psi region leave much to be desired. Also, there is little reason to suppose that the pressure-distance curve from atomic bombs should have the same shape as a curve for pentolite since the blast phenomena in the two cases may never be similar. An atomic bomb is obviously much more nearly a point source than is HE. The total consequence of this fact is that, compared with HE explosions releasing the same energy, the pressure-distance curves for atomic bombs should display greater pressures at near distances and lower pressures at far distances.

(b) Pressure-Distance Curve from Bomb on Tower. Experimental pressure-distance data from bombs burst on towers are unsatisfactory because (1) there is considerable scatter in the data and (2) the curves have anomalies in shape which, if assumed genuine, might indicate jets, both perpendicular to and down the blast lines. There exist no overhead photographs taken at such times as to settle this question of asymmetries.

In view of this situation and because of the lack of both a free-air curve and fundamental reflection data, the most that can be done is the application of scaling laws to the best tower data

[redacted]

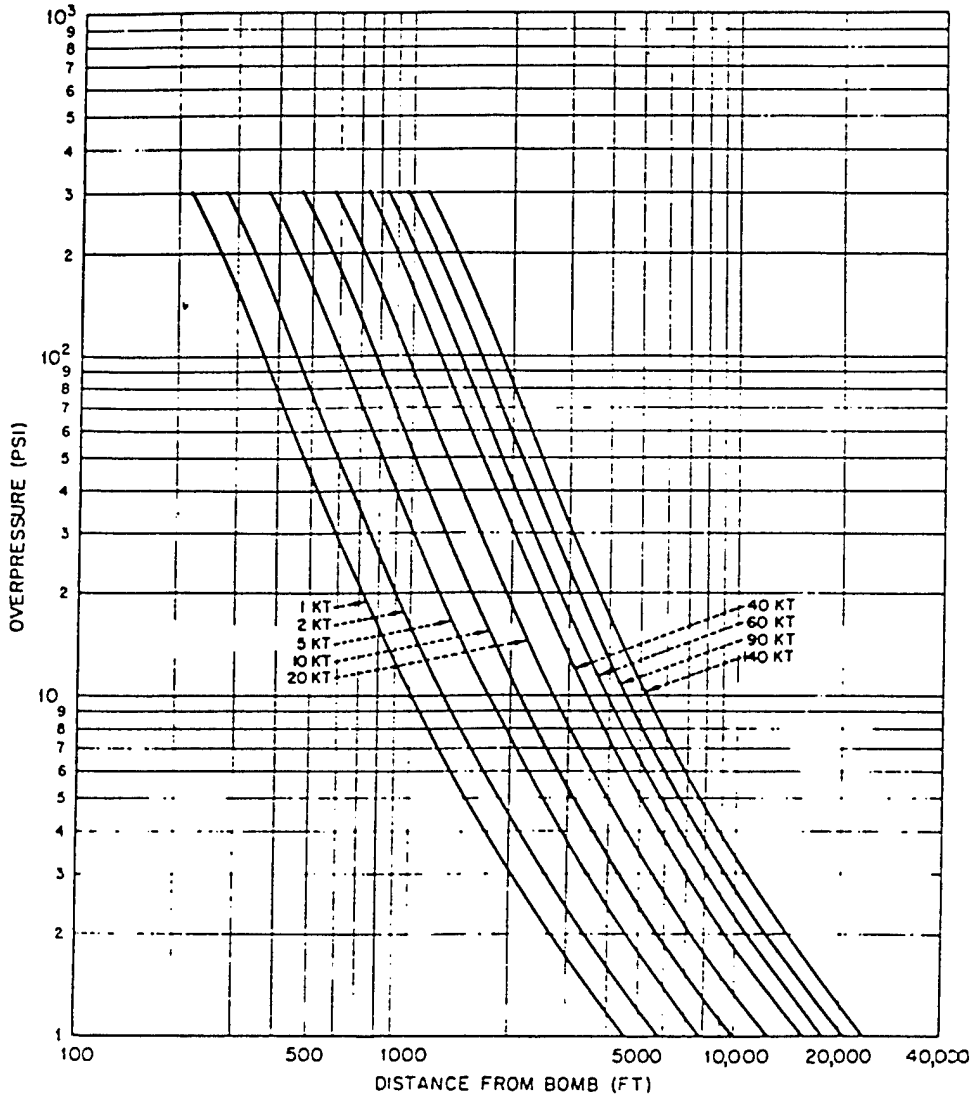

Fig. 4.4 Free-air-pressure–Distance Curves for Atomic Bombs. Derived from Bleakney-Stoner-Kirkwood curve[6,7] for TNT and based on the assumption that the pressure-distance curve for an atomic bomb is the same as that for three-fourths the same tonnage of pentolite (1 lb of pentolite equals 1.18 lb of TNT).

so far obtained. This has been done in Fig. 4.5. To obtain the curve for a tonnage W_2, in terms of the known curve for W_1, multiply the distance at which each pressure occurs for W_1 by $(W_2/W_1)^{1/3}$.

(c) Length of Positive Phase. The forward end of the spatial profile of the blast wave will propagate faster since at any instant it contains higher pressures than those regions closer to the explosion. Consequently the length of the positive phase should increase.

Figure 4.6 is a graph, scaled from HE, of the duration of the positive phase at large distances vs distance from the explosion. Duration for other energy releases may be obtained by scaling according to the cube root of the tonnage. When calculating positive phase durations for tower shots, it must be remembered that the blast wave appears as one from a bomb greater in energy release by a factor of 1.5 to 2.0, the precise value being uncertain.

In the region where most of the blast measurements will be made, the negative phase can be expected to have a duration greater than the positive by a factor of between 2 and 5.

(d) Reflected Blast-wave Variables Under 300-ft Tower for 50 Kt (F. B. Porzel). The values of pressure, density, and material velocity and their time variation in the region of regular reflection beneath the tower have been calculated[8] for a 50-kt bomb detonated on a 300-ft tower. Using a theory of strong shocks with variable γ, all pertinent hydrodynamic variables in the incident wave at the ground were calculated from Sandstone fireball measurements. The necessary equations of state were based on several sources.[9-11] The corresponding peak values in the reflected wave were then calculated, using regular reflection theory modified to include the variation in γ. These data furnished the boundary conditions at the front of the reflected wave for regions close to the ground. From these conditions the mass flow behind the reflected shock was derived, the procedure being similar to the IBM run but using more rapid graphical and computational techniques.

Density, material velocity, and pressure were necessarily carried forward during the integration, and temperatures were deduced, using equations of state for high pressures.

Figures 4.7 to 4.10 give for various distances from ground zero the results of this calculation for the time variation of pressure, density, material velocity, and temperature, respectively. Peak values vs time or distance and shock arrival times are included. The early wave form is markedly different from that of a free-air burst, mostly because of the large entropy changes involved.

These curves were prepared and should be regarded primarily as an exercise in strong shock hydrodynamics but probably constitute a reasonable estimate for 50 kt on a 300-ft tower. In general, the results cannot be scaled to different tonnages or different tower heights, except for rough orders of magnitude.

(e) Calculation of Ground Pressures from Air-burst Bombs. The pressure of a reflected shock depends on both the pressure of the incident shock and its angle of incidence. Figures 4.11 and 4.12, adapted from reference 12 and extrapolated for reflected pressures greater than 20 psi, constitute a summary of the available information obtained from experiments with small charges. To obtain the pressure distribution on the ground from air-burst bombs, proceed as follows:

1. Draw a free-air-pressure–distance curve for the given tonnage by scaling from Fig. 4.4.
2. For the given height of burst, compute, for the values of cos θ listed in Figs. 4.11 and 4.12, the radial distances from the bomb to the ground and the corresponding distances from ground zero.
3. Knowing the radial distance for each cos θ, find the corresponding incident pressure P_f from the curve of step 1.
4. From Figs. 4.11 and 4.12, read the value of the reflected pressure P_r, corresponding to each value of P_f at its particular value of cos θ.
5. Plot the reflected pressures obtained from step 4 against the corresponding distance from ground zero.

This procedure has been carried out in Figs. 4.13 and 4.14 for yields of 60 and 100 kt [redacted] The heights of burst in these figures are of tactical interest.

The following limitations on the accuracy of the procedure must be emphasized:

1. The free-air-pressure–distance curve is uncertain.
2. The reflected pressure curves were extrapolated for reflected pressures greater than 20 psi.

(Text continues on page 41.)

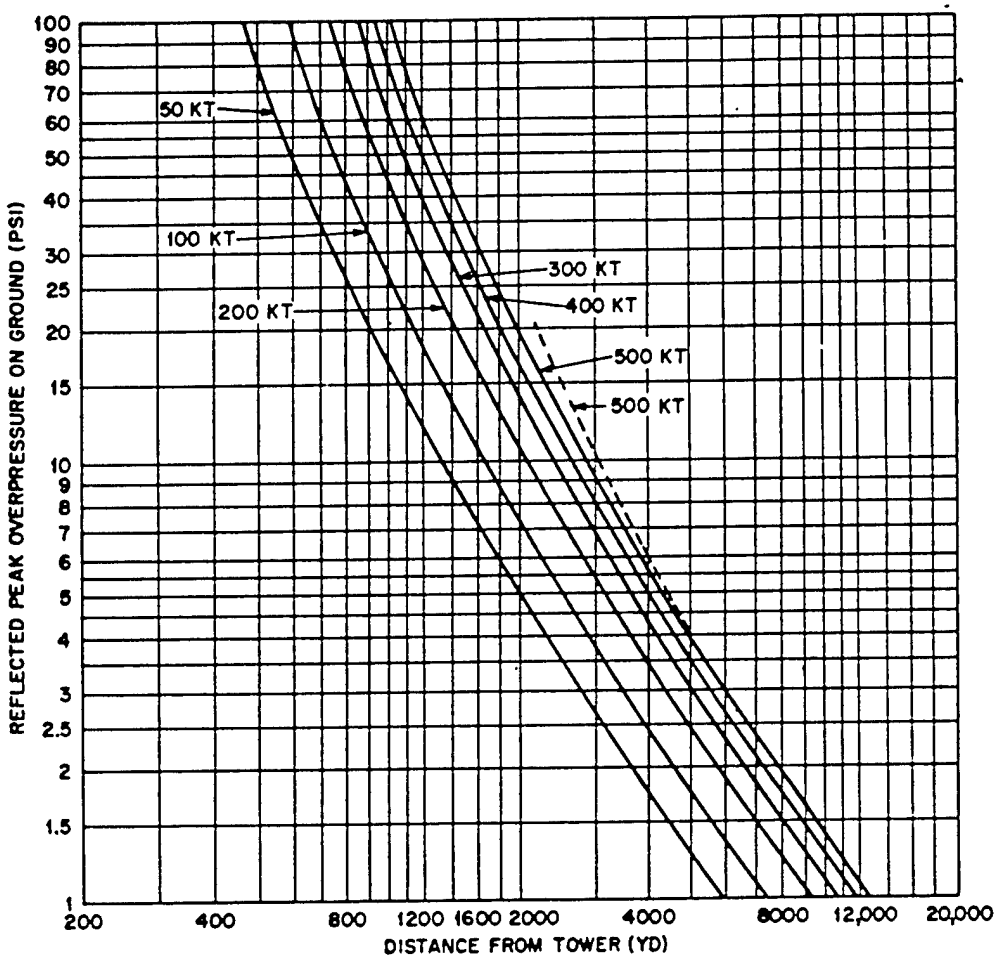

Fig. 4.5 Reflected Pressure vs Distance, 50 to 500 Kt from 200- to 300-ft Towers. ——, scaled from Operation Sandstone and Crossroads after Lampson. -----, from Report LA-743R, 500 kt. Actual pressures for larger bombs will be somewhat lower because the energy loss to ground increases rapidly for low heights of burst. The solid-line curve for 500 kt allows for this loss for approximately 400-ft height; the dashed curve considers loss for a high height of burst greater than 1600 ft.

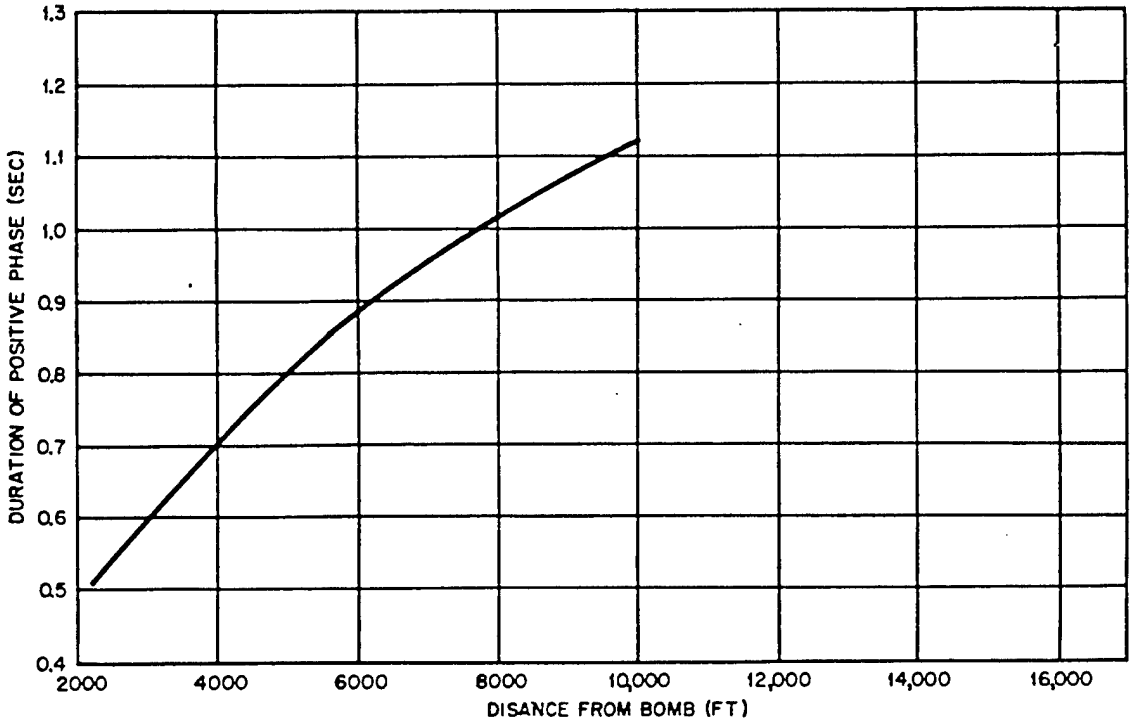

Fig. 4.6 Duration of Positive Phase vs Distance from a 20-kt Bomb Exploded in Free Air. Durations for other yields may be obtained by scaling according to the law $t_2/t_1 = (W_2/W_1)^{1/3}$, constant pressure.

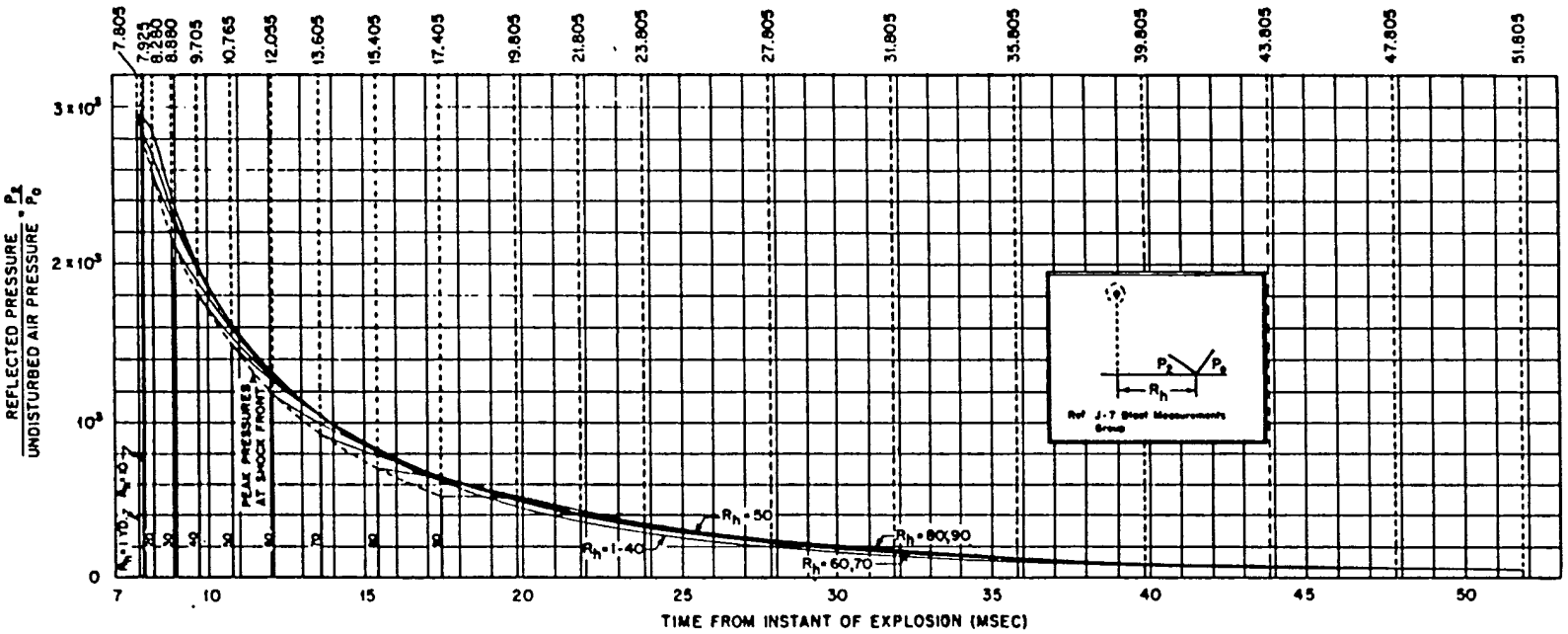

Fig. 4.7 Reflected Pressure on the Ground vs Time for 50 Kt, 300-ft Height of Burst, at Several Horizontal Distances R_h

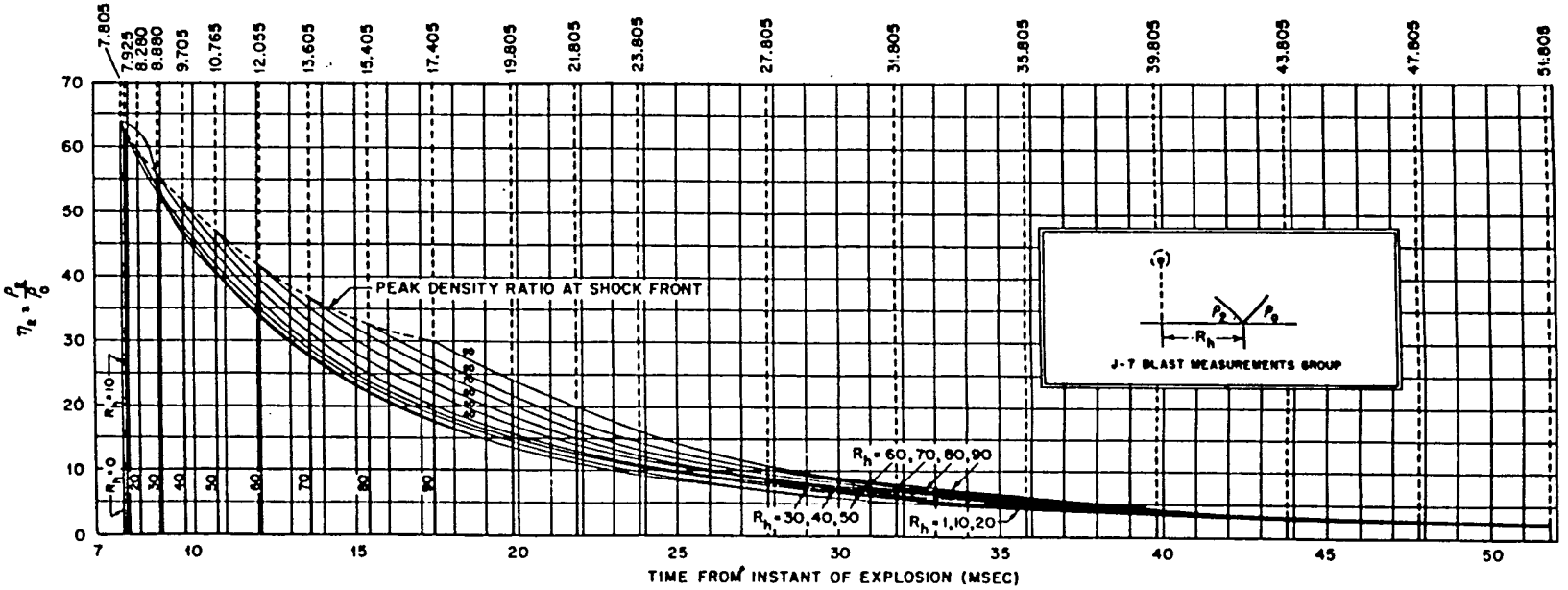

Fig. 4.8 Ratio of Air Density in Reflected Region on the Ground to Density of Undisturbed Air vs Time for 50 Kt, 300-ft Height of Burst, at Several Horizontal Distances R_h

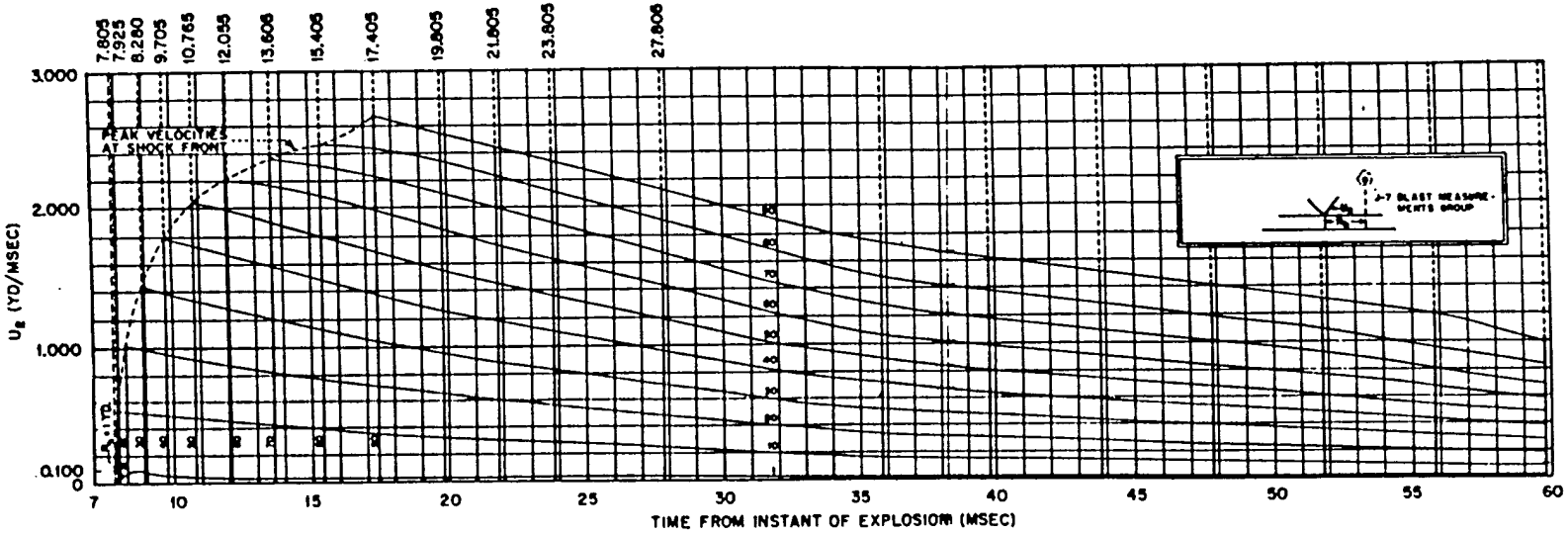

Fig. 4.9 Material Velocity U_s in Reflected Region on the Ground vs Time for 50 Kt, 300-ft Height of Burst, at Several Horizontal Distances R_g

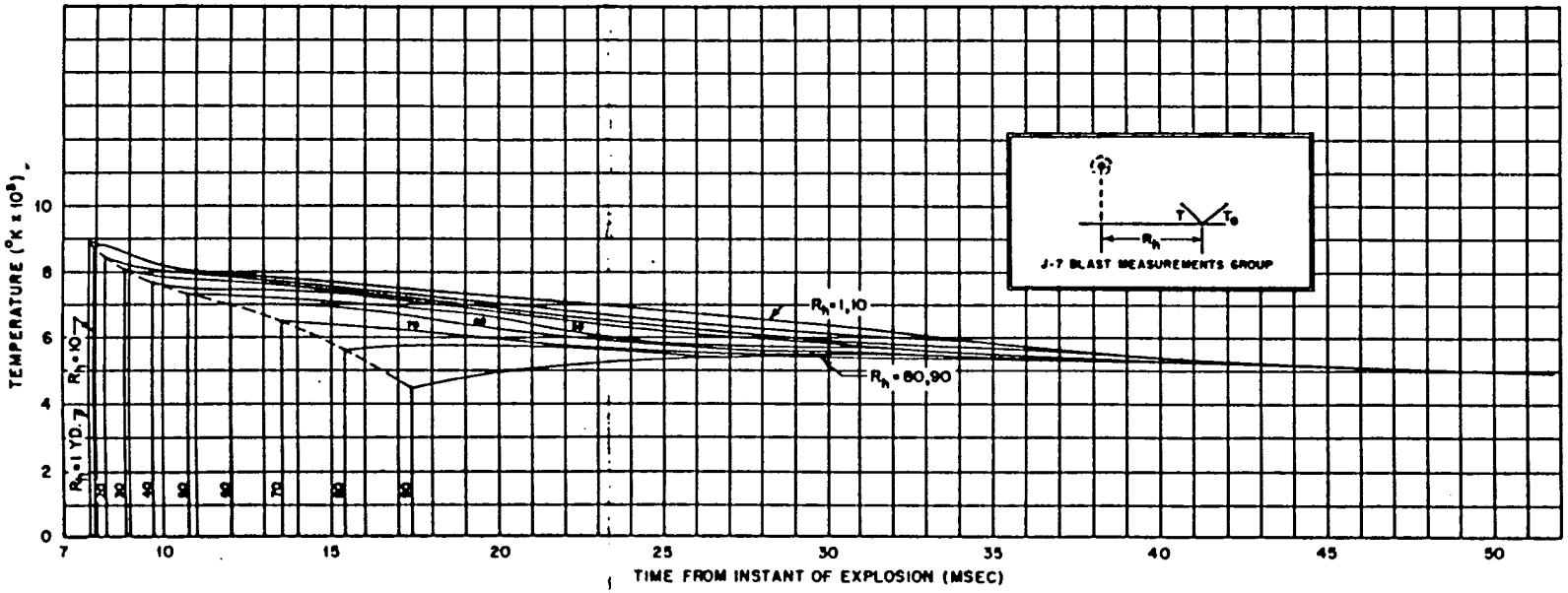

Fig. 4.10 Temperature on the Ground vs Time for 50 Kt, 300-ft Height of Burst, at Several Horizontal Distances R_h

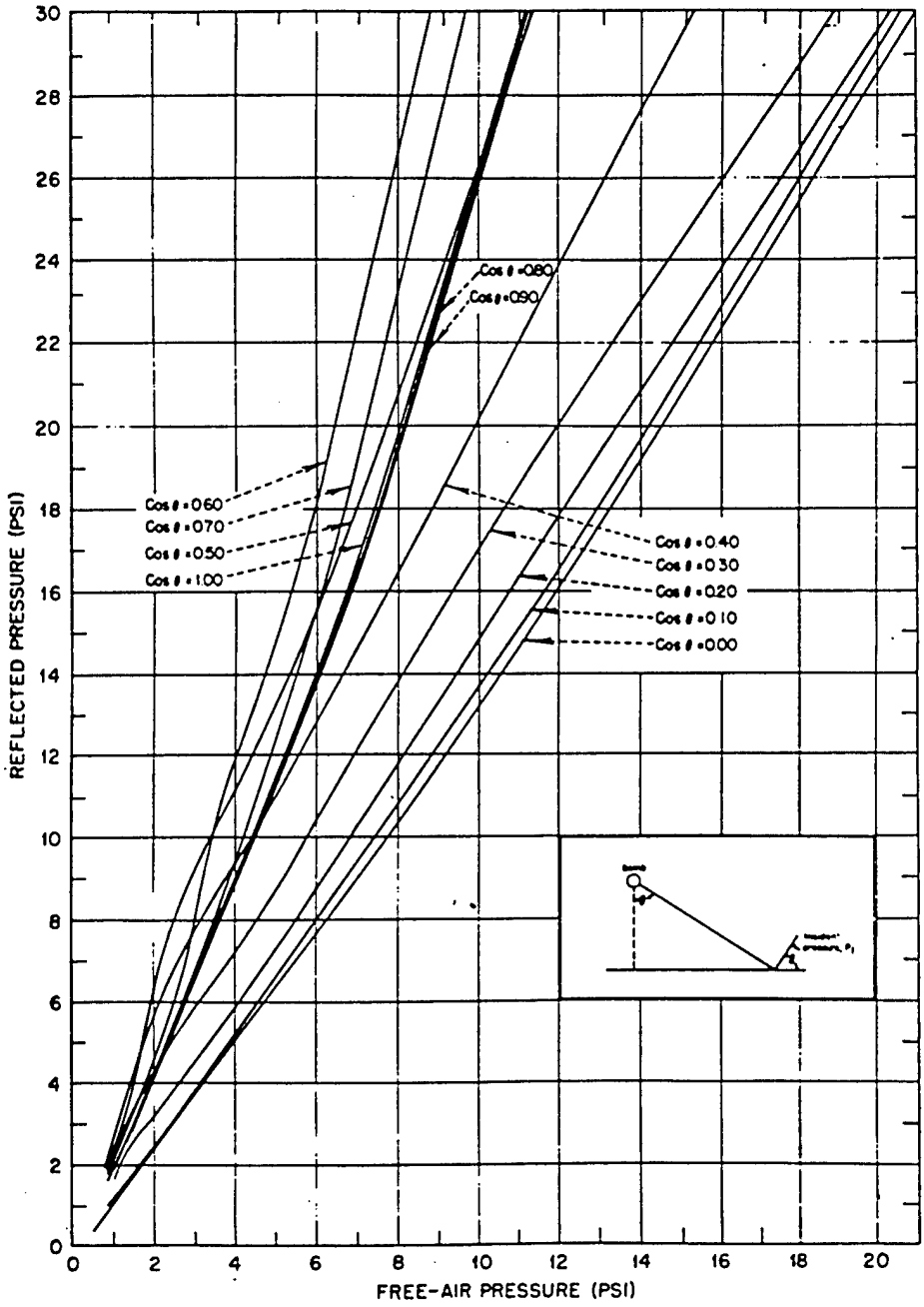

Fig. 4.11 Reflected Pressure P_r vs Free-air Pressure P_f at Cos θ = Constant. Based on Fig. 6 of Report LA-743R. Values greater than 20 psi for P_r were obtained by linear extrapolation.

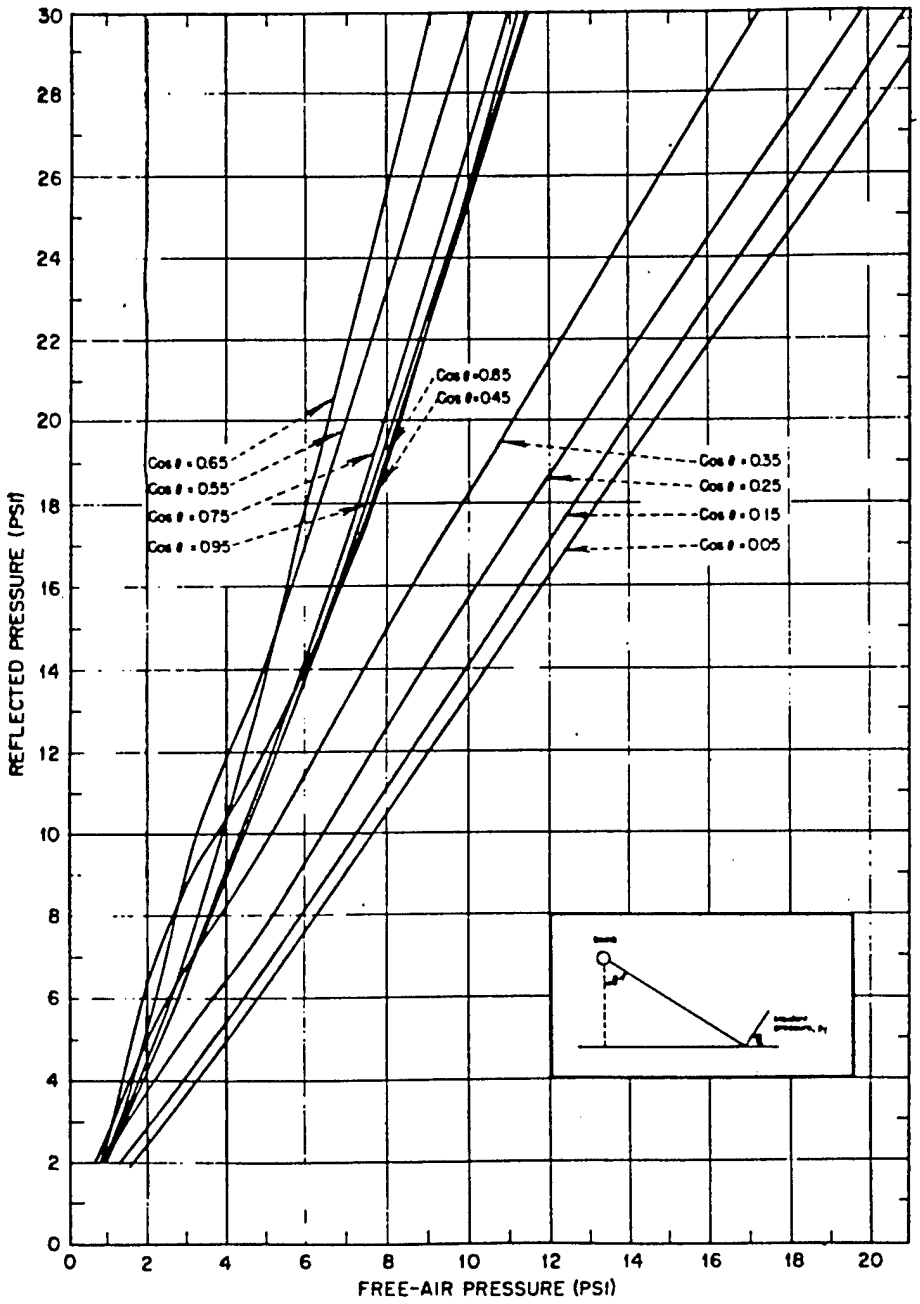

Fig. 4.12 Reflected Pressure P_r vs Free-air Pressure P_f at Cos θ = Constant. Based on Fig. 6 of Report LA-743R. Values greater than 20 psi for P_r were obtained by linear extrapolation.

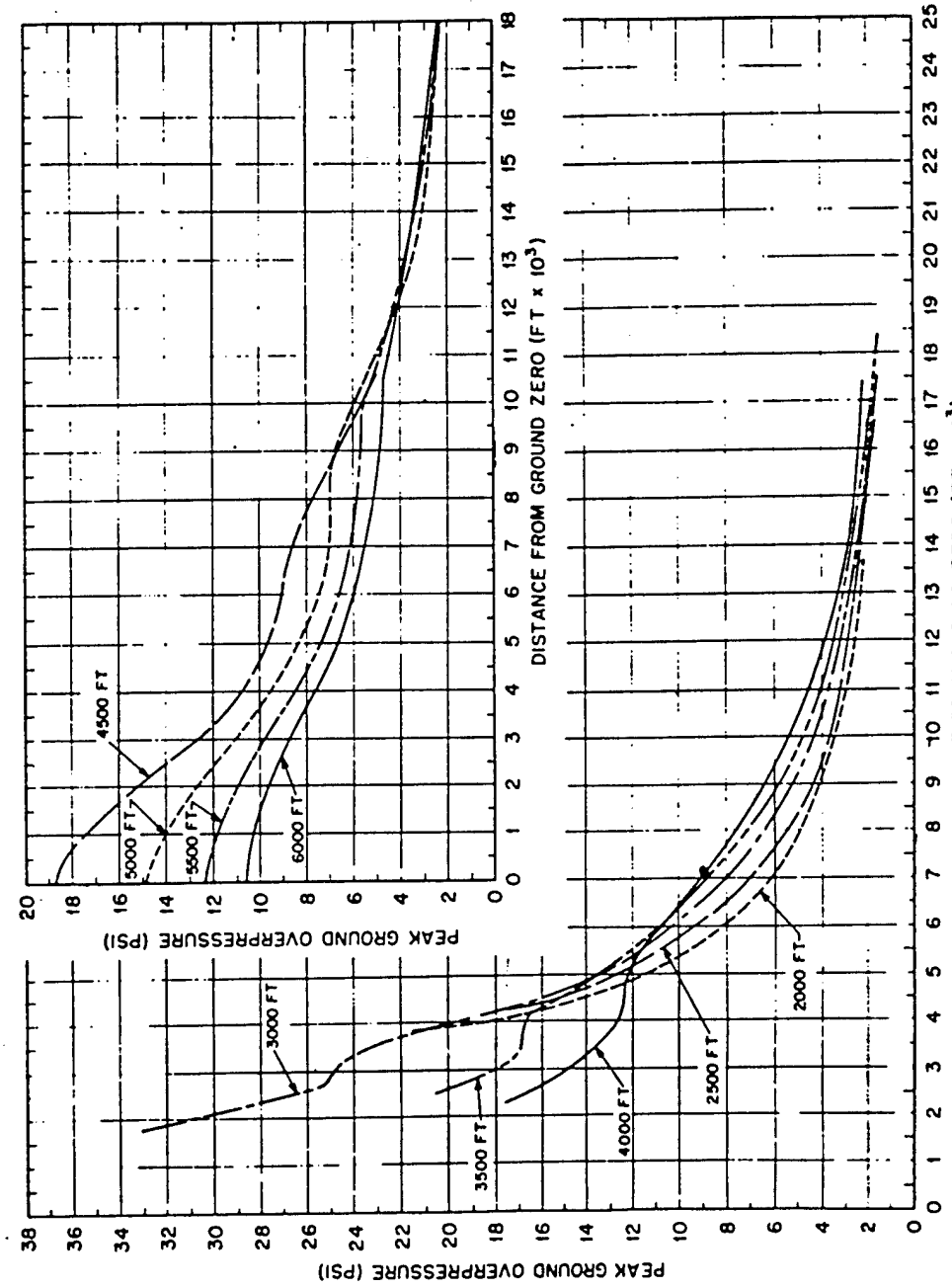

Fig. 4.13 Reflected Ground Overpressure vs Distance from Ground Zero [redacted] (60 Kt) for Various Heights of Burst. Based on Report LA-743R.

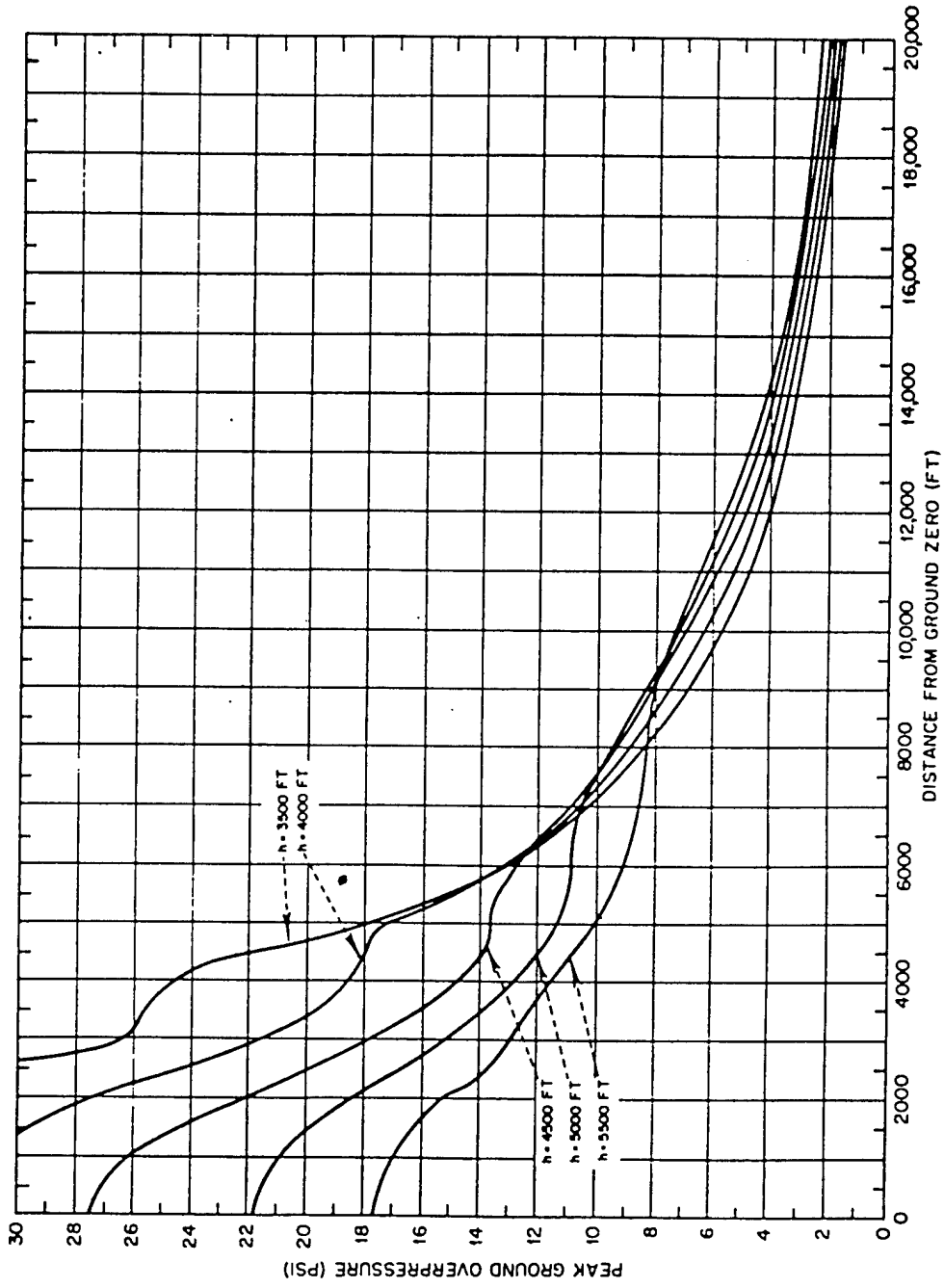

Fig. 4.14 Reflected Ground Overpressure vs Distance from Ground Zero [redacted] (100 Kt) for Various Heights of Burst. Based on Report LA-743R.

[redacted]

3. The reflection data were obtained during the war and their accuracy is uncertain. The genuineness of all the wiggles in the P_r-vs-P_f curves cannot be vouched for.

(f) Maximization of Overpressure Areas Produced by Air-burst Bombs.[12] It is possible, as a consequence of the curves in Figs. 4.11 and 4.12, to maximize for an air-burst bomb of given energy release the area over which a specified overpressure is exerted. The area maximization is accomplished by suitable choice of the height of burst.

In Fig. 4.15 are plotted, for several tonnages, the heights of burst required to maximize ground overpressure areas up to 20 psi. These curves assume a homogeneous atmosphere of sea-level density and pressure and have inherent in them the same uncertainties as P_r-vs-P_f curves.

To obtain curves for other tonnages, multiply at each pressure the heights of burst given in Fig. 4.15 by the cube root of the tonnage ratios.

(g) Triple-point Trajectories (F. B. Porzel). Triple-point trajectories may be estimated by combining data for (1) low heights of burst (photographic measurements of Trinity, X-ray, and Yoke shots[13]) and (2) high heights of burst (small-charge data[12]). The small-charge data are extrapolated downward and made to agree with photographic observations for low heights of burst.

From this procedure result the curves of Fig. 4.16, which give, for various Mach stem heights, the height of burst vs horizontal distance from ground zero. The curves are drawn for 1 kt. To obtain corresponding curves for another tonnage, W_2, multiply all distances, including Mach stem heights, by $(W_2)^{1/3}$. Figure 4.17 is a graph of the triple-point trajectories expected from [redacted] weapons detonated on 300-ft towers.

Because of the uncertainties in the fundamental data, both sets of curves should be used with caution.

(h) Peak Values of Pertinent Blast-wave Parameters. Figure 4.18 is a graph of peak overpressure vs the peak magnitude of the more important hydrodynamic variables immediately behind the shock front. The curves were computed from the Rankine-Hugoniot equations using $\gamma = 1.4$. They should be quite accurate up to overpressures of 150 psi; above that pressure they are indicative but not accurate because γ begins to vary. If accurate values of the variables above 150 psi are required, more elaborate works should be consulted.[9]

4.1.4 Summary of Gaps in Current Knowledge of Nuclear Blast Waves

Gaps in current knowledge relative to the blast waves produced by nuclear explosions fall into two categories: uncertainties in the free-air region and uncertainties in the reflected regions.

(a) Uncertainties in Free-air Region. The free-air blast wave from a nuclear explosion is essentially unknown because (1) there is no experimental information at distances greater than approximately the breakaway diameter and (2) no completely realistic calculation has been performed.

(b) Uncertainties in Reflected Regions. Experimental information does not establish the precise shape of the pressure-distance curve because of data scatter and possible existence of jets. Small-charge data are uncertain and do not extend to low heights of burst or reflected pressures greater than 20 psi. No realistic calculation is possible at this time.

4.1.5 Summary of Greenhouse Program for Reduction of Gaps in Current Knowledge of Nuclear Blast Waves

The Greenhouse blast measurements program is summarized in Table 4.1. If successful, results from the program should fill in considerable portions of the nuclear blast-wave picture.

4.2 THERMAL RADIATION

4.2.1 Pertinent Characteristics

The theoretical aspects of the nature of the thermal radiation emitted by atomic bombs exploded in air have been adequately treated elsewhere.[3,6,14] The following sections summarize briefly the state of knowledge relative to thermal radiation.

Pertinent characteristics may be divided into three categories:

1. Fraction of energy released appearing as thermal radiation.
2. Time variation of thermal radiation.
3. Spectral character of thermal radiation.

(a) Fraction of Energy Appearing As Thermal Radiation. Measurements of the total thermal

[redacted]

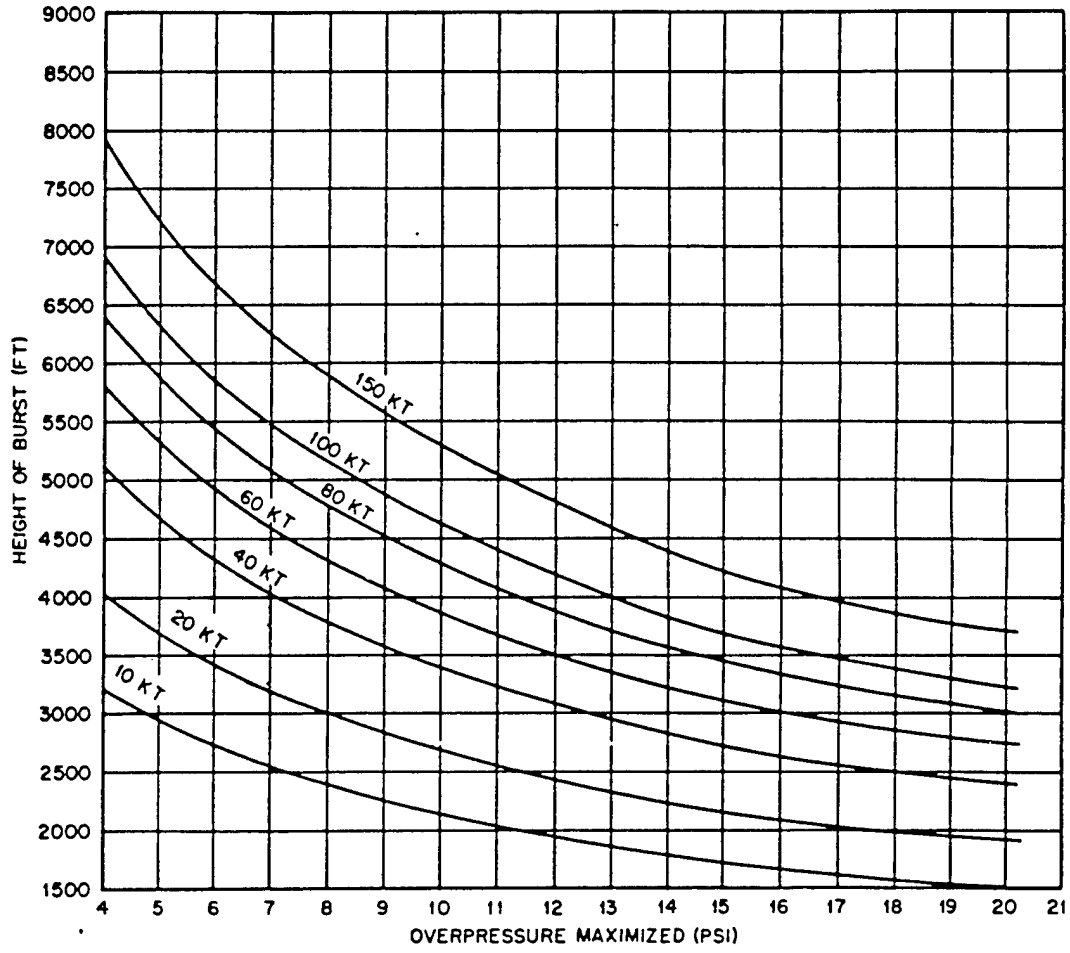

Fig. 4.15 Height of Burst vs Overpressure Area Maximized. Based on Report LA-743R, assuming uniform sea-level atmosphere.

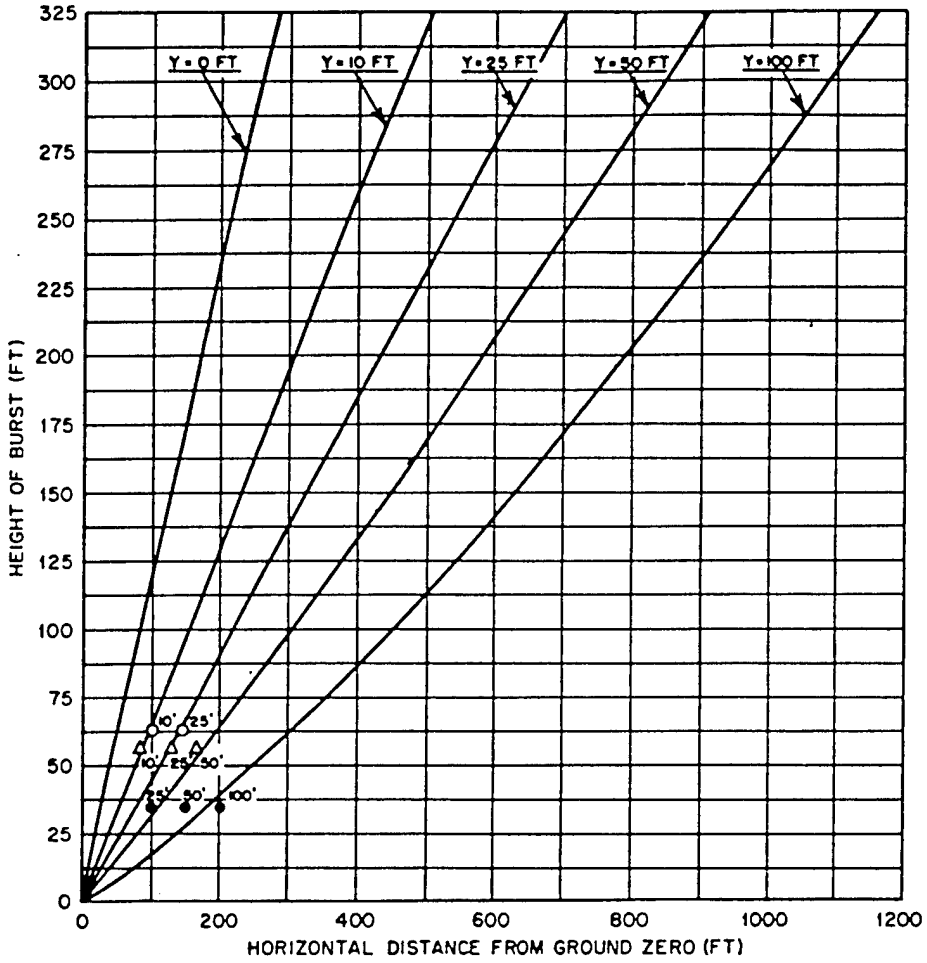

Fig. 4.16 Mach Stem Height Y As a Function of Height of Burst and Horizontal Distance, 1 Kt. Reference: Report LAB-J-705 with extrapolation down from Report LA-743R. Δ, Yoke films. O, X-ray films. ●, Trinity films.

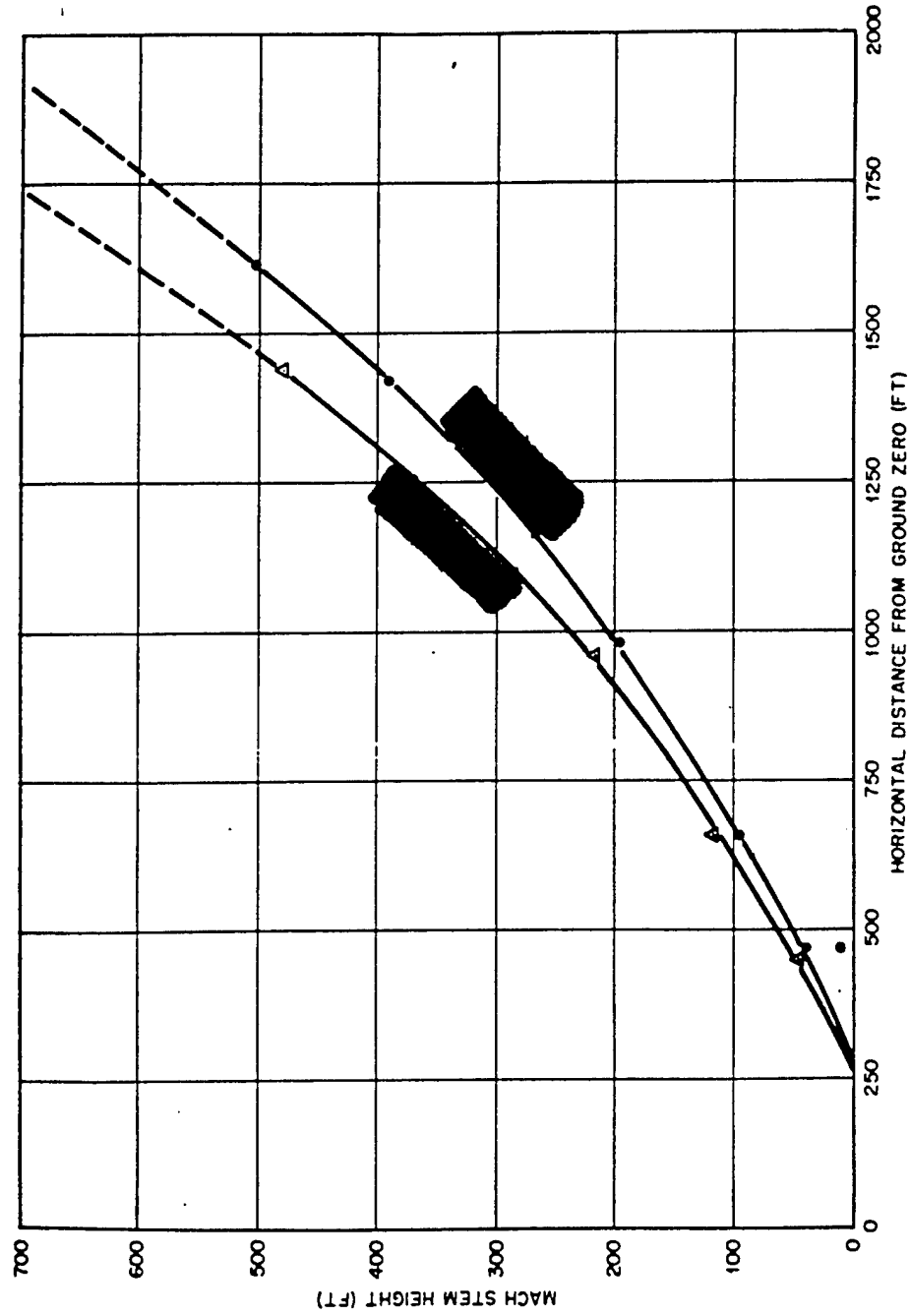

Fig. 4.17 Estimate of Mach Stem Height vs Horizontal Distance [redacted] 300-ft tower. References: Reports LAB-J-705 and LA-743R.

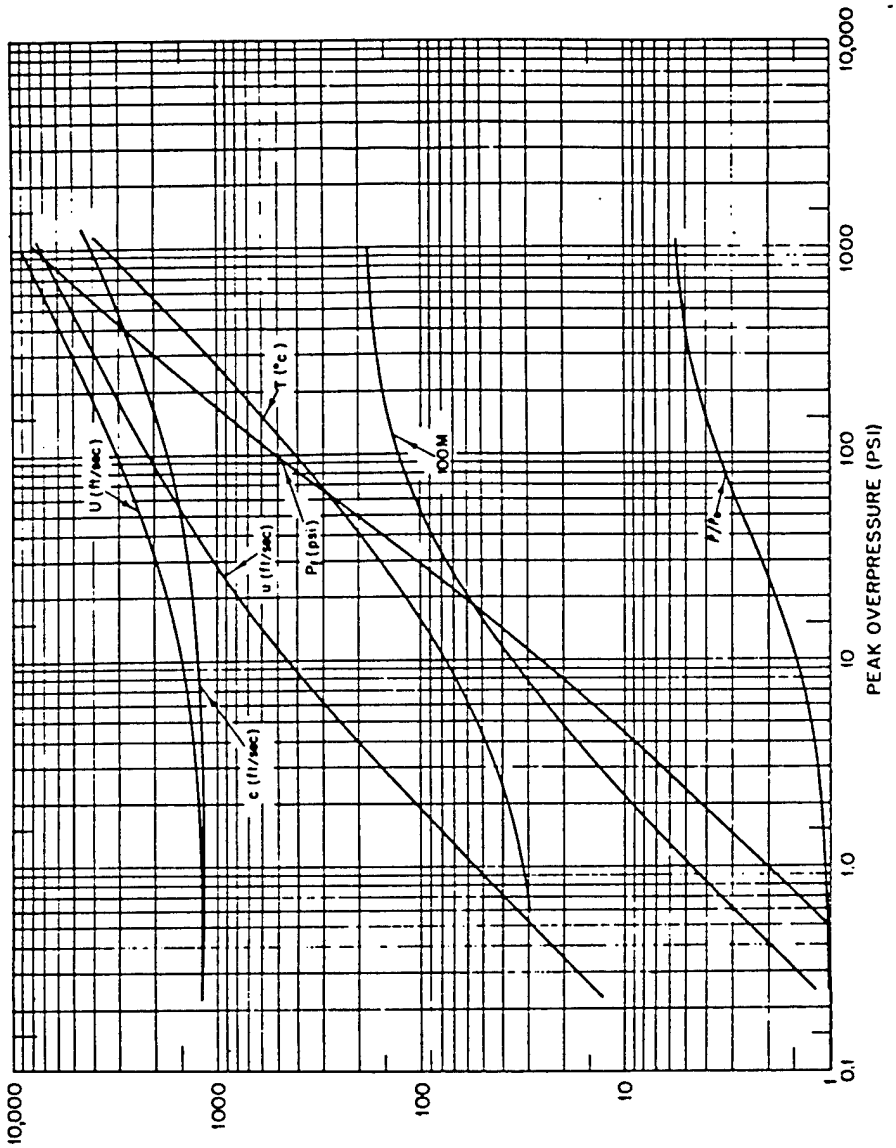

Fig. 4.18 Calculated Peak Values of Pertinent Blast-wave Characteristics. ρ, density; U, shock velocity; u, particle velocity; c, sound velocity; M, Mach number (u/c); P_f, reflected overpressure after normal incidence. Assumptions: $\gamma = 1.4$ = constant; $P_0 = 14.7$ psi; $\rho_0 = 0.00117$ g/cm^3; $c_0 = 1142$ ft/sec; $T_0 = 25.6°C = 78.1°F$. Relative humidity, 80 per cent.

TABLE 4.1 SUMMARY OF PRINCIPAL GREENHOUSE BLAST MEASUREMENTS

Experiments	Purpose
Free-air Region	
Fireball photography before ground strike	Determination of yield Calculation of fireball pressures up to time of breakaway, i.e., ~4000 psi Location of jets and asymmetries
Balloon telemetering of shock arrival times	Free-air peak pressures, ~300 to ~40 psi
Rocket smoke-trail photography to give shock position vs time	Free-air peak pressures, possibly down to ~5 psi Possible information on triple-point trajectory after breakaway
Reflection Region	
Fireball photography after ground strike	Calculation of reflected pressures in fireball Determination of triple-point trajectory in fireball stage and, possibly, beyond breakaway Location of jets
Ball-crusher gauges near base of tower	Measurement of reflected pressures in fireball continuously from regular through Mach reflection regions, ~10,000 to ~1000 psi Possible determination of asymmetries
Measurement of shock arrival times by blast switches	Accurate determination of pressure-distance curve from tower shot, ~1000 to ~3 psi
Measurement of peak pressures by foil and indenter gauges	Backup for blast switches, ~200 to ~7 psi
Measurement of pressure vs time by inductance gauges	Accurate measurement of pressure vs time characteristic, ~200 to ~7 psi
Measurement of pressure vs time by spring piston gauge	Backup for inductance gauges, ~200 to ~7 psi
Overhead photography from airplane	Determination of asymmetries Possible calculation of reflected pressure-distance curve

(Text continues on page 56.)

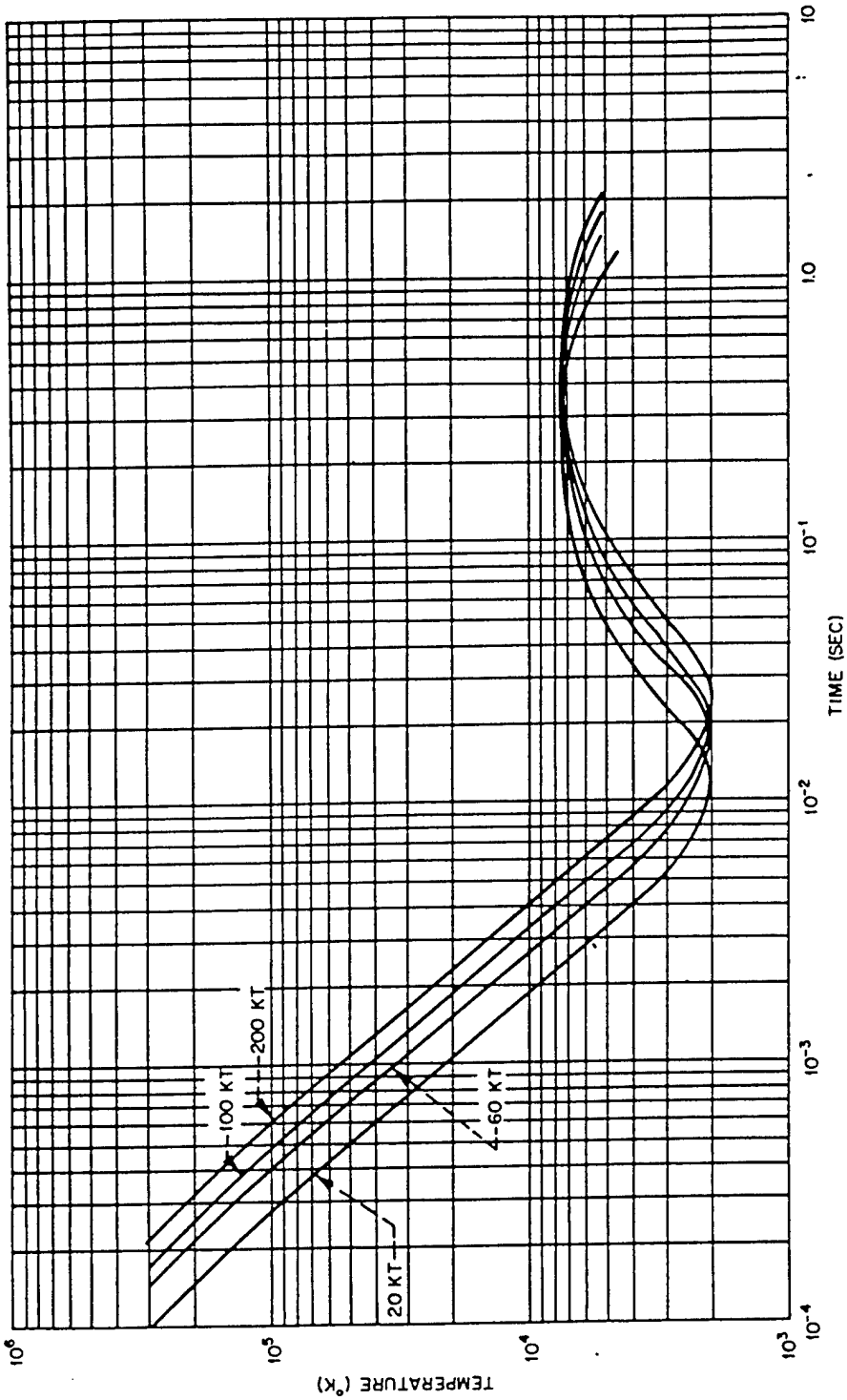

Fig. 4.19 Fireball Temperature vs Time

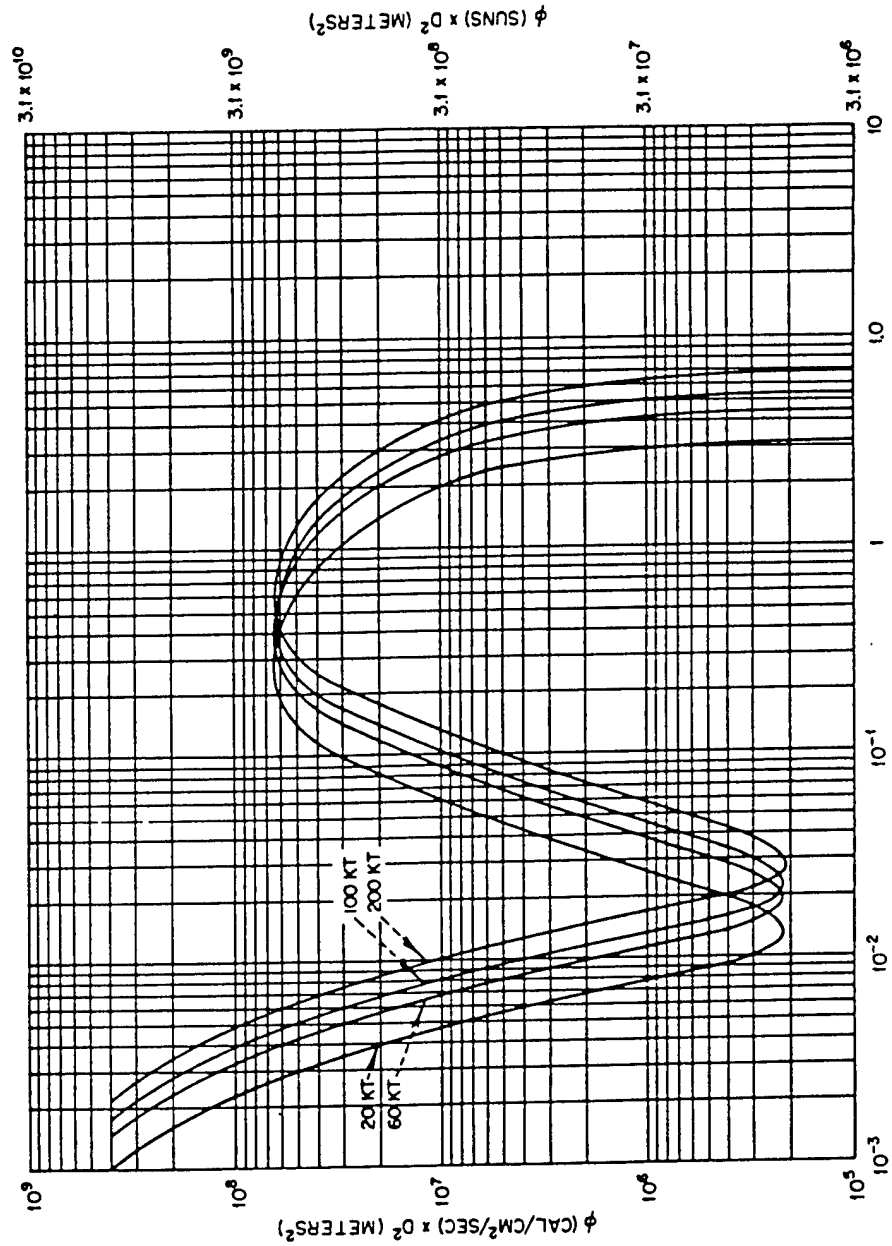

Fig. 4.20 Fireball Illumination vs Time. 1 sun = 1.35×10^6 ergs/cm^2/sec, or 3.23×10^{-2} cal/cm^2/sec; D, distance from bomb to point of observation.

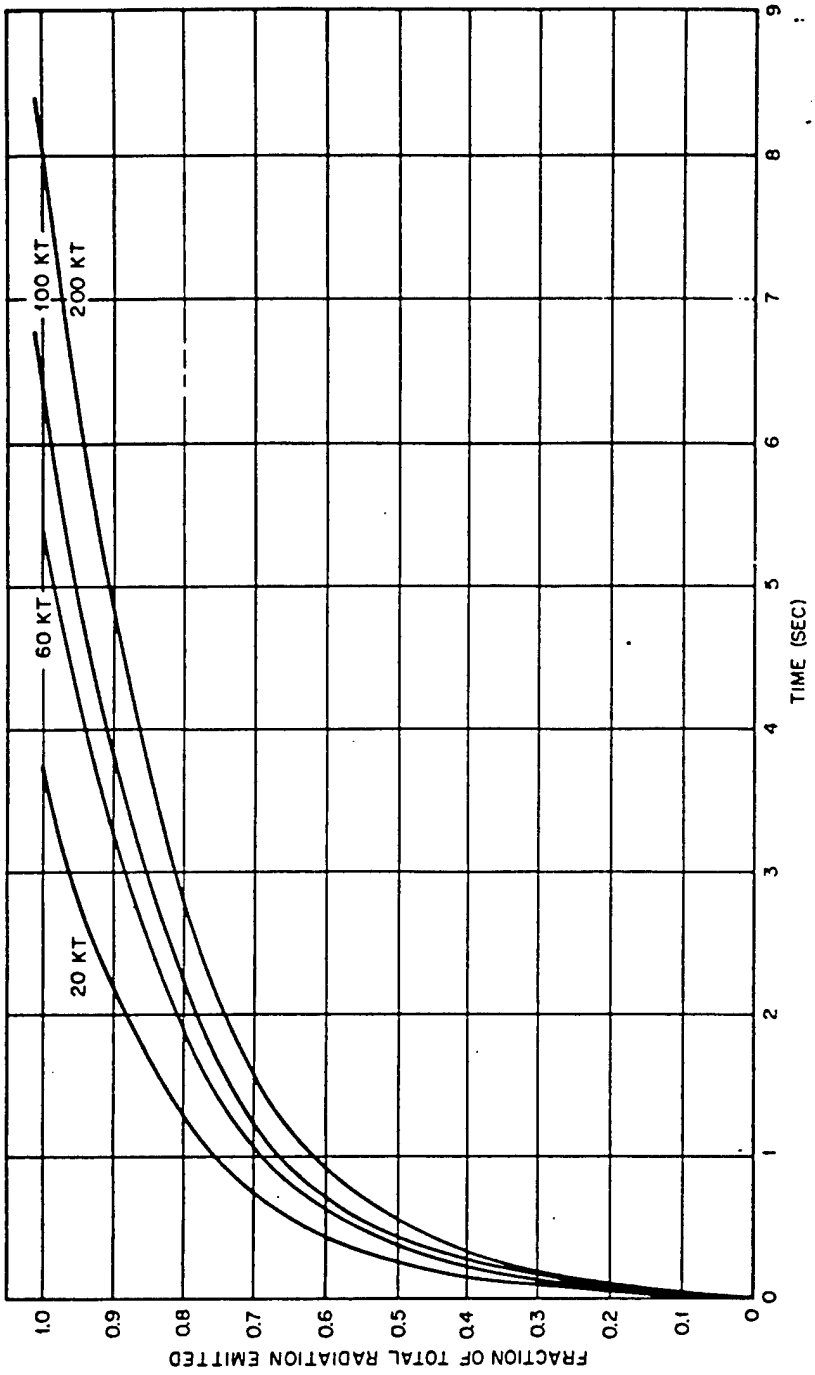

Fig. 4.21 Fraction of Total Thermal Radiation Emitted vs Time. Based on Sandstone Zebra.

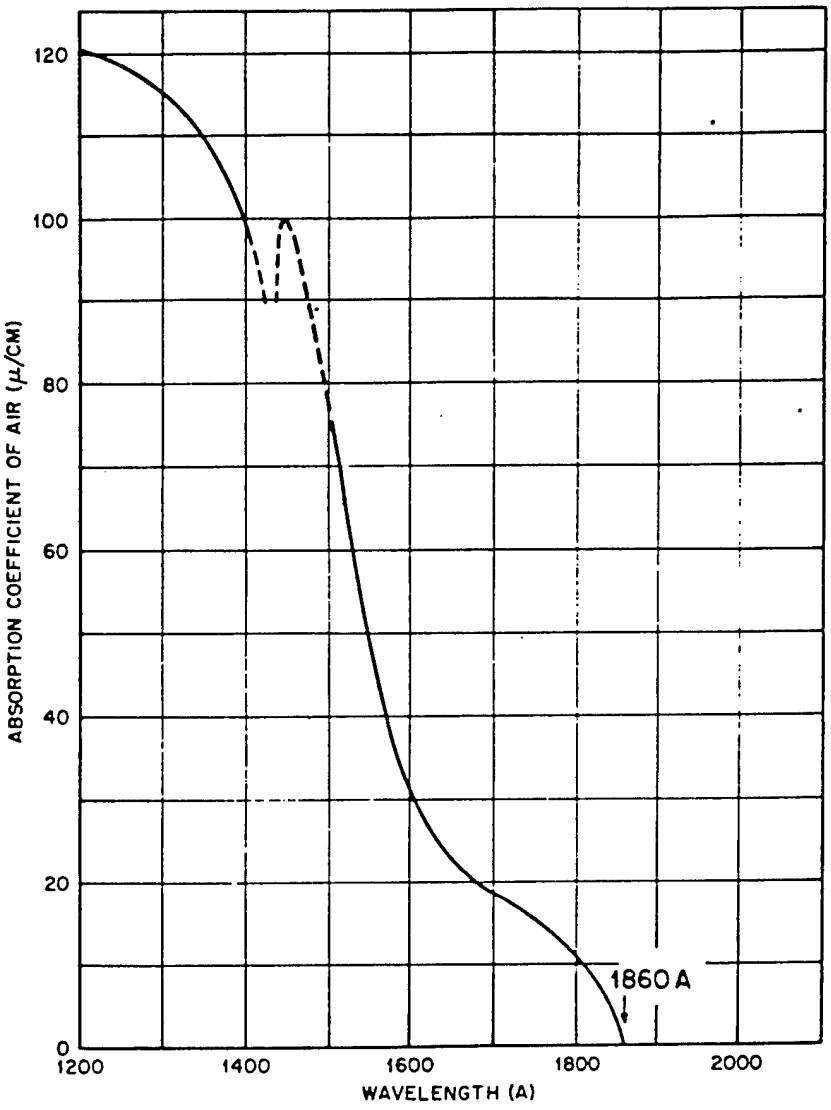

Fig. 4.22 Absorption Coefficient of Air vs Wavelength

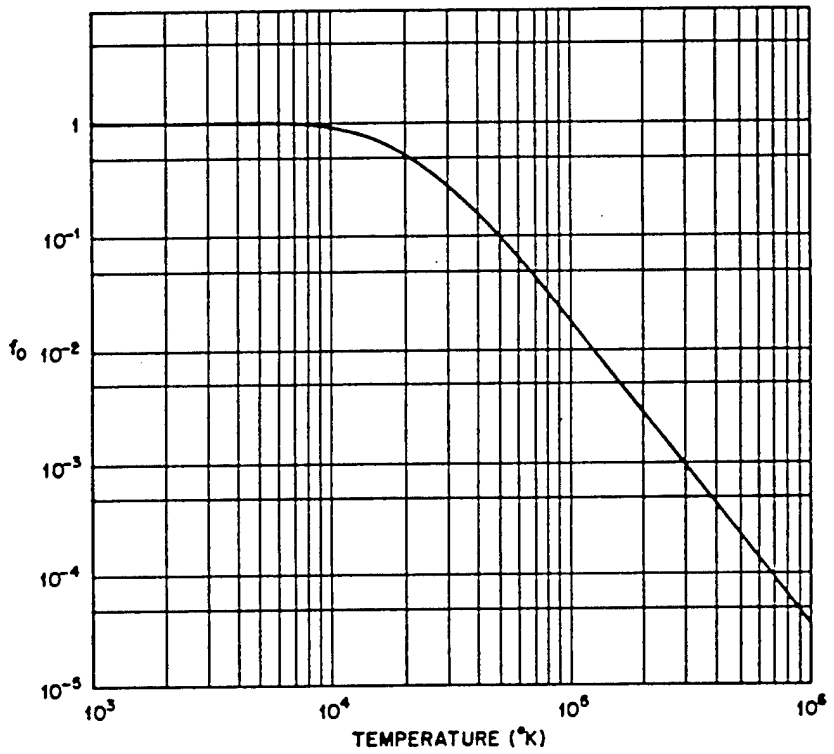

Fig. 4.23 Fraction of Radiation Penetrating Air As a Function of Fireball Temperature. $f_0 = (\int_{\lambda_0}^{\infty} e_\lambda \, d\lambda)/(\int_0^{\infty} e_\lambda \, d\lambda)$; λ_0 = 1860 A; e_λ = Planck function.

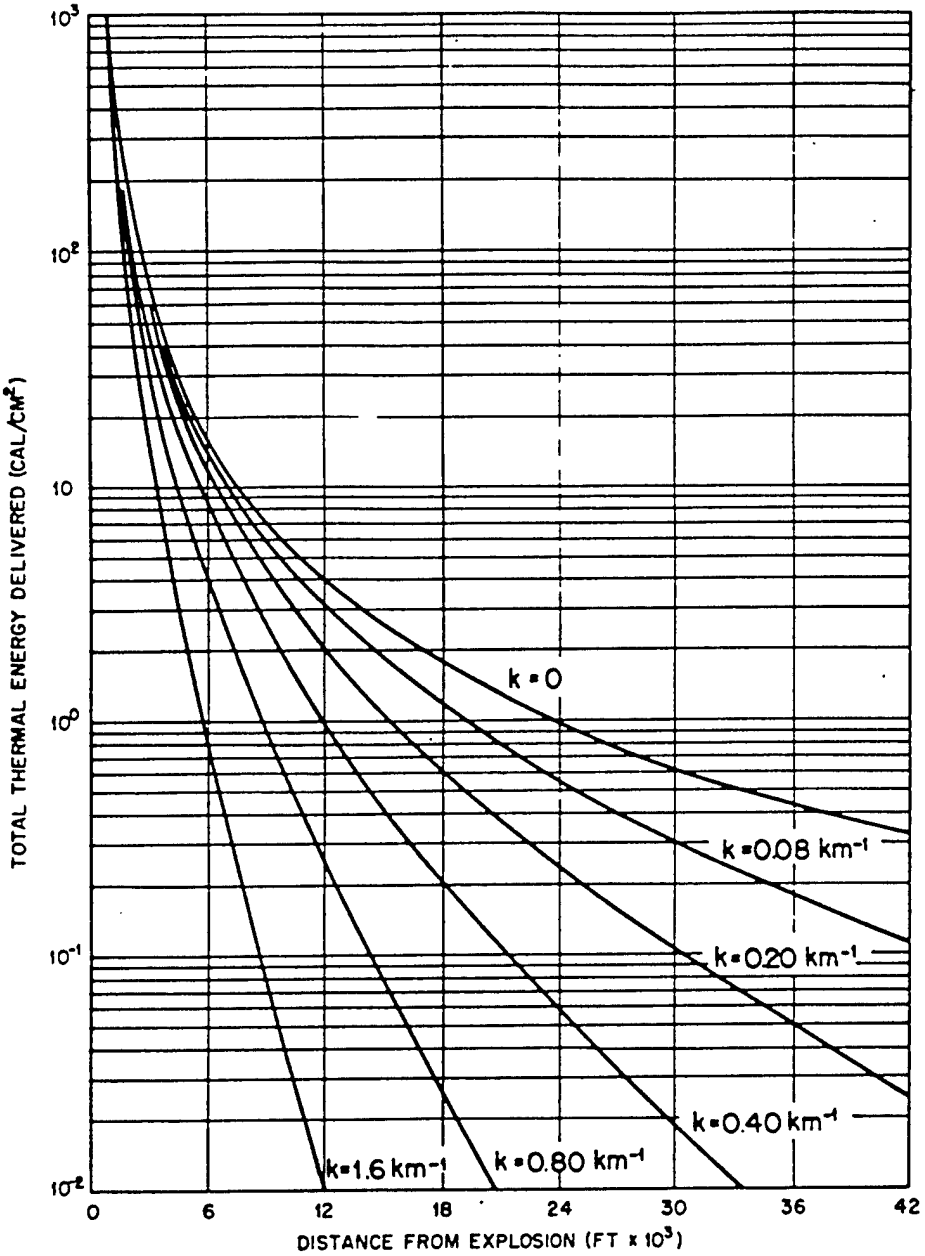

Fig. 4.24 Thermal Energy Delivered vs Distance As a Function of Attenuation Coefficient, 20 Kt

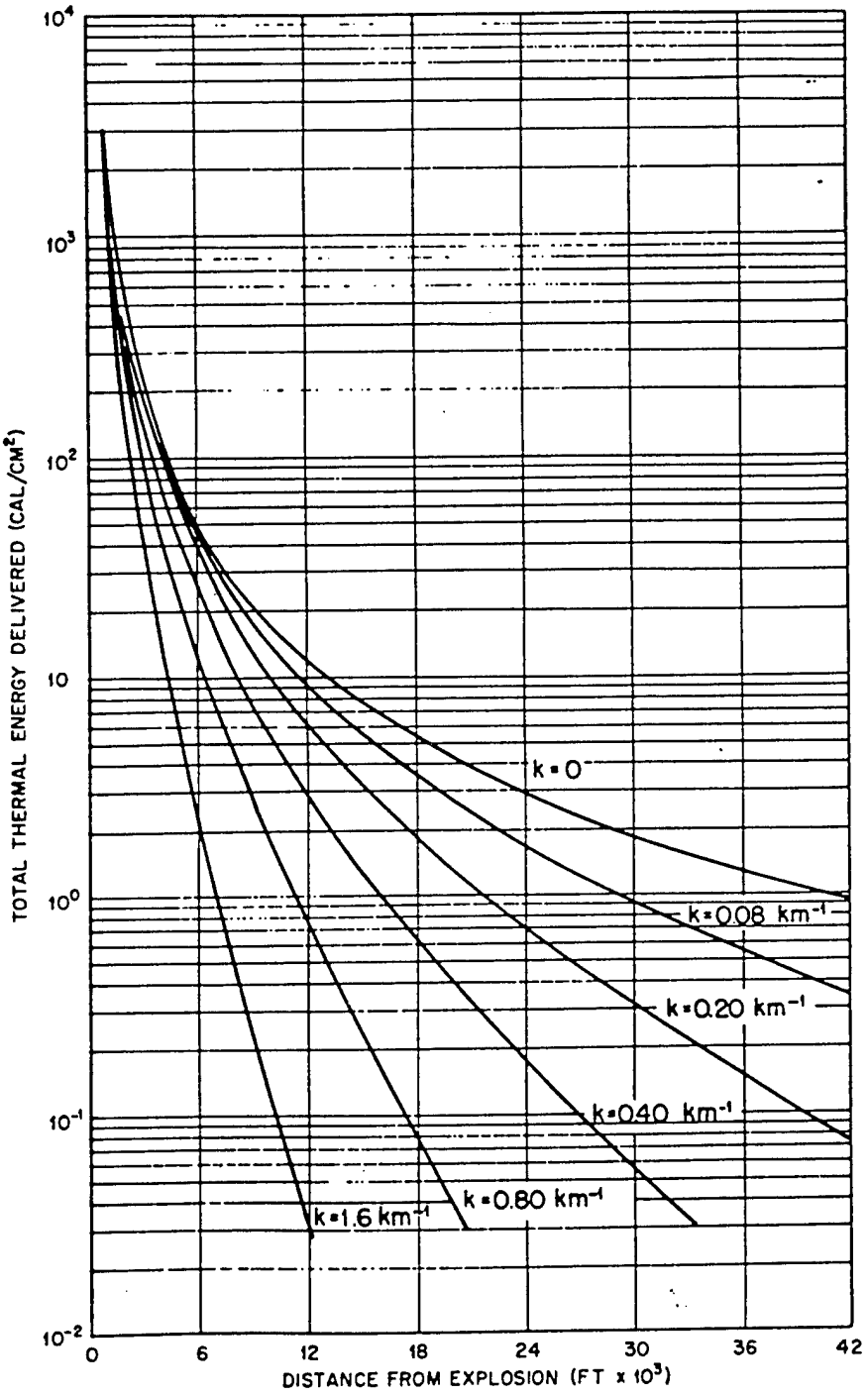

Fig. 4.25 Thermal Energy Delivered vs Distance As a Function of Attenuation Coefficient, 60 Kt

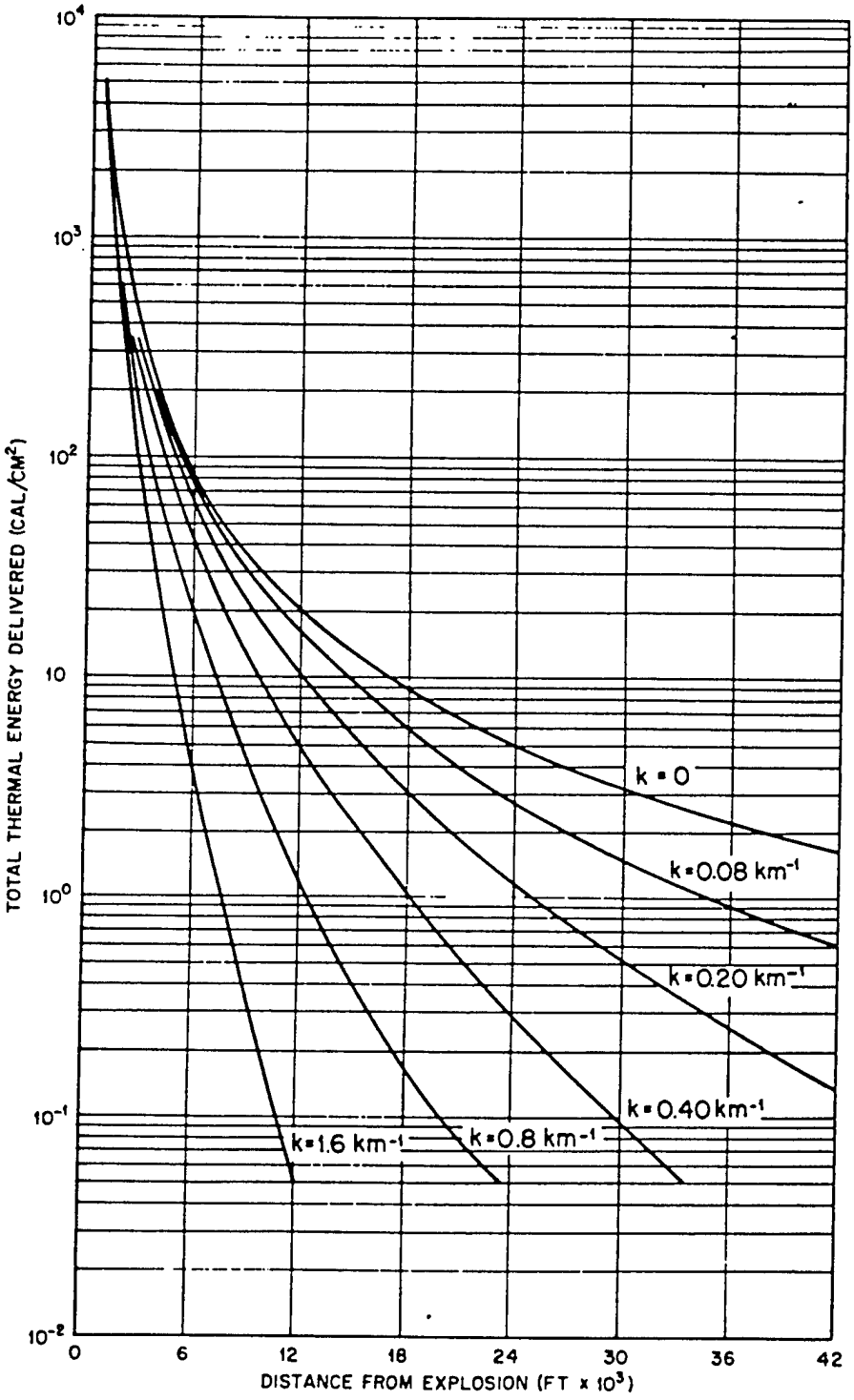

Fig. 4.26 Thermal Energy Delivered vs Distance As a Function of Attenuation Coefficient, 100 Kt

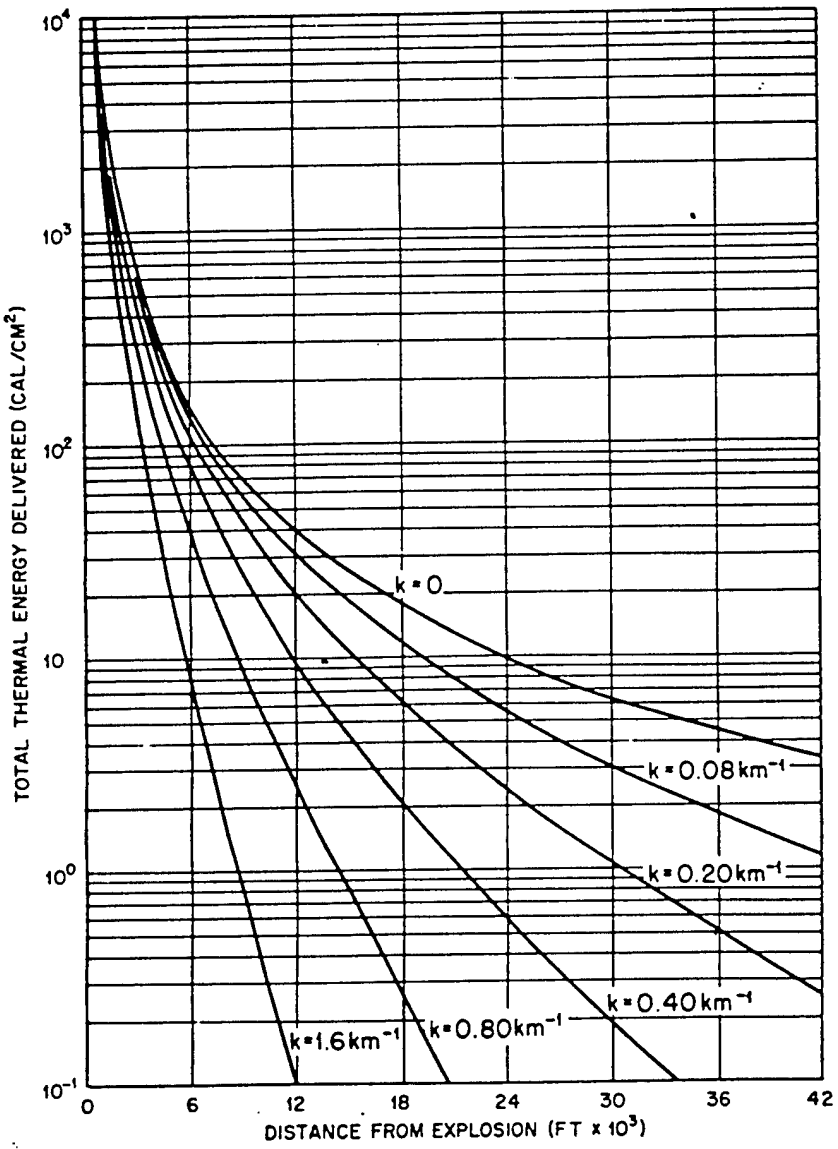

Fig. 4.27 Thermal Energy Delivered vs Distance As a Function of Attenuation Coefficient, 200 Kt

radiation emitted were made at Trinity, Bikini, and Sandstone. The results are inconclusive and uncertain for the following principal reasons:

1. No precise measurements were made of atmospheric attenuation.
2. The contribution by reflection from land and water is unknown.
3. In the case of tower shots it is difficult to evaluate precisely the effects of ground absorption of energy, reflected shock traveling up the fireball, dust, etc.

In view of these uncertainties, the most that can be said from the composite results of previous measurements of thermal radiation is that approximately $\frac{1}{3} \pm \frac{1}{6}$ of the total energy of the bomb appears as thermal radiation.*

(b) Time Variation of Thermal Radiation. The time rate of variation of thermal radiation is fairly well known (except for very early stages) from theory and experiment. By far the largest fraction is emitted after the illumination minimum resulting from the formation of the oxides of nitrogen.

Figures 4.19 to 4.21 give the time variation (for various tonnages) of fireball temperature, fireball illumination, and total emitted radiation. The curves are combinations of theoretical and experimental results. To obtain curves for other tonnages, multiply all times by the cube roots of the ratios of the tonnages.

(c) Spectral Character of Thermal Radiation. Although some spectral observations of the fireball have been made, the results have not been conclusively analyzed or corrected for atmospheric attenuation, and the spectrum is essentially unknown. There is no reason to believe that it should differ greatly from that of a black body.

(d) Atmospheric Attenuation. Figures 4.22 and 4.23 give some data on the absorption characteristics of air as a function of wavelength.

The character of thermal radiation at large distances from an explosion is sensitively dependent on the exponential attenuation coefficient. Figures 4.24 to 4.27 give the thermal energy delivered vs distance for various values of the attenuation coefficient. To obtain the curves for other tonnages, multiply the ordinates by the ratio of the tonnages.

*This refers to the prompt thermal radiation seen by detecting instruments in times of, say, less than 5 sec. Ultimately, essentially all the energy released by the bomb is degraded into heat.

4.2.2 Summary of Greenhouse Thermal Radiation Measurements

The following is a brief summary of thermal radiation measurements to be made at Greenhouse.

Atmospheric Attenuation: Measurements will be made of atmospheric attenuation for wavelengths up to 25,000 A at times near to that of the detonation. Such measurements should make possible the more accurate determination of the total thermal energy as well as the fireball spectrum.

A deficiency exists in the fact that attenuation measurements will not be made of the perturbed atmosphere resulting from ionizing radiations.

Ballistic Measurements of Total Radiation: Long-time-constant instrumentation will measure the integrated radiation flux over the entire radiation period.

Total Radiation As a Function of Time: Total radiation as a function of time will be recorded with 50-μsec resolution using a modulated bolometric system.

Spectral Distribution of Energy As a Function of Time: Spectrographic equipment with 25-μsec resolution will record spectrum vs time.

Equivalent Black-body Temperature: Photocells will measure up to approximately 4 msec the spectral emission in wavelength bands selected so as to avoid strong groups of atomic lines.

High-resolution Spectroscopy: A high-resolution spectrograph will be used to identify the absorption bands of ozone and the oxides of nitrogen.

REFERENCES

1. B. R. Suydam, Scaling of a Blast From One Medium to Another, Los Alamos Scientific Laboratory Report LA-1137.
2. F. B. Porzel, Rate of Growth of Atomic Fireballs, Los Alamos Scientific Laboratory Report LA-1214.
3. Sandstone Report, Vol. 9, Chap. 6 (Revised).
4. Los Alamos Scientific Laboratory, "The Effects of Atomic Weapons," Chap. 3, U. S. Government Printing Office, Washington, 1950.

5. J. Hirschfelder and J. Magee, Radiation Phenomena in Air Blast of Gadget, Los Alamos Scientific Laboratory Report LA-1020, Chap. 4.
6. R. G. Stoner and W. Bleakney, The Attenuation of Spherical Shock Waves in Air, J. Applied Phys., 19(7): 670-678 (1948).
7. J. G. Kirkwood, private communication.
8. J-7 Blast Measurements Group, LASL: W. Baker, P. FlorCruz, R. Houghten, F. Porzel, J. Smith, and J, Whitener, private communication.
9. C. F. Curtiss and J. O. Hirschfelder, Thermodynamic Properties of Air, Department of Chemistry, University of Wisconsin, Naval Research Laboratory, Navy BuOrd Contract NOrd 9938, Task Wis-1-A, June 1, 1948.
10. S. R. Brinkley, J. G. Kirkwood, and J. M. Richardson, Properties of Air Along a Hugoniot Curve, Report OSRD-3550, Apr. 27, 1944.
11. K. Fuchs and R. E. Peierls, The Equation of State of Air, Los Alamos Scientific Laboratory Report LA-1020, Chap. 3, Apr. 6, 1948.
12. F. Porzel and F. Reines, Height of Burst for Atomic Bombs, Los Alamos Scientific Laboratory Report LA-743R.
13. R. A. Houghten and J. M. Smith, Mach Stem Height vs Horizontal Distance Determinations, Los Alamos Scientific Laboratory Report LAB-J-705 (not available).
14. Los Alamos Scientific Laboratory, "The Effects of Atomic Weapons," Chap. 4, U. S. Government Printing Office, Washington, 1950.

[redacted]

Chapter 5

Biomedical Program

By W. H. Langham

5.1 INTRODUCTION

The purpose of the biomedical program of Operation Greenhouse is to provide information considered important to the national security in the event that the United States is attacked with atomic weapons. Although there is an abundance of physical data regarding blast, thermal radiation, and ionizing radiation emitted by an atomic blast, such data are quite often partially inadequate for purposes of medical and civil defense planning. As an example of the need for more applicable data regarding radiation casualties from an atomic explosion, it is interesting to consider the accuracy of the gamma-radiation-vs-distance curve given in the weapons effects manual.[1] The general consensus is that the curve is accurate only to within a factor of 2. If it is assumed that the casualty threshold of gamma radiation for man is 200 r, then the casualty threshold distance from a 20-kt atomic explosion, read from the gamma-ray curve in the weapons effects manual, is approximately 1580 yd, and the spread, as a result of the uncertainty of a factor of 2, is from 1410 to 1750 yd. At the standard population density for a large American city of 40 persons per acre, this spread would represent a difference in potential casualties of approximately 28,000 persons. If 1580 yd is taken as the casualty threshold distance from an average 20-kt explosion, a difference of 100 yd in that distance would mean an additional 8000 potential casualties in an American city having the standard population density. It therefore seems imperative that an attempt be made to determine the potential casualty threshold range of atomic weapons somewhat more accurately than that which can be derived from physical measurements alone. Therefore one purpose of the biomedical program is to obtain more exact data as to the potential casualty production of the ionizing radiation from an atomic detonation.

A second purpose of the biomedical program is to provide an adequate biological basis for the correlation of physical data of the bomb with medical and biological response observed in the commonly used experimental animals, namely, the mouse, the dog, and the pig.

The third purpose of the program is to collect field data on the commonly used laboratory animals, for purposes of correlation with the vast amount of laboratory data available and to provide orientation for further laboratory programs.

As an illustration of this purpose it is quite possible, in the laboratory, to produce flash burns on experimental animals which may then be used for therapeutic study of the biological damage. However it is important that information on the character and quality of the flash burns produced by an atomic explosion be known in order that the results obtained in the laboratory may be unquestionably correlated with those occurring under field conditions.

The fourth purpose of the program is to collect quantitative field data under controlled conditions for purposes of correlation with the uncontrolled qualitative data collected in Japan.

The fifth purpose of the test is to give biological and medical experimenters actual field experience in studying the various casualty-producing phenomena of atomic weapons.

The major casualty-producing phenomena of the bomb are blast, ionizing radiation (including gamma rays, neutrons, and beta rays), and thermal radiation. The experiments selected for the

[redacted]

biomedical program were selected with these various phenomena in mind.

Blast studies were eliminated from this specific series of tests because of the inherent difficulty of exposing experimental animals to the blast effect without exposing them to the more serious effects from the ionizing and thermal radiations. This particular series of projects is therefore concerned with studying the biological effects of ionizing and thermal radiations. The criteria for selecting the various projects were:

1. The experiment had to be one which could not be performed in the laboratory but only under field conditions.
2. The project had to be useful toward fulfilling one of the five purposes of the biomedical test program.
3. The project had to be one with a reasonable degree of assurance of giving some usable information regarding either the fundamental knowledge of the biological effects of an atomic detonation or knowledge strictly applicable to civil defense and medical planning.

A brief description of the nature of each of the projects is given in the following sections.

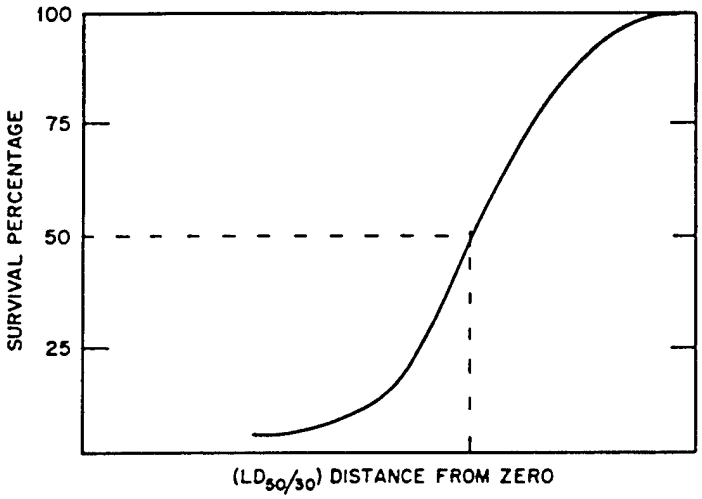

Fig. 5.1 $LD_{X/30}$ Survival Curve. Percentage of a large group of animals surviving for 30 days after exposure plotted against distance from the bomb or against radiation damage.

5.2 LD_X STUDY USING MICE

The mouse is the standard experimental animal for laboratory study of the biological effects of ionizing radiations. Knowledge of the response of the mouse to ionizing radiation in the field is considered highly important in order to provide a basis for the correlation of the vast amount of laboratory data with conditions occurring in the field. This experiment was introduced for the purpose of determining the lethal effect of radiation from an atomic explosion of known energy release as a function of distance from the detonation using the mouse as the biological test unit.

Large groups of mice are being placed at various distances from zero point to cover the predicted gamma-dosage range of from approximately 100 to 1200 r. Observation of these animals for a period of 30 days following the blast will permit the establishment of the characteristic $LD_{X/30}$ curve shown in Fig. 5.1, as a function of distance from the explosion. The $LD_{X/30}$ response of mice to X rays is well known for a wide variety of laboratory conditions. Collection of the data demonstrated in Fig. 5.1 under field conditions will permit the correlation between the data on radiation dosage emitted by the bomb and similar data collected in the laboratory.

5.3 SERIAL-SACRIFICE STUDY USING SWINE

Good pathological material was collected following the atomic bombings in Japan. The cir-

cumstances under which this material was collected prevented the pathologists from obtaining pathological specimens that demonstrated the early pathology of acute radiation damage. This experiment for Operation Greenhouse is designed to supply such material for observation of very early radiation damage, thereby filling the gap in the Japanese data. A large group of swine is being placed at a distance from the bomb where the gamma-ray intensity is predicted to be approximately 1000 r. These animals will be sacrificed serially and autopsied. Samples of their tissues will be prepared histologically and studied for pathological changes as a function of time after the bomb detonation. These pathological observations are to be correlated with the observations made in Japan.

5.4 SERIAL-SACRIFICE STUDY IN DOGS

The dog is recognized as the standard large animal for physiological studies in the laboratory. In exactly the same manner as specified in Sec. 5.3, dogs are to be exposed at a point where the predicted gamma-ray dosage is approximately 1000 r. The dogs are to be serially sacrificed, and their tissues will be observed for early pathological effects of lethal doses of gamma radiation. These pathological observations are to be correlated with the Japanese studies and with those made on swine. For both the swine and dogs, blood cultures will be made to determine the time of onset and the degree of septicemia following an acute lethal dose of gamma radiation from an atomic blast. These observations are expected to give some indication of the importance of septicemia in acute radiation death.

5.5 LD_X STUDIES IN SWINE

From the point of view of civil defense planning and the medical care of potential atomic bomb casualties, the $LD_{X/30}$ dose of gamma radiation for man is extremely important. At this time the $LD_{50/30}$ for the human being is not known, but it is estimated to be approximately 400 r. The body thickness and contour of the pig are quite similar to that of man, and the response to ionizing radiation is quite comparable. This experiment is designed to determine the gamma-ray $LD_{X/30}$ dose for swine exposed under actual field conditions. A relatively accurate determination of the $LD_{X/30}$ for the pig will permit a more dependable extrapolation to the $LD_{X/30}$ for man. Pigs of suitable size are being placed in containers and exposed to the radiations from the bomb at various distances from zero where the dosage of gamma rays is predicted to be between 100 and 800 r. Observation of these animals for a 30-day period following the blast will permit the construction of the standard LD_X curve shown in Fig. 5.1. These data may then be extrapolated to man and correlated with pretest studies made in the laboratory by exposing pigs to more conventional sources of radiation.

5.6 LD_X STUDIES IN DOGS

Since the dog is the standard animal for physiological studies in the laboratory, it was considered worth while to determine the $LD_{X/30}$ for the dog. Groups of dogs are being placed at varying distances from the atomic explosion such that the predicted gamma-ray dosage ranges between 100 and 800 r. Observation of these animals for a 30-day period will permit the determination of the percentage of 30-day survival of animals as a function of distance from the blast. These results may then be correlated with similar observations made in the laboratory using X rays. These data, when correlated with the observations in mice and swine, will permit a more accurate estimation of the casualty threshold radius of an atomic explosion for man.

5.7 THERMAL-BURN STUDIES

Thermal burns account for an extremely high percentage of the total casualties following an atomic bomb detonation. Little is known about the specific characteristics of the flash burns created by an atomic weapon.

Anesthetized pigs are to be placed in shelters at varying distances from zero point. The flank of the animal will be placed against a port containing movable shutters and various types of filters. Observation of the burns produced on these animals will give information as to the type and quality of the burn as a function of dis-

tance from the explosion. It is also expected to give information as to which components of the thermal radiation from the bomb are contributing most to the thermal injury produced. The purpose of this experiment is to define the type of burn suffered by atomic casualties in order that it may be reproduced under laboratory conditions. Once this definition is established it will be possible to study the therapy and management of such thermal burns in the laboratory.

5.8 DEPTH DOSE AND PHANTOM DOSIMETRY

The energy spectrum of the gamma rays emitted from an atomic explosion has not been well defined. Obviously the biological effects produced are directly dependent on the spectrum of the radiation. Film badges and ionization chambers are being placed in unit-density phantoms approximating the body size and contour of the various experimental animals and man. These phantoms are to be placed at varying distances from zero. Determination of the degree of film blackening will permit a correlation of the physical measurements of energy spectrum, the depth dose in unit-density material, and the biological results observed in the experimental animals. The purpose of this experiment is to give information on the depth-dose characteristics of the gamma rays emitted from an atomic detonation and their relation to the biological effects observed in animals.

5.9 HEMATOLOGICAL STUDIES

Whole blood from the serially sacrificed swine and dogs will be preserved in the field and returned to the United States, where it will be transported to a number of laboratories interested in studying the biochemical changes produced in the blood of animals as a result of lethal doses of atomic bomb radiations. The purpose of this experiment is to provide a large amount of material for biochemical studies.

5.10 STUDIES OF SURVIVAL MICE

Exposure of experimental animals to chronic doses of X rays is known to shorten the life span and increase the incidence of malignancies and cataract. There has been no previous opportunity to study the effect of radiations from an atomic detonation on these factors. A large number of mice surviving the bomb detonation for greater than 30 days will be returned to the United States where they will be observed for the duration of their lives. The purpose of these observations is to study the effects of the gamma rays from an atomic detonation on the shortening of life span and on the incidence of neoplasia, cataract, and other delayed symptoms of radiation damage as a function of distance from zero.

5.11 STUDY OF NEUTRON-INDUCED CATARACT

Observation of cyclotron workers who received chronic neutron exposure seems to indicate that neutrons are extremely effective at inducing cataract. Groups of mice shielded from gamma rays are to be exposed at distances where the total neutron flux is predicted to range between 5×10^9 and 1×10^{11} neutrons/cm^2. These animals will be observed for the incidence and time of appearance of cataract. The biological results observed are to be correlated with the physical measurements of neutron flux as a function of distance from the bomb. The results of this study will be compared with the incidence of cataract following gamma-ray exposure.

5.12 INHALATION OF FISSION PRODUCTS

There exists considerable doubt as to the hazards involved in the event that a manned aircraft is forced to fly through an atomic cloud. The anticipated hazards involve the amount of gamma radiation received from the cloud and the amount of fission products inhaled by the plane crew during cloud passage. This experiment is designed to give at least qualitative information on both these potential hazards. Groups of mice are to be placed in the drone planes that will make two passes each through the cloud to collect fission-product samples for radiochemical analysis. Several groups of these mice will be sacrificed, and the gamma-radiation exposure that they sustained will be measured by the decrease in their splenic and thymic weights. The remaining groups of animals will be sacrificed immediately, and their lungs and other tissues

will be analyzed for inhaled fission-product activity. The data obtained are expected to give quantitative information on gamma-ray exposure and at least qualitative information as to the inhalation hazard associated with flying through an atomic cloud.

5.13 BIOLOGICAL DOSIMETRY USING *TRADESCANTIA*

Pretest studies at the Oak Ridge National Laboratory showed that the number of chromosome aberrations produced in *Tradescantia* by radiation is quantitatively related to the total dosage received. *Tradescantia* blooms are to be placed in containers at varying distances from zero and on the drone aircraft, after which the number of chromosome aberrations will be determined. These data are expected to give an indication of the total radiation dosage delivered during the passage of the drone aircraft through the cloud and a measure of the total neutron and gamma-ray dosage delivered as a function of distance from the detonation on the ground. The neutron studies will be accomplished by shielding the *Tradescantia* blooms from the gamma radiation by means of lead shields.

5.14 BIOLOGICAL DOSIMETRY OF GAMMA RAYS USING MICE

Pretest studies conducted at LASL have shown that the weight decrease in the spleen and/or thymus of the mouse following exposure to radiation is quantitatively related to the total radiation dose. Five days after irradiation, a graph of the log of the spleen and/or thymus weight decrease vs the total dosage of 250-kv X rays gives a straight line with an error of ±10 per cent. By using this relation it is possible to determine the effective biological doses of various types of radiation in terms of the splenic and thymic weight decrease produced by known amounts of 250-kv X rays. Groups of mice are to be placed at varying distances from zero, and their splenic and thymic weight decrease is to be determined 5 days after the detonation. These data will permit an estimation of the biological effectiveness of the gamma radiation received by the animals as a function of distance from the detonation. The relative radiation dosage at the various distances may then be expressed in terms of equivalent roentgens of 250-kv X rays. It is anticipated that this experiment will give a very accurate measure of the gamma-radiation dosage delivered at various distances from an atomic bomb of known energy release. These data may then be correlated with the physical measurements of gamma radiation and the symptoms observed in mice, dogs, and swine used in the various other projects.

5.15 BIOLOGICAL DOSIMETRY OF NEUTRONS USING MICE

Pretest observations of the effect of radiation on splenic and thymic weight decrease mentioned in Sec. 5.14 were extended to include the measurement of the biological effectiveness of varying doses of neutrons. Much uncertainty still exists as to the biological and medical importance of the neutrons emitted from an atomic explosion as a function of distance from the detonation. Groups of mice are to be placed in lead-shielded containers (to protect them from gamma rays) at varying distances from the zero point. The lead-shielded containers are to be placed at distances such that a predicted neutron density ranging from 5×10^9 to 5×10^{11} neutrons/cm^2 is covered. Five days after the detonation, the decrease in weight of the spleens and thymuses of the various groups of animals will be determined. From these measurements it will be possible to estimate the relative biological effectiveness of the neutrons emitted from the bomb as a function of distance from zero. Biological effectiveness will be expressed in terms of equivalent roentgens of 250-kv X rays. The results will be correlated with physical measurements of neutron flux made by Task Unit 3.1.1.

5.16 STUDIES OF MISCELLANEOUS DOSIMETRY AND GENETIC MATERIALS

All the previous projects have dealt with the study of the radiation doses in the range of a few hundred roentgens. It was considered advisable to introduce a few studies involving radiation doses in the range of several thousand roentgens. There are numerous miscellaneous dosimetry materials (for example, crystal do-

simeters) which are capable of measuring doses of several thousand roentgens. This experiment includes the placement of such high-level dosimeters at distances of from 300 to 900 yd from the zero point. These materials are expected to give a quantitative measure of the total radiation in the high dosage range.

Corn seeds, *Glomerella*, and other biological materials are known to give very high mutation rates when exposed to large doses of ionizing radiation. A number of such materials are to be placed in containers with the miscellaneous dosimetry materials at varying distances of from 300 to 900 yd from the zero point. These materials will be returned to the United States where they will be studied for the incidence of mutations. The induced mutational changes are to be observed both quantitatively and qualitatively. The results observed are to be compared with those obtained from comparable doses of X rays and other conventional radiations under laboratory conditions.

5.17 DISSEMINATION OF BIOMEDICAL INFORMATION

The information collected from all these projects is to be carefully studied and correlated with the physical data collected by Task Unit 3.1.2 and with the physical data collected by all other task units. Whenever possible the information will be interpreted in terms most applicable to medical and civil defense planning in the event of an attack on the United States involving the use of atomic weapons. The information so obtained is to be declassified as soon as possible and made available to the various agencies concerned with medical and civil defense planning.

REFERENCE

1. Los Alamos Scientific Laboratory, "The Effects of Atomic Weapons," U. S. Government Printing Office, Washington, 1950.

[redacted]

Chapter 6

Military Test Program

By P. G. Galentine

6.1 INTRODUCTION

The purpose of this chapter is to describe briefly that portion of the Task Group 3.1 responsibility that is commonly referred to as the "Military Tests." Task Unit 3.1.3, under the command of Col R. E. Jarmon, is responsible for the accomplishment of this program. Since the TU 3.1.3 program is separated into six relatively independent subdivisions, this summary is organized accordingly.

6.2 EFFECTS ON STRUCTURES

Prior to the advent of the atomic bomb, with its attendant long positive blast-pressure phase, the criteria of impulse ($\int \Delta p\, dt$) had been successfully applied in evaluating damage to structures. This was made eminently feasible because of the very short duration of the positive pressure phase in the blast wave produced by a conventional bomb. Whenever this duration is increased by a factor of 100 or more, as is the case with atomic weapons, the impulse method breaks down experimentally as a criterion for prognosticating damage. As a result, another criterion was arbitrarily selected, that of overpressure in the blast wave. Hence the Department of Defense is faced with two basic and related problems at this time:

1. If a potential enemy has a structure which should be denied to him, how many pounds of overpressure must that structure be subjected to for the desired amount of damage to be obtained? (The statement of this problem assumes, of course, that "the desired amount of damage" is well defined.*) If such a structure requires X pounds of overpressure, it might be referred to as an "X-pound structure."

2. If a facility F, whose worth is such that F must be housed in an X-pound structure, how should such a structure be fabricated? Also, if F is housed in a Y-pound structure (Y is greater than X), how can the existing structure be reinforced so that it may be converted into an X-pound structure? The statement of this problem assumes, of course, that structural strength is a well-defined function of military worth.*

This portion of the experimental program is designed to collect data of use in solving these problems. More specifically, a method must be established for predicting structural blast damage.

Beginning with the survey of damage resulting from the atomic bombing of Japan, considerable effort has been devoted to the development of a method of analysis of structures subjected to blast loading of long duration. Both elastic and plastic theories have been employed in the study of damage to Japanese buildings. However, uncertainties with respect to blast loading and in the design and quality of construction have hampered such efforts. Also the resistance of materials and structural elements under rapid rate of loading was not well known. As a result of tests under dynamic loading of materials at the National Bureau of Standards and the California

*This assumption is reasonable for the purposes of this chapter. In actuality the problem, whose solution is assumed, is very difficult in itself. Its treatment, however, has no place in this discussion.

[redacted]

Institute of Technology, on reinforced-concrete beams and slabs at the Massachusetts Institute of Technology, and the extensive researches of Bleakney, much better information is available. This fact made it much more feasible to design test structures properly, for use in conjunction with a fission weapon on Engebi.

In order to predict damage, it is necessary to know, first, the loads that will result from blast on the different portions of the structures. Such loads are affected by a number of factors such as size, shape, orientation, openings, and partial failure of weaker portions of the structure. There are local blast effects, such as on the panels of a building, and the translational or shearing effect on the structure as a whole.

Second, it is necessary to know what the response of the structure and panels will be under the blast loading. Such response involves the mass and resistance to deformation of the panels and the frame as it is affected by loads transmitted to it by panels. Since criteria of damage are required, plastic yield is of direct interest.

The data to be obtained consist in blast-pressure measurements on the exposed and interior portions of the structures, measurement of blast pressures transmitted through an earth cover on semiburied structures, soil pressure under footings, relative displacements of portions of structures, accelerations of panels and frames, and strains on members. The time of failure of weaker structures will be measured, and the mechanics of failure will be observed by high-speed photography. Physical-damage surveys will provide essential data on damage.

The data collected by transient measurements and by survey of physical effects will verify or indicate the required modifications to present methods of analysis. The data will also provide check points for diffraction studies and model tests which should be made in the Zone of the Interior (ZI) to complement these experiments.

No attempt is made here to describe the various test structures in detail or to catalog them according to uses. The Army has 2 test structures, the Navy 12, the Air Force 12, and the Public Buildings Service 1; hence there are 27 basic test structures in addition to a number of the service buildings, such as recording stations for instrumentation and housing for high-speed cameras. It is possible, however, to make the following general statements, which hold true for all or a large portion of the program:

1. It is desirable to conduct the tests under good daylight conditions in order that the high-speed photography of deformation and failures will be facilitated.

2. The overpressure-vs-distance curves drawn by C. W. Lampson, of the Ballistic Research Laboratories, were used for placement of all structures. Based on these curves, the Army structures were designed for best results with a weapon yield range of 50 to 60 kt, whereas the Navy and Air Force structures were designed for best results with a weapon yield range of 40 to 50 kt.*

3. A "dud" will leave the structures program essentially intact for future use.

In view of statement 2, it is interesting to estimate the dependence (for success) of these experiments on weapon yield. Doing this in turn requires an appreciation of the methods used by the structural-design personnel. As an example, consider the Navy portion of the program. The Navy was interested in testing certain structural designs of given size, shape, cost, method of construction, material, etc. Such structures were designed, and subsequent analysis of each indicated that it would be deflected an interesting amount (for experimental purposes) by Z-psi overpressure. The Lampson curve for 50 kt was then entered at Z-psi overpressure to determine the proper location of such a structure. This location technique was employed because the Navy had been previously notified by the AEC that the following facts could serve as a guide: (1) The weapon yield would be 50 ± 10 kt, and (2) the Lampson overpressure-vs-distance curve was as reliable as any available curve and would be used as the standard reference for Greenhouse planning.

Consider Navy Structure 3.2.6, a concrete dome located 1080 yd from ground zero. The Lampson curves for 40 and 50 kt indicate, then, that the building was designed to be tested in an overpressure range of 12.5 to 14 psi. A strong deviation in overpressure from this range of values, in either direction, would have deleterious effects. A small overpressure would deflect or damage the structure so little that great extrapolations would have to be made in anal-

*This information was obtained verbally from LCDR W. H. Rowen, Assistant Program Director for the "effects on structures" program.

ysis—a process little better than guesswork. A large overpressure would undoubtedly demolish the structure to such an extent that no data would be forthcoming. As mentioned, much of the design is in the plastic range, and the instruments to be employed on the structures are set to operate within previously established ranges; hence the overpressure experienced at a given point becomes a rather critical parameter for these experiments.

It must not be concluded from this, however, that the success of Structure 3.2.6 as an experiment is critically dependent on the yield lying in the 40- to 50-kt range. If the source of the Lampson curve is inspected, it is found that an uncertainty of ±20 per cent in the Sandstone experimental pressure data (in the 10- to 15-psi range) is somewhat conservative. The reason for the selection of a specific structure is now apparent since the variation in yield associated with a pressure uncertainty of ±20 per cent is a function of the pressure range in question. In particular, it is reasonable to say that $W \sim P^{\frac{1}{2}}$ for an overpressure in the 10- to 20-psi range. Hence the uncertainty of 20 per cent in overpressure leads to an uncertainty of 30 per cent in yield. This indicates that the pressure range of 12.5 to 14 psi, for which Structure 3.2.6 is intended, is associated with a probable yield range of 30 to 65 kt rather than 40 to 50 kt.

Thus the following conclusions are made:

1. Although the entire structures program is rather critically dependent on the overpressure field for success, and therefore on the weapon yield, it is not necessarily dependent on the yield lying within the range of 40 to 50 kt for the Navy and Air Force (50 to 60 kt for the Army).

2. It is probable that a weapon yield exists in the range of 30 to 65 kt for the Navy and Air Force (38 to 78 kt for the Army*) which will supply an overpressure field that is most desirable from the point of view of success for the structures experiment.

6.3 CLOUD PHYSICS

The mechanics of formation, rise, and dispersion of the atomic cloud are not well known. A certain amount of experimental data is available from both Bikini and Sandstone, but it is lacking in significant details. Detailed experimental data and the subsequent development of an adequate theory of these phenomena are very desirable for many reasons, a few of which are:

1. The use of airborne instrumentation, by any means whatever, in atomic tests involves planning which is dependent on both the trajectory and the thermodynamic structure of the cloud.

2. Atomic tests must be carefully evaluated from the point of view of attendant radiological hazards, direct and indirect, to personnel. The use of the word "indirect" here denotes the denial of a critical area to personnel due to contamination. Prediction and/or control of the fall-out from the atomic cloud is therefore of the greatest importance. This is particularly true when tests are to be conducted in the ZI, where the population density is relatively high.

3. Should an atomic bomb be used in a strike against an enemy, it is possible that the presence of its atomic cloud over enemy territory can be put to advantage. The use of artificial seeding agents to induce precipitation from the cloud, with its attendant concentration of fall-out contamination, might well serve to deny a critical area to enemy personnel. Even if the denial were not complete or lasting, the psychological effect of such a tactic could be very valuable.

4. Especially in the case of a multiple bomb strike at night, there is the problem of aircraft evasion of the contaminating cloud. Detection of the cloud at a sufficient distance to allow an aircraft to avoid contact successfully is therefore a problem.

5. After the cloud has dispersed to the extent that it becomes invisible to the eye, concentrations of fission particles may be present in sufficient amount to make contamination a real danger either to the surface by means of fall-out or to airborne vehicles by means of direct contact. It is therefore necessary that provision be made for detecting and tracking such concentrations.

There are obvious extensions and ramifications to these items which the limitations of space prevent treating in greater detail. Certainly the five items listed offer sufficient justification for a rather extensive experimental program. Such a program has been collected under the title of "cloud physics," and the in-

*Obtained by an analysis similar to that given for Navy Structure 3.2.6, applied to Army Structure 3.1.1, the multistory building.

dividual parts of this program are briefly described in the following sections.

6.3.1 Thermodynamic Structure of the Cloud

The instrumentation plans for this phase of the experiment call for measurement of temperature and relative humidity at various pressure altitudes in and around the cloud. This will be accomplished with 18 drone-carried aerographs. The drones are being vectored into the cloud at altitudes varying from 6000 to 28,000 ft. Each aerograph will detect and automatically record information on ambient air temperature, relative humidity, pressure, altitude, airspeed, and time.

The problem of the feasibility of inducing precipitation from atomic clouds using artificial seeding agents is under theoretical attack at this time. The factors which are important in the formation of precipitation have been isolated and are being individually studied. Accordingly, drop-size distribution, liquid-water content, temperature, air motions, cloud thickness, and sublimation nuclei are the important variables which are influential in the precipitation process. The results of seeding trials carried out during the past 3 years have been studied and evaluated with the conclusion that the possibility of producing rain artificially depends very greatly on the magnitude of the variables mentioned. Therefore it is imperative to know the values of these factors in the atomic cloud in order to determine theoretically the possibility of inducing precipitation from it.

6.3.2 Photographic Documentation of the Cloud

Sequential photographic records of the cloud will be obtained from three fixed ground positions and from two B-50D aircraft. Colored photography will be used in addition to black and white. One of the fixed ground stations will be on Rigili Island and will be equipped with six K-17 cameras, arranged to give views of the cloud over a vertical angle of 60° and across a horizontal angle of 120°, with slight overlaps. The other ground stations will be at opposite ends of a base line on Eniwetok and will each be equipped with one Mitchell camera. The two B-50 aircraft will be used as photographic aircraft after their primary mission in the blast program is completed. They will circle the cloud at H+30 min, one above and one below the cloud, to obtain aerial photographs of any significant phenomena such as "rain-out" and shears.

This photographic documentation proposes to be of such high quality that it will yield useful data for computing dimensions, rate of rise, and for giving aid in determining "rain-out" from the cloud, as well as determining physical aspects of the ice cap and assisting in the development of a theory for the formation of the ice cap.

6.3.3 Wind Measurement

The wind data to be obtained are continuous measurements of the intensity of the afterwind induced by the rising fireball of an atomic explosion. This afterwind is a wind directed toward the blast center which springs up within a few seconds after the passage of the shock wave. Measurements of material velocities during the passage of the shock wave will be obtained as a by-product. The data will be compiled and analyzed to obtain more complete understanding of the meteorological effects of a large blast. This knowledge can subsequently be used in studies in which the wind structure is a factor. Two of these studies are the "base-surge" problem and the "seeding" of radioactive clouds.

The base-surge problem is one which has received emphasis under the program of research on the geophysics aspect of atomic warfare. The term "base-surge" is usually applied to the phenomenon of a cloud formation in the lower levels of the atmosphere, rapidly expanding around the periphery of the blast. At this time it appears probable that this phenomenon is a single manifestation of a somewhat more complex circulation structure; it therefore appears appropriate to measure the winds caused either directly or indirectly by the blast. It is anticipated that such studies will be capable of analysis for use during the course of a theoretical study of the entire circulation problem.

The seeding of radioactive clouds involves an operational requirement for observations of the afterwind structure. In seeding the cloud, either to induce fall-out or to render the cloud visible after nightfall, it is necessary to introduce the seeding material after the cloud has cooled to a temperature at which this material will not vaporize. It may be most practical to introduce

the seeding material into the afterwind draft so that it will be carried into the cloud when appropriate temperatures have been reached. In such an operation the particle size of the seeding material would depend on the afterwind structure.

Twenty-five wind-measuring devices, with their accompanying automatic recording equipment, will be installed in the area of the tests. Two shots will be monitored, that on Engebi and that on Eberiru. Each measuring device consists of a pitot tube and a vane with self-synchronous link for direction indication, mounted on a steel mast. Measurements will be taken 6 and 12 ft above the surface to detect vertical variation of the wind. In order to check the assumption that only radial distance from the blast will affect the afterwind speed, the instruments will be staggered at different azimuths from the center of the blast.

6.3.4 Tropical Meteorology

This project involves general research in the meteorology of tropical regions with special emphasis on improving the accuracy of forecasts for atomic testing so that radiological hazards may be minimized. Special emphasis will be placed on the collection of all types of meteorological data before, during, and after the tests, over a wide portion of the Pacific area.

6.3.5 Atmospheric Conductivity

Previous theoretical and experimental work has shown that the presence of radioactive matter in the air can be detected from measurements of electrical conductivity in the atmosphere. This has been found to be more effective than any other existing method for detecting the presence of a cloud and determining its distribution of radioactive matter with respect to both space and time. This indicates the desirability of using airborne conductivity equipment for such experiments at Eniwetok.

Two B-50 aircraft and one L-13 aircraft will be equipped with ion-conductivity chambers and atmospheric nuclei counters in order to obtain the following data:

1. Before the blast, conductivity measurements will be made to determine background value for the surrounding area. After the blast, planes will first search for the radioactive cloud and, after finding it, will carry out experiments in and around it.

2. Diffusion of the cloud shortly after the blast (1 or 2 hr) will be determined by measuring the variation of atmospheric conductivity as a function of distance near the edge of the cloud.

3. Measurement of time rate of change of conductivity in the fringes of the cloud for several days after the blast will give the rate of both vertical and horizontal cloud diffusion.

4. Measurements will be made in order to map contours of radioactive intensity as a function of time over the island where the blast occurred. From these measurements the time rate of decay of radioactivity and the variation in intensity as a function of distance from the blast center can be determined.

5. Determination will be made of cloud contours and its possible disintegration into smaller radioactive clouds. During this time the variation of height and width of the clouds with time can also be measured, and position and speed of the cloud will be determined.

The dependence of the cloud physics program on weapon yield or time of firing can be summarized as follows:

1. The photographic documentation requires sufficient light for taking pictures.

2. The wind-measuring devices have been designed in a fashion similar to that outlined for the structures program (Sec. 6.2). Hence they are physically placed so as to operate most effectively in the overpressure field defined by the Lampson 50-kt curve. A strong deviation from this on the high side would cause undue damage to the close-in units, with an attendant loss of data.

6.4 RADIOLOGICAL INSTRUMENT EVALUATION

The evaluation and test of radiological instruments is part of a continuing program directed toward the design and development of instruments satisfactory for issue to military and civil defense organizations.

Dosimeters have been developed to the point that they are adequate for industrial use under controlled conditions, with very low permissible dosages and dose rates and with radiation of known energies. Military dosimeters, however, require use under uncontrolled conditions of

dosage levels approaching and even exceeding lethal amounts at very high dose rates and unknown energies. Controlled laboratory experiments cannot provide the dose rates and the wide range of energies which result from an atomic detonation. Hence a realistic test of military instruments can be carried out only in conjunction with an actual detonation.

Airborne radiation detection instruments are also of great interest for at least two reasons: (1) to afford better methods of long-range detection and (2) to obtain information as to the gamma-radiation intensity, distribution, and decay characteristics in the blast area. The reader will note that here is an excellent example of the interdependence of experimental programs. As was the case with dosimeters, realistic tests of airborne instruments can be carried out only in conjunction with an actual atomic bomb explosion. The experimental program will be summarized briefly in Secs. 6.4.1 and 6.4.2.

6.4.1 Service Tests of Dosimeter Devices

The following types of dosimeter devices will be used both on the ground and in drone aircraft, in order that they will be exposed to a wide range of dosages, dose rates, and blast conditions: (1) quartz-fiber electrometer, (2) ionization chamber, (3) photographic, (4) color-changing alkali-halide crystal, (5) energy-storage phosphor, (6) conduction crystal, (7) color-changing glass, and (8) chemical. Measurements will be made of the change in color density of certain minerals, notably the alkali halides, as a result of exposure to ionizing radiation. Changes in fluorescence of activated phosphate glasses will be determined, and any other effects of the radiation on these "crystals" and "phosphors" will be observed and measured.

In connection with these determinations, tests will be carried out to evaluate portable survey instruments for measuring radiation intensity of contaminated areas resulting from atomic explosions. An evaluation will also be made of a mobile radiological field laboratory containing equipment for determination of the necessary information for formulation of an estimate of the hazard in occupying a given area, including nature, quality, energy, and decay rate of the contamination.

Dosimeter data obtained from this experiment will be used to aid in determining the adequacy of the instruments with respect to tactical uses and applications; stability and reliability under field use; blast, heat, and light; physical design; component stability under irradiation; decontamination; saturation; reusability; and shielding. Some dosimeters will be carried by the radiological safety monitors, and others will be placed on panels mounted inside drone aircraft. The crystal dosimeters will be enclosed in lighttight boxes and located on the ground at fixed distances from the weapon. The survey instruments will be carried into the area after the detonation. The radiological field laboratory will be stationed outside the area expected to be affected by the explosion, and personnel will bring samples to the laboratory for analysis.

6.4.2 Evaluation of Airborne Radiac Equipment

This portion of the experiment will test four recently developed instruments: (1) two types of droppable gamma-intensity telemetering equipment, (2) an airborne surface-radiation-intensity survey device, and (3) an airborne radioactive-cloud detector and tracker. An Air Force B-17 will carry the latter and will track the radioactive cloud from the time of the explosion until the cloud has dissipated to nondangerous radiation intensities. The other instruments will be carried by a Navy P2V. The gamma-telemetering transmitters will be dropped into the crater as soon as practicable after the blast; the P2V will contain the receiver for these and will remain in the area for several hours to monitor the transmitting units. Simultaneously with the latter, the P2V will make an aerial survey, at various altitudes, over the crater area, this survey being continued periodically for several days.

A large portion of the radiological instrument evaluation program is not affected by weapon yield. The fixed ground stations, however, are dependent on weapon yield in much the same manner as is the structures program.

6.5 PHYSICAL TESTS AND MEASUREMENTS

As the vague nature of the title would indicate, this portion of the program is a somewhat heterogeneous collection of experiments, the de-

tailed objectives of which are widely divergent. Generalizations about the philosophy behind such experimentation are not attempted; instead the experiments are merely listed, and the object and content of each are briefly stated.

6.5.1 Cloud Particle Size and Distribution

Each drone aircraft will be equipped with the following apparatus, designed to obtain representative samples of the cloud for the determination of particle size and distribution:

1. A cascade impactor designed to separate the particle contaminant into four size fractions.
2. A centrifuge designed to separate the cloud contaminant into a continuous spectrum of particle-size fractions.
3. A 10-cu ft snap sampler designed to obtain a cloud sample for ultimate analysis, including gaseous and particulate determination as well as microchemical and radiochemical analysis.
4. Two isokinetic samplers designed to precipitate cloud particles out of a decelerating stream of air, one using an electrostatic precipitator and the other using a thermal precipitator.

Data will be obtained on the composition, concentration, specific activity as a function of particle size, and particle-size distribution of the particulate matter of the radioactive cloud. These data will supplement previous atomic bomb phenomena observations in the determination of:

1. The requirements for airborne protective equipment.
2. Those properties of cloud contamination which will provide a guide in developing simulated contaminants for laboratory use.
3. Fall-out, extent and severity of areas of contamination, and extrapolation to other environmental conditions of detonation.
4. The correlation of particle size with chemical composition, total radioactivity, and the chemical conditions under which the radiocontaminants exist in the cloud.
5. The relative value of nonisokinetic methods of cloud sampling.
6. The prediction of the gross decay rate of a cloud which might settle out in habitated areas as a result of a nearby atomic burst.

6.5.2 Effects of Thermal Radiation on Material

For an assessment of the ability to simulate and measure in the laboratory the thermal effects of atomic bomb detonations on materials, pretested materials and instruments will be exposed at operationally important distances. Whenever feasible, protected instruments will be placed to record the instantaneous environmental conditions so that the important attributes of the associated detonation phenomenology can be selected for future laboratory reproduction.

In addition, small samples of "standard" materials, which are believed to be important as potential sources of primary fire hazard, will be exposed. The standard materials are to be selected, if possible, on the basis of their response to the following important parameters of the exposure: total energy, spectral distribution, intensity as a function of time, ambient conditions, and orientation of the receiving surface. The number of standards will be minimized by previous laboratory studies. Hence each standard material will represent an entire class of substances which may vary, for example, in color, density, and chemical composition.

Defensive plans, including recommendations for the selection of materials, design of equipment and structures, disaster planning, etc., will be based on the foregoing information plus knowledge of factors contributing to the origin and spreading of fires. One very important problem to attack in this connection is the determination of whether primary fires constitute a significant factor in the defense planning, particularly from the point of view of target vulnerability estimates.

6.5.3 Exposure of Combat Vehicles

Ten medium tanks will be placed at various distances from the weapon, each being supplied with and surrounded by instrumentation designed to obtain information about the following:

1. Total ionizing radiation and, whenever necessary, ionization as a function of time, at various points in the interior and in the vicinity of the combat vehicle.
2. The interior wall temperature of the combat vehicle as a function of time.
3. The adiabatic heating of the air inside the vehicle caused by the passage of the blast wave.
4. The rise in interior pressure as a result of the blast-wave passage.
5. The normal and cross accelerations and overturning moment imparted to the vehicle by the incident shock wave.

[redacted]

6. Certain stress and strain measurements on critical structural members of the vehicle.

The data obtained will be used in the evaluation of the tactical effectiveness of atomic weapons against armor concentrations and in the formulation of tactical doctrine for such situations in both offense and defense.

The experiment is based on experience gained with armor at previous tests and is expected to provide calibration data for both calculations and laboratory experiments involving the test tanks and other armored weapons.

6.5.4 Fall-out Distribution

Glass collection plates will be placed at selected locations on the islands which make up Eniwetok Atoll. After the detonation the plates will be recovered and examined for any radioactive particles which may have fallen on them. The experiment is designed to determine the test-site fall-out pattern, particularly as it is affected by meteorological conditions. In addition, it is desired to appraise the potential health from external and internal exposure to the fall-out products.

The information gathered will be valuable in predicting fall-out patterns for tactical detonations as well as other tests. It will also indicate probable hazards to personnel who are in the fall-out areas or who must enter them at a later time.

In particular, the fall-out samples will be analyzed to obtain the following data:

1. Distribution of fission products and fissile materials in samples.
2. Concentration pattern of fall-out products.
3. Particle-size distribution of fall-out products.
4. Radiochemical composition of fall-out products.

6.5.5 Interpretation of Survey-meter Data

Greased metal collection strips will be attached to the outer surfaces of the drone planes for the purpose of obtaining samples of radioactive contaminant aloft. From these samples data will be obtained concerning the energy spectrum of the composite radiation from surfaces contaminated with fission materials. Spectra will be obtained as soon as possible following the initial contamination, and changes in spectral distributions will be observed for as long a period thereafter as is interesting. Ionization dose-rate measurements of both beta and gamma radiations will be made with available absolute and secondary standards.

The data obtained will be used to interpret the response of portable survey instruments in terms of the actual radiation dose received. It will also lead to a more correct estimation of the health hazard associated with atomic weapon–induced contamination.

6.5.6 Evaluation of Filter Materials

Each of five types of filter material will be arranged in multilayer pads and placed in drone planes. A sample of the radioactive cloud will subsequently be passed through the pads. At the test site, as soon after the test as possible, the individual layers of the pads will be measured for gross radioactivity. Further analysis will be made in the ZI by counting and radioautograph techniques to obtain data on the penetration efficiency of the filter materials and to check qualitatively particle-size measurements made by other methods.

The data obtained will be used to determine the protection afforded by gas-mask canisters and collective protectors against radioactive particulates resulting from an atomic explosion. Techniques of sampling and efficiency of collection of airborne contaminants will also be evaluated.

6.5.7 Contamination and Decontamination Studies Aloft

Thin metal test surfaces will be prepared and attached to the drone planes, whenever feasible, at such spots as to accumulate a maximum amount of radioactive contaminant. After the passage of the drone planes through the atomic cloud and the subsequent contamination of the test surfaces, the metal plates will be removed as soon as possible and subjected to decontamination analysis. A small portion of the laboratory work will be done in the Forward Area, but the majority of the samples will be shipped to laboratories in the ZI.

The data to be obtained are those which determine:

1. The contamination and decontamination characteristics of various standard surfaces ex-

[redacted]

posed to an atomic cloud. This will take into account the surface material or the protective coating on the material and the physical characteristics of the surface, such as roughness.

2. The efficiency of decontamination methods and agents as a function of time after exposure.

3. The capabilities of existing methods with respect to full-scale operational decontamination.

The results obtained will be compared to the results of laboratory experiments on both contaminability and efficiency of decontamination methods in order to determine the extent of correlation between field and laboratory tests. The data will lead to a better understanding of the factors that influence the contamination and decontamination of materials and hence make probable the creation of better field operational decontamination procedures. It will also aid in the development of new contamination-resistant material and will provide improved design criteria for materials employed in military equipment and construction.

In addition, the data will yield a better understanding of:

1. The chemical and physical nature of the contaminants in the atomic cloud.

2. The fractionation of fission products in the cloud due to differences in chemical and physical properties.

3. Preferential decontamination.

4. Activity levels obtainable in decontamination.

6.5.8 Cloud Radiation Field

Each of the drone planes will be equipped with two recording-type gamma-ray intensity measuring instruments, one for 0 to 10 r/hr and the other for 1 to 100,000 r/hr. A graph will thus be obtained of radiation intensity as a function of time. This graph, in conjunction with data from other projects on cloud position vs time and drone location vs time, will enable a graph to be made of gamma-ray intensity vs distance from the center of the cloud at various cloud heights.

The latter data will aid in determining the potential health hazards to airborne personnel in the region of an atomic cloud as a function of time after detonation. It is also essential for determining the criteria to be applied in designing airborne warning instruments and protective equipment.

6.5.9 Evaluation of Protective Clothing

This experiment is a part of a continuing program which includes studies of protection from and decontamination from radioactive contamination for both atomic bomb bursts and radiological warfare dissemination of radioactive particulates. Two phases are included, the first being devoted to a study of the decontaminability of those materials.

The materials considered to be of interest for phase 1 are plain cotton fabric, water-repellent-finished cotton fabric, plain woolen fabric, worsted fabric, impregnated cotton cloth, synthetic resin-coated fabric, unwoven cotton fabric, elastomeric film, and filament rayon fabric.

Items of protection clothing needed for wear by personnel entering the contaminated areas will be manufactured in both reusable and "throw-away" types. Protective items will be monitored upon removal from the contaminated areas and subsequently transported to the decontamination unit for further study.

Data will be obtained on the following:

1. Evaluation of materials as to protective value, susceptibility to contamination, susceptibility to decontamination, and serviceability.

2. The handling and disposal of contaminated clothing under field conditions.

3. The effectiveness of various types of laundering decontamination procedures.

4. Susceptibility of existent mobile laundry equipment to contamination due to processing of contaminated clothing and susceptibility of the same laundry equipment to decontamination.

5. The problem of contaminated waste-water disposal.

Such data will obviously be applicable to both military and civil defense planning.

6.5.10 Evaluation of Collective-protector Equipment

This experiment is essentially a test of two items of equipment: (1) a filter which is called the "field collective protector, E24R4" and (2) a valve which closes when its entrance port is subjected to a given overpressure, known as the "antiblast closure." The collective protector will be installed in a reinforced-concrete structure equipped with air locks containing antiblast closures. Additional antiblast closures will be installed at various distances from zero point,

the protected side of each closure being instrumented to indicate peak pressure. The latter phase of the experiment will determine if particulate filters, having bursting pressures of 7 psi, can be protected with antiblast closures.

The primary objective is to determine the efficiency of existent collective-protector equipment in preventing the entrance of radioactive contaminants into a shelter. Supporting instrumentation will supply the following data in connection with the concrete shelter:

1. Radioactive penetration through the collective protector as a function of time.
2. Total activity from radioactive particulates within the shelter.
3. Total activity retained by the protector.
4. Pressure as a function of time, both outside and inside the shelter.

These data will afford a basis for continuing development work in this field.

Only those portions of the physical tests program which will exist as fixed ground installations are dependent on the weapon yield, and those few items are dependent on yield in the manner outlined in Sec. 6.2 for the military structures program.

6.6 LONG-RANGE DETECTION

This portion of the military tests program, as its name implies, is devoted to a consideration of those parameters associated with the detection of an atomic explosion at great distances. The importance of such techniques was made obvious by the President's announcement of the Russian explosion in 1949. A number of interrelated but independent experiments will be carried out in this connection. No attempt is made to describe their methods since insufficient information exists at this time. The objectives, however, are presented in Secs. 6.6.1 to 6.6.8.

6.6.1 Radiochemical, Chemical, and Physical Studies of Atomic Bomb Debris

1. To calibrate certain fission-product ratios for bomb neutron energies.
2. To determine the relation between fission-product yields, type of fissionable material, and neutron energy.
3. To compare fission-product ratios for bombs and fast reactors and to make estimates of bomb neutron spectra.
4. To make a determination of possible fractionation of fission products and fissionable material in the original cloud.
5. To evaluate previous estimates of total energy as a function of capture to fission ratio and tamper content of debris.
6. To obtain more information on the relation between particle size and the conditions of an atomic bomb explosion.
7. To determine the effect of different types of carrier material on properties of the debris and any influence on radiochemical and other analyses.
8. To determine the effect of small proportions of large particles on an estimate of total activity from distant measurements.
9. To estimate the relation between total energy and the combination of specific activity and tamper content of the debris.
10. To determine the feasibility and accuracy of newly developed analytical techniques for fission-product and neptunium analyses, alpha-particle emitters, ultramicrochemical analysis of the debris, and physical properties of particles.

6.6.2 Infrasonic Wave Propagation Studies

This experiment is designed to provide a basis for an estimate of the effectiveness of acoustic detection stations in providing an early warning of an atomic blast accomplished by another nation. Acoustical data, if obtainable, permit an accurate determination of the time and location of the blast. This information, together with techniques of nuclear detection and conventional intelligence, is used to ensure the collection of adequate early samples of bomb debris for chemical analysis and to assist in the interpretation of the nature of the atomic event. Specific objectives are:

1. To establish the change in character of the acoustical signal with distance from the blast.
2. To establish the existence of directional effects in wave propagation to great distances from large explosions.
3. To compare the effectiveness of several types of acoustical equipment during actual field test.
4. To establish, if possible, the correlation between infrasonic wave propagation to great distances from large explosions and to short distances from small explosions.

5. To establish the optimum characteristics to be desired in acoustical detection equipment (frequency range, maximum sensitivity, etc.).

6. To establish the effect of meteorological conditions on the accuracy of azimuth determinations made at a considerable distance from the blast.

6.6.3 Location of an Atomic Bomb Cloud by Observation of Air Currents

Upper-air weather observation stations will be established, in addition to those in permanent operation, to improve the coverage of meteorological data over the areas of interest. These data will be analyzed and correlated with radiological observations.

1. To study the rates of diffusion and settling of particles.

2. To test cloud-tracking and forecasting techniques.

3. To facilitate the collection of samples of debris at great distances.

6.6.4 Collection of Bomb Debris by Airborne Filters

1. To support other experiments requiring collection of bomb debris.

2. To delineate the radioactive cloud for approximately 5000 miles.

3. To test a large "super-sampler" filter unit designed to provide a sufficiently large sample for analysis in the event that only very low concentrations of weapon debris are available in the atmosphere.

6.6.5 Instantaneous Detection of Atomic Bomb Debris by Airborne Detectors

1. To determine the feasibility of measuring at long range the concentration of atomic bomb debris continuously from ground level to 90,000 ft.

2. To ascertain the reliability of scintillation-counter equipment developed for balloon-borne and aircraft-borne instrumentation in detecting and measuring the concentration of widely dispersed weapon debris.

3. To obtain a vertical profile of the distribution of debris from Eniwetok at key locations.

6.6.6 Collection of Atomic Bomb Debris at Ground Level and Analysis of Samples

1. To compare relative amounts of activity collected by different methods.

2. To determine fractionation of fall-out material as a function of distance from the explosion.

3. To determine the physical characteristics of transported material.

4. To evaluate the relative efficiencies of the various collection systems located at ground level.

5. To investigate chemical methods for separation of active material.

6. To obtain experimental data on yields from an actual bomb explosion for calibration of results which might be obtained at various distances from the site of future atomic explosions of unknown origin.

6.6.7 Seismic Wave Propagation Studies

1. To establish criteria for distinguishing between an earthquake and an atomic explosion.

2. To clarify the limits on range at which seismic observations of atomic explosions can be made as a function of weapon yield.

3. To ascertain the effectiveness at long range of seismic methods of determining the time, place, and magnitude of an atomic explosion.

6.6.8 Detection of Atomic Bomb Debris by Atmospheric Conductivity

1. To locate particular sources of atomic bomb debris in the vicinity of the site as an aid to collection of specific samples, such as (a) fall-out below the cloud, (b) fringes of the moving cloud shortly after formation, and (c) body of the cloud after it becomes invisible but before extensive dispersal.

2. To determine the feasibility of detecting the presence of bomb debris instantaneously in an aircraft at great distance with atmospheric-conductivity apparatus.

6.7 EFFECTS ON AIRCRAFT

At this time the only available medium of atomic weapon delivery is that of manned aircraft. This fact presents the Air Force with serious planning problems, which in the past have been solved only in a very naive manner owing to a lack of, or the unreliability of, basic data. It is hoped that the results of the Greenhouse Program will alleviate the latter difficulty, at least in part, and that weapon-delivery mission

planning can be subsequently made more specific and reliable.

A few of the basic problems involved can be stated briefly as follows:

1. Given an atomic-fission-produced energy release of known magnitude, what are the undisturbed details of the following influence fields established by such a phenomenon: (a) overpressure, (b) gamma radiation, (c) thermal radiation, (d) neutron flux, and (e) material velocity?

2. Given the solution of problem 1, how are such fields perturbed by the introduction of a disturbance such as an aircraft? Suppose that the undisturbed overpressure field produced by a given weapon is completely known. Then, if an instrumented aircraft is placed on a known point p in this field and a pressure P is measured at a time t, how is the number P to be related to the pressure P′ that would have existed at p at time t if the aircraft had not been present?

3. Given that an aircraft is to be exposed to known values of overpressure, thermal radiation, and material velocity, how will the aircraft and its occupants be affected? The solution to this problem depends strongly on the answers to problems 1 and 2, as well as on static and dynamic structural studies and thermal-radiation reflection and transmission studies, etc.

In the past the philosophy of weapon-delivery planning has been ultraconservative from the point of view of safety to the dropping aircraft and its crew. Such a philosophy has at least two disadvantages: (1) Increasing weapon yield requires constant revision of aircraft performance criteria, with its associated problems, and (2) the cost of destroying some targets becomes too high for feasibility. Recent theoretical work has indicated that such ultraconservative planning is unwarranted, and the "effect on aircraft" portion of the Greenhouse Program is designed to implement and check this theoretical work. The experimentation is subdivided into six parts (Secs. 6.7.1 to 6.7.6).

6.7.1 Tests of Airborne Aircraft

The data to be obtained concern the nature and magnitude of the loads and forces induced in aircraft structures in flight adjacent to an atomic explosion. Four radio-controlled drones and three manned aircraft will be located in space and time in such a manner as to instrument seven points in the overpressure field. The seven points have been carefully selected for all shots in accordance with theoretical analysis. Two points are included at which aircraft structures should be stressed to limit loads.

At each point the following measurements will be taken:

1. Altitude.
2. Air speed.
3. Location in space vs time, accomplished with ground-based radar.
4. Aircraft response, accomplished by measuring accelerations at the center of gravity, at the tail, and at elements such as engines and wing panels as are appropriate.
5. Positions of flight control surfaces.
6. Structural loads: bending moments and shear and torsional measurements taken at appropriate points.
7. Aerodynamic loads, accomplished by taking pressure measurements at the surface of the aircraft.

To assure collection the data from the drones will be telemetered as well as recorded in the plane.

6.7.2 Static Tests of Aircraft Panels

Specified aircraft components will be placed in the Mach reflection region of the shock wave. Controlled measurements are to be taken to evaluate the effects of blast, heat, and radioactivity on these components. The following specific data are to be obtained:

1. Air-load and air-pressure measurements on an ideal rigid wing.
2. Structural measurements on an ideal simple wing, both straight and swept design.
3. Qualitative data on vented and unvented components.
4. Qualitative data on secondary items such as canopies, antennas, pitot tubes, fuel tanks, and rudders.
5. Qualitative data on new experimental structures utilizing new materials and/or new design principles.

6.7.3 Interferometer Gauges

This experiment is designed to measure pressure vs time on sites E, S, P, and Q. The information received on site E will be checked by

different methods of obtaining the same data, hence affecting a calibration of the new gauge used.

This method of pressure measurement utilizes the principle of the interference bands of light produced on the mirrored surfaces of a quartz diaphragm. Since the pressure on the diaphragm varies the thickness of the film of air which separates the plates, the interference fringes are displaced. This displacement is a direct measure of the pressure on the diaphragm.

Twenty-four gauges will be used: eight in conjunction with the structures program on Engebi and sixteen in conjunction with the static tests of aircraft panels on the four sites mentioned.

6.7.4 Radar-scope Photography

It is proposed to take photographs of radar scopes during the shot periods.

Detailed analysis of radar-scope data available from Crossroads and Sandstone indicates that proper use of radar-scope photography may furnish a direct measurement of bombing accuracy and an estimate of bomb damage.[1] The accomplishment of this proposal would supply more data from which to draw conclusions.

A special high-light-intensity-output type of scope plus a high-speed camera will be used in each of two manned aircraft in conjunction with the standard radar equipment. Any quantitative data on ionization and pressure distributions at shot time will be of value in making a more complete analysis of the recorded data.

6.7.5 Effects of Atomic Explosions on Radio Wave Propagation

It is proposed to cause radar and radio transmitters on selected sites to transmit on frequencies spaced throughout the spectrum and be received or reflected through the blast and recorded on magnetic tape for subsequent measurement and analysis.

Considerable difference of opinion exists as to influences or effects on the propagation and reception of radio and radar signals in the vicinity of atomic blasts. An analysis of the data from this experiment will provide basic knowledge on these phenomena for application in future planning and design. The data from this experiment and that from radar-scope photography will be complementary and each will aid in the analysis and interpretation of the other.

6.7.6 Aerial-photography Damage Study

This experiment is designed to determine the feasibility of determining structural damage from aerial photographs. The operational importance of such a technique is obvious.

Vertical and oblique aerial photographs will be taken of the various structure groups on sites E, S, and T, both before and after the Easy shot. A comparison of the before and after photographs of any given structure will lead to an estimate of the damage sustained by that structure. Such estimates will be checked and calibrated by subsequent detailed physical inspection of building damage.

The experiments of Secs. 6.7.1 and 6.7.2 are dependent on the yield of the weapon in much the same manner as is the structures program (see Sec. 6.2). It should be pointed out, however, that the aircraft positioning in Sec. 6.7.1 is also dependent on knowing the attenuation of the blast wave with passage through the atmosphere. Since this problem has never been solved, approximations must be used. It is concluded, then, that the probability of a given aircraft experiencing the overpressure range for which it was positioned is somewhat lessened.

REFERENCE

1. Operation Sandstone, Airborne Radar Strike Photography of Atomic Explosions, Operations Analysis Section, Headquarters USAF, Special Report No. 3.

AEC, Oak Ridge, Tenn., A-33255